AD NUMBER

AD431959

LIMITATION CHANGES

TO:

Approved for public release; distribution is unlimited.

FROM:

Distribution authorized to U.S. Gov't. agencies only; Administrative/Operational Use; JAN 1964. Other requests shall be referred to Aeronautical Systems Div., Wright-Patterson AFB, OH 45433.

AUTHORITY

AFFDL ltr 2 May 1979

ASD-TDR-63-783

THERMAL STRESS DETERMINATION TECHNIQUES FOR SUPERSONIC TRANSPORT AIRCRAFT STRUCTURES

PART II - DESIGN DATA FOR SANDWICH PLATES AND CYLINDERS UNDER APPLIED LOADS AND THERMAL GRADIENTS

TECHNICAL DOCUMENTARY REPORT NO. ASD-TDR-63-783, PART II

JANUARY 1964

Supersonic Transport Research Program
Sponsored by the
Federal Aviation Agency

Flight Dynamics Laboratory
Aeronautical Systems Division
Air Force Systems Command
Wright-Patterson Air Force Base, Ohio

(Prepared Under Contract AF33(657)-8936 by
R.A. Gellatly and R.H. Gallagher of Textron's
Bell Aerosystems Company, Buffalo, New York)

NOTICES

The information contained herein is a part of a national undertaking sponsored by the Federal Aviation Agency with administrative and technical support provided by the Department of Defense, Aeronautical Systems Division, Air Force Systems Command with contributing basic research and technical support provided by the National Aeronautics and Space Administration.

When Government drawings, specifications, or other data are used for any purpose other than in connection with a definitely related Government procurement operation, the United States Government thereby incurs no responsibility nor any obligation whatsoever: and the fact that the Government may have formulated furnished, or in any way supplied the said drawings, specifications, or other data, is not to be regarded by implication or otherwise as in any manner licensing the holder or any other person or corporation, or conveying any rights or permission to manufacture. use. or sell any patented invention that may in any way be related thereto.

Copies have been placed in the DDC collection. U.S. Government agencies may obtain copies from DDC. Other qualified DDC users may request through:

Office of the Deputy Administrator
for Supersonic Transport Development
Federal Aviation Agency
17th Street N.W. and Constitution Avenue
Washington 25, D.C.

DDC release to OTS not authorized.

This report must not be cited, abstracted, reprinted, or given further distribution without written approval of the above-named controlling office.

Copies of this report should not be returned to the Research and Technology Division, Wright-Patterson Air Force Base, Ohio, unless return is required by security considerations, contractual obligations, or notice on a specific document.

FOREWORD

This report was prepared by Textron's Bell Aerosystems Company, Buffalo, New York, under Contract AF33(657)-8936. The work was administered under the direction of the Flight Dynamics Laboratory, Aeronautical Systems Division, by Mr. G. E. Maddux, Project Engineer. The work was performed by the Structures Section of the Aerospace Engineering Department, Bell Aerosystems Company, in the period of 15 June 1962 to 31 July 1963. Mr. Richard H. Gallagher was Technical Director of the study.

The authors wish to acknowledge the contributions to this work of P.P. Bijlaard, Professor of Engineering Mechanics at Cornell University and consultant to the Bell Aerosystems Company. Prof. Bijlaard formulated the techniques employed to obtain solutions for the instability of flat sandwich panels and for the thermal stresses and instability of sandwich cylinders supported by rigid bulkheads. Major contributions to this work were also made by Mrs. Leona Barback, and Miss Penelope Miller of the Bell Electronic Data Processing Department, who coded the computer programs used in development of the design data presented herein.

ABSTRACT

Structural design data are presented for various applied load and thermal gradient conditions for flat rectangular sandwich panels and sandwich cylinders. The flat panel solutions pertain to instability under nonuniform stress, and also to the stresses and displacements resulting from normal pressures and temperature gradients across the panel thickness in the presence of uniform midplane compression.

Sandwich cylinder design data are given for buckling under nonuniform circumferential and axial stress, respectively, and for stresses due to radial or axial temperature gradients. The range of stiffness parameters extend, at one limit, to the isotropic forms of construction.

PUBLICATION REVIEW

This report has been reviewed and is approved.

W.A. SLOAN, JR.
Colonel, USAF
Chief, Structures Division
AF Flight Dynamics Laboratory

TABLE OF CONTENTS

TABLE OF CONTENTS (CONT)

ILLUSTRATIONS

ILLUSTRATIONS (CONT)

ILLUSTRATIONS (CONT)

ILLUSTRATIONS (CONT)

TABLES

LIST OF SYMBOLS

a	panel length, in.
b	panel width, in.
c	cylinder half length, in.
D_c	sandwich cylinder stiffness parameter, $\frac{r^2 D_q}{D_s}$
D_p	sandwich panel stiffness parameter, $\frac{b^2 D_q}{D_s}$
D_p'	D_p / π^2
D_q	sandwich shear stiffness $(h+t)G_c$
D_s	sandwich bending stiffness $\frac{Et\,(h+t)^2}{2(1-\mu^2)}$

} or as specified in reference 3

E	modulus of elasticity, psi
G_c	shear modulus of sandwich core, psi
H_d, H_l, H_x	constants defined by Eqs. V-4, V-5, V-6
h	depth of sandwich core, in.
K	constant, $\frac{2(1-\mu^2)\,r^2}{(h+t)^2}$
M	bending moment per unit width, lb. in/in.
m_1, m_2	constants defined by Eqs. V-2, V-3
N_x	midplane loading in flat sandwich panel, lb/in.
p	surface pressure, psi
S	stress ratio, defined in Chapters II and IV
R	ratio of outer and inner radii of sandwich cylinder, $\frac{r_o}{r_i}$
r	cylinder radius, in.

T	temperature, °F
t	face thickness of sandwich panel, in.
u, v, w	displacements in x, y, z direction respectively
x, y, z	rectangular or cylindrical coordinates
α	coefficient of thermal expansion
β	wavelength parameter defined by Eq E-7
Λ	aspect ratio of finite sandwich panel, a/b
λ,Λ	wavelength parameters
μ	Poisson's ratio
Π	eigen value and critical stress parameter
ρ	stress distribution parameter, defined in Appendix A
σ	stress
η	non-dimensional form of midplane loading, $\frac{N_x}{D_q}$

CHAPTER I

INTRODUCTION

The development of thermal stress determination techniques for supersonic transport aircraft structures has consisted of a threefold effort. First, a survey of the literature pertinent to thermal stress analysis was performed, resulting in publication of an annotated bibliography of the subject for the period 1955-1962 (Reference 1); a bibliography covering thermal stress analysis literature prior to 1955 had been published elsewhere. The second portion of this study effort has been concerned with the development of graphical design data for various applied load and thermal gradient conditions for flat rectangular sandwich panels and sandwich cylinders. This work is presented in the subject report. Finally, computer programs for the more complex problems encountered in beam, plate, and cylindrical constructions were coded with the purpose of making them available to eligible recipients in the airframe industry. A description of these programs is given in Reference 2.

Sandwich panels and cylinders provide attractive constructional forms for large high-performance vehicles and will undoubtedly be given consideration during the developmental phase of the SST airframe. They are extremely efficient from a weight standpoint and can be fabricated using materials suitable for an elevated temperature environment exceeding 1000°F. Sufficient data have been accumulated to permit their design for conventional loadings and uniform temperature conditions (c.f., Reference 3) but design data is lacking for nonuniform temperature conditions. It is the intent of this report to provide such data. In addition, it is to be noted that the design curves to be presented extend, in one limit, to the conventional isotropic thin plate and cylinder constructions.

The design curves are presented in the chapters of this report with a discussion of their basis, use, and limitations and with illustrative examples, but without a detailed description of the related formulations and solution techniques. The latter are given in a series of Appendixes.

Solutions to flat sandwich panel problems are found in Chapters II and III. One of the most important problems in flat plate analysis is the prediction of elastic instability in the presence of nonuniform stress produced by temperature gradients. Hoff[4], Klosner and Forray [5], and van derNeut [6], among others, have presented procedures and isolated results for this problem as it pertains to thin isotropic plates; there are no known solutions for sandwich construction. In Chapter II of this report, curves are presented which allow the prediction of the elastic instability conditions for long honeycomb sandwich panels with equal thickness isotropic skins under nonuniform longitudinal stress, for both fixed and simply supported longitudinal edges.

Manuscript released by authors in July, 1963 for publication as an ASD Technical Documentary Report.

Chapter III is coneerned with the stresses and displacements at the eenter of simply-supported rectangular sandwich panels subjected to temperature gradients through the panel thiekness and to pressure loadings. The presence of fixed uniaxial midplane forees is also taken into aeeount. The graphs eover a wide range of aspect ratios, stiffnesses, and midplane loadings. A limited number of results for eonditions of fixed support along two edges is also presented. Teehniques for solving this type of problem have been published by Bijlaard [7] and Ebeioglu [8]. Referenee 7 eonsiders only the problem of temperature gradients and in neither Referenee 7 nor in Referenee 8 are design eurves presented. The formulation of the governing differential equations for this problem, as deseribed in Appendix B, has not been formally presented elsewhere.

Chapters IV through VII deal with various problems in the analysis of heated sandwieh cylinders. Curves for the prediction of the elastie instability of sandwieh cylinders subjeeted to cireumferentially varying axial stress are found in Chapter IV. Conditions which produee this type of stress distribution inelude both nonuniform eireumferential temperature gradients and also eombinations of bending and axial eompression. Graphical means of determining the stresses due to temperature for this problem have not been eonsidered since the applicable procedures involve the use of either thermoelastie beam theory or the diserete element teehniques of matrix struetural analysis. In neither ease are graphieal solutions feasible.

Published references have not as yet considered the above-cited instability problem. Bijlaard and Gallagher [9] and Abir and Nardo [10] studied the ease of the isotropie eylinder under circumferentially varying axial stress. Both references coneluded that the small defleetion theory maximum stress amplitude for elastie instability under varying stress is effeetively equal to that for uniform compression. This eonelusion is found to be essentially correet in the present ease of sandwich cylinders. Comparisons are made with the results of past studies of the stability of sandwieh eylinders under uniform compression (References 11-13).

Chapters V and VI treat the stress and instability analysis of heated cylinders supported by unheated rigid bulkheads. Fixed and simple support conditions are ineluded. Graphical methods for determining the maximum stresses under such eonditions appear in Chapter V. This class of problem, for isotropic cylinders has been previously dealt with by Hoff [14], Przemienieeki [15], and Johns [16]. Based on the results of Chapter V, a series of elastic instability analyses were performed and from these latter results a set of graphical representations of the data were drawn. These appear in Chapter VI. Results for the limiting case of the isotropic cylinder are compared with solutions given by Hoff [14], Johns [17] and Anderson [18].

The final design data given in this report pertain to the stresses in a sandwich cylinder due to radial temperature gradients. Means for computing the stresses due to either internal or external pressure are also presented. A similar problem, but with different core properties, was treated by Yao [19]. Yao proposes a numerical approach to analysis, based on a method of suceessive approximations. The radial

temperature gradient problem is limited to stress solutions since considerations of general instability are involved.

As noted earlier, all theoretical questions associated with the computation of the data employed in construction of the graphical representations are examined in detail in a series of Appendixes (Appendixes A through E).

CHAPTER II

BUCKLING OF SANDWICH PANELS UNDER NONUNIFORM STRESS

This chapter presents graphical representations with which the elastic instability conditions for honeycomb sandwich panels with equal thickness isotropic skins under nonuniform longitudinal stress can be predicted. The panels are assumed to be "long" (i.e., aspect ratio effects and the significance of the transverse support conditions are excluded) and clamped or simply supported along their longitudinal edges. The conditions of analysis are illustrated in the insert in Figure II-1.

A detailed treatment of the formulations and procedures employed in the derivation of the presented curves is given in Appendix A. The governing differential equation is that which was derived by Reissner in Reference 20; the method employed for its solution was the finite difference approximation technique. A special purpose computational program was coded and utilized in the development of the required data.

It is shown, in Appendix A, that the critical stress is a function of two parameters, a stiffness parameter (D_p) and a parameter defining the stress distribution. The stiffness parameter is given as

$$D_p = b^2 \frac{D_q}{D_s} \tag{II-1}$$

where b is the panel width and D_q and D_s are the core shear stiffness and the panel bending stiffness, respectively. The analyst has at his disposal the choice of a number of formulas for D_q and D_s, dependent upon the details of sandwich panel construction; these choices are developed and discussed in Reference 3, Section 3.1. The simplest and most appropriate formulas for these parameters are

$$D_q = (h + t)\, G_c \tag{II-2}$$

$$D_s = \frac{Et\,(h+t)^2}{2(1-\mu^2)} \tag{II-3}$$

where h is the core depth, G_c is the core modulus of rigidity, t is the thickness of one of the panel faces, and E and μ are the modulus of elasticity and Poisson's ratio of the face material, respectively. These designations of geometry, stiffness, material properties, etc. are applicable to all chapters of this report.

In the strictest sense, the stiffness paratmeter D_p can range from nearly zero to infinity. At infinity the case of the isotropic plate with infinite shear stiffness prevails. This condition is nearly achieved at much lower values and it is

satisfaetory to eonsider the maximum D_p to equal 10^4. At the lower range of D_p it is found that an entirely different mode of instability, wrinkling, is eneountered. This mode is eharaeterized by a zero wavelength buekling condition due to an initial assumption that the individual bending stiffnesses of the faees eould be neglected. It is not the intention of the present analysis to deal with wrinkling. The curves have eonsequently been terminated at $\frac{N_x}{(h+t)G_c} = 1$, whieh is a limit imposed by wrinkling assoeiated with shear instability failure of the eore. Thus, evaluations of the critical stress were performed for a range of D_p values from 10^4 down to values where this shear instability limit appeared.

Only the simplest forms of stress distribution are of general interest and therefore suitable for inclusion in design eharts. The results presented herein were developed for linear and trigonometric-shaped stress distributions. Linear or nearly linear distributions exist on panels in wings sustaining overall nonuniform chordwise temperature gradients and also when the bending stress distribution on a wing cross-seetion departs from the uniformity predicted by elementary theory (as is generally the case). Trigonometric-shaped stress distributions are good approximations to conditions where the panel longitudinal edge members (e.g.. the spar caps) provide signifieant heat sinks, thereby resulting in extreme, loeal, transverse variations of the longitudinal thermal stress. Similar eomments as to applicability could be made for both types of stress distribution for fuselage skin panels.

A linear variation of stress which is equivalent to a uniformly distributed load superimposed upon a bending moment is conveniently deseribed by the ratio (S) of the stress levels at either side of the panel. Using the convention that the denominator is always the larger positive (compressive) value, any purely eompressive load is covered by the range $1 \geq S \geq 0$. This range has been extended into the mixed compressive-tensile region to the value S = -1.0, i.e. pure bending. This range of S from +1.0 to -1.0 has been covered in intervals of 0.25. The selected trigonometric cases are simply sin y, sin 2y, eos y, cos 2y.

Figures II-1 to II-4 present the results in graphieal form. Figures II-1 and II-2 are for the simply supported case while Figures II-3 and II-4 relate to fixed support of the longitudinal edges. It was intended to depict in Figure II-1 the results from Reference 3 for uniform compression (S = 1.0), but due to the excellent level of agreement it is not possible to differentiate between those results and the present solutions for S = 1.0. The eurves are terminated at the lower end by the wrinkling boundary diseussed previously.

Figure II-5 depicts the variation of buckling stress for the isotropic plate subject to linear stress distributions for each boundary condition. These curves have been obtained by considering large values of D_p. Here, the form of the abeissa has been altered slightly to eliminate the shear stiffness of the core (D_q). The new abcissa is thus taken as $\frac{t_i \sigma_{cr} b^2}{D_s}$, where $t_i = 2t$ is the thickness of the isotropic plate.

Illustrative Examples

Example (1) Sandwich Plate with simply supported edges

Width of panel	= 40 in.
Core Thickness	= 0.50 in.
Modulus of faces	= 10^7 lb/in^2
Face Thickness	= 0.036 in.
Shear Modulus of Core	= 2 x 10^4 lb/in.^{2}

The panel is subjected to a triangular compressive load (S = 0). Utilizing the above data and formulas 3.12E and 3.13B from Reference 3, one obtains $D_s = 5.68 \times 10^4$ and $D_q = 1.0 \times 10^4$. From this paper, $D_p = \frac{D_q b^2}{D_s} = 282$. From figure II-1, for S = 0 at $D_p = 282$, the buekling load parameter $\frac{2t}{D_q}\sigma_{er}$ is found to be 0.257. Henee,

$$\sigma_{cr} = \frac{0.257\ D_q}{2t} = 35700 \text{ lb/in}^2$$

Total applied load = $2t\ \sigma_{cr}\frac{b}{2} = 51400$ lb.

Example (2) Isotropic Plate with simply supported edges

Width of panel	= 40 in.
Modulus of panel	= 10^7 lb/in^2
Thickness	= 0.388 in.
Thus D_s	= 5.343 x 10^4

This panel is also subjected to a triangular eompression (S = 0). From Figure II-5 at S = 0, $\frac{t_i b^2}{D_s}\ \sigma_{cr} = 77.05$

$$\text{Thus } \sigma_{cr} = \frac{77.05\ D_s}{t_i b^2} = 6625 \text{ lb/in.}^2$$

Here again total applied load = $t_i\ \sigma_{cr}\frac{b}{2} = 51400$ lb. Thus, the two panels carry the same loading but, as can be seen, the sandwich panel has a considerable advantage over the isotropic plate on a weight basis.

The few published solutions for buckling of long panels under nonuniform loading are entirely restricted to the case of isotropic plates. Timoshenko (21) has considered an isotropic plate with a linearly varying stress. The parameter used by Timoshenko is the factor k in the expression.

$$\sigma_{cr} = k\ \frac{\pi^2 D_s}{b^2 t}$$

Using this parameter the following comparison is obtained

S	k	
	Timoshenko	Present Report
+1.0	4.00	3.98
0	7.81	7.79
-0.5	13.40	13.35
-1.0	23.90	23.63

Hoff [4] has considered a trigonometric distribution of load, corresponding to the cos 2y case of the present paper. The value obtained by Hoff, k = 7.67, shows good agreement with the present work where k = 7.68.

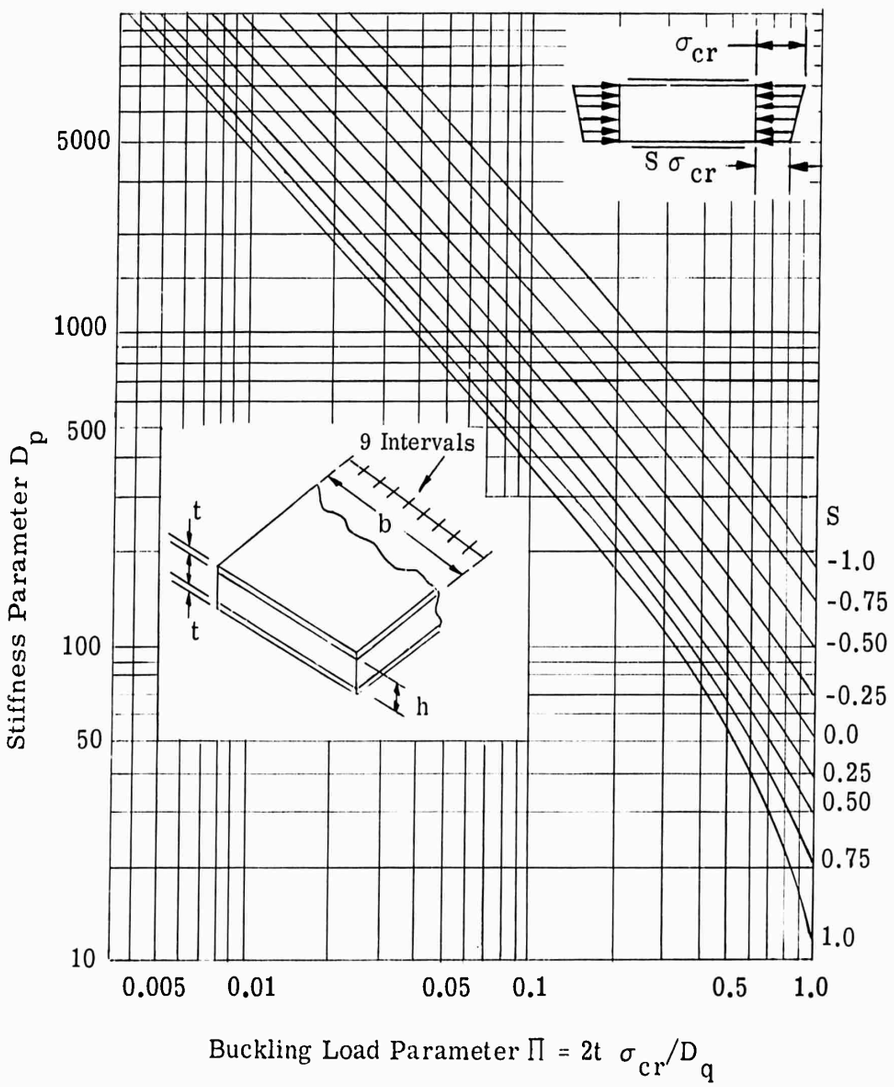

Figure II-1. Buckling Load of a Long Sandwich Panel Subjected to Linearly Varying Edge Stress (Long Edges Simply Supported)

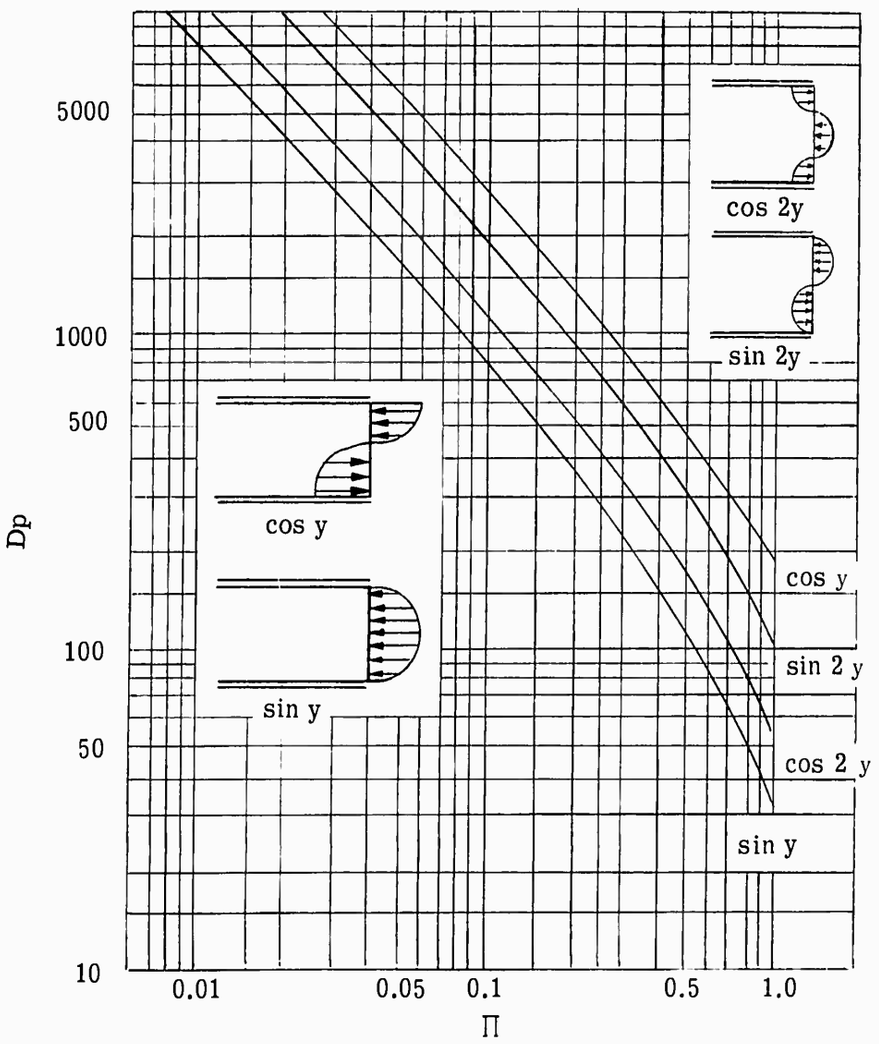

Figure II-2. Buckling Load of a Long Sandwich Panel Subjected to Trigonometric Edge Stresses (Long Edges Simply Supported)

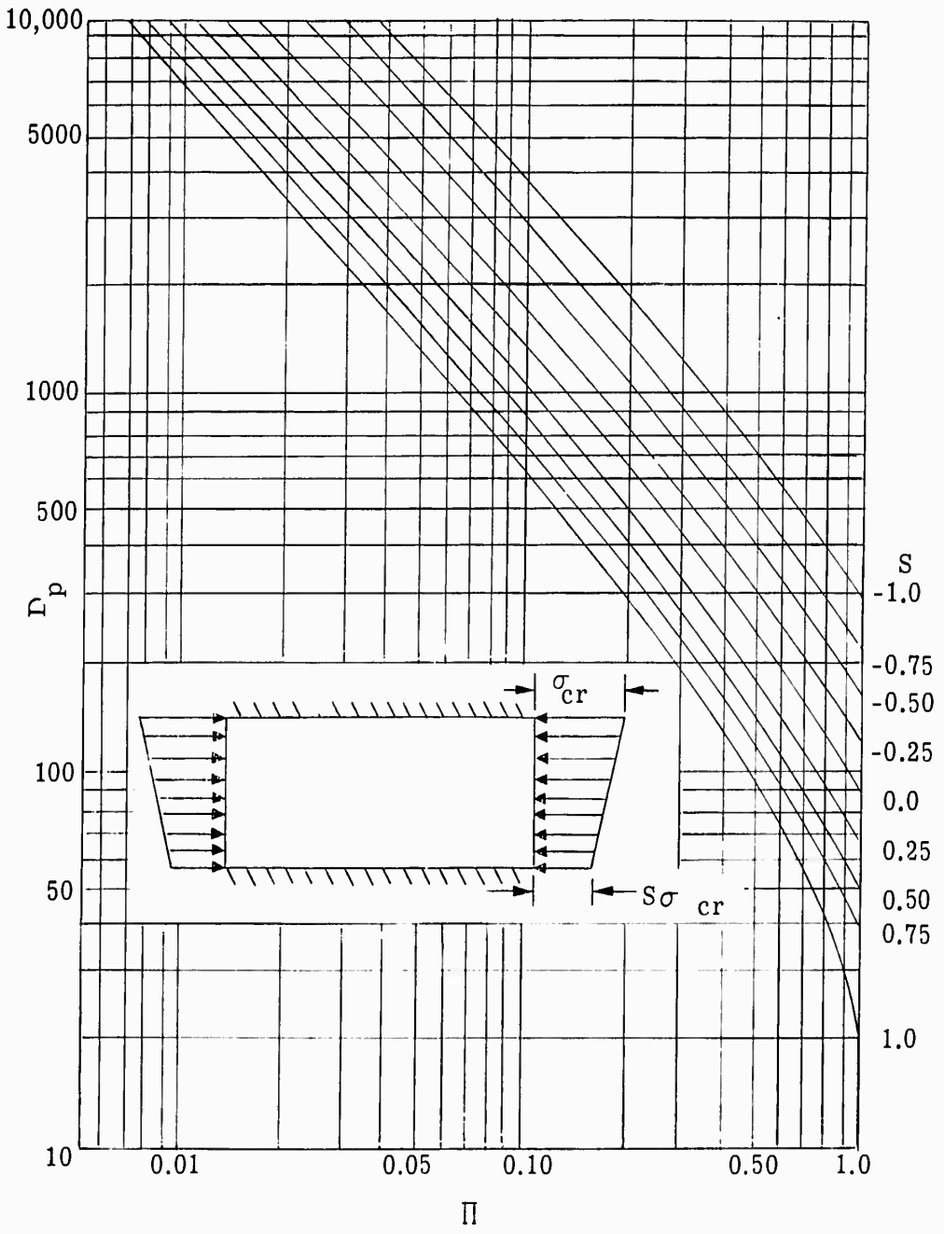

Figure II-3. Buckling Load of a Long Sandwich Panel Subjected to Linearly Varying Edge Stress (Long Edges Fully Fixed)

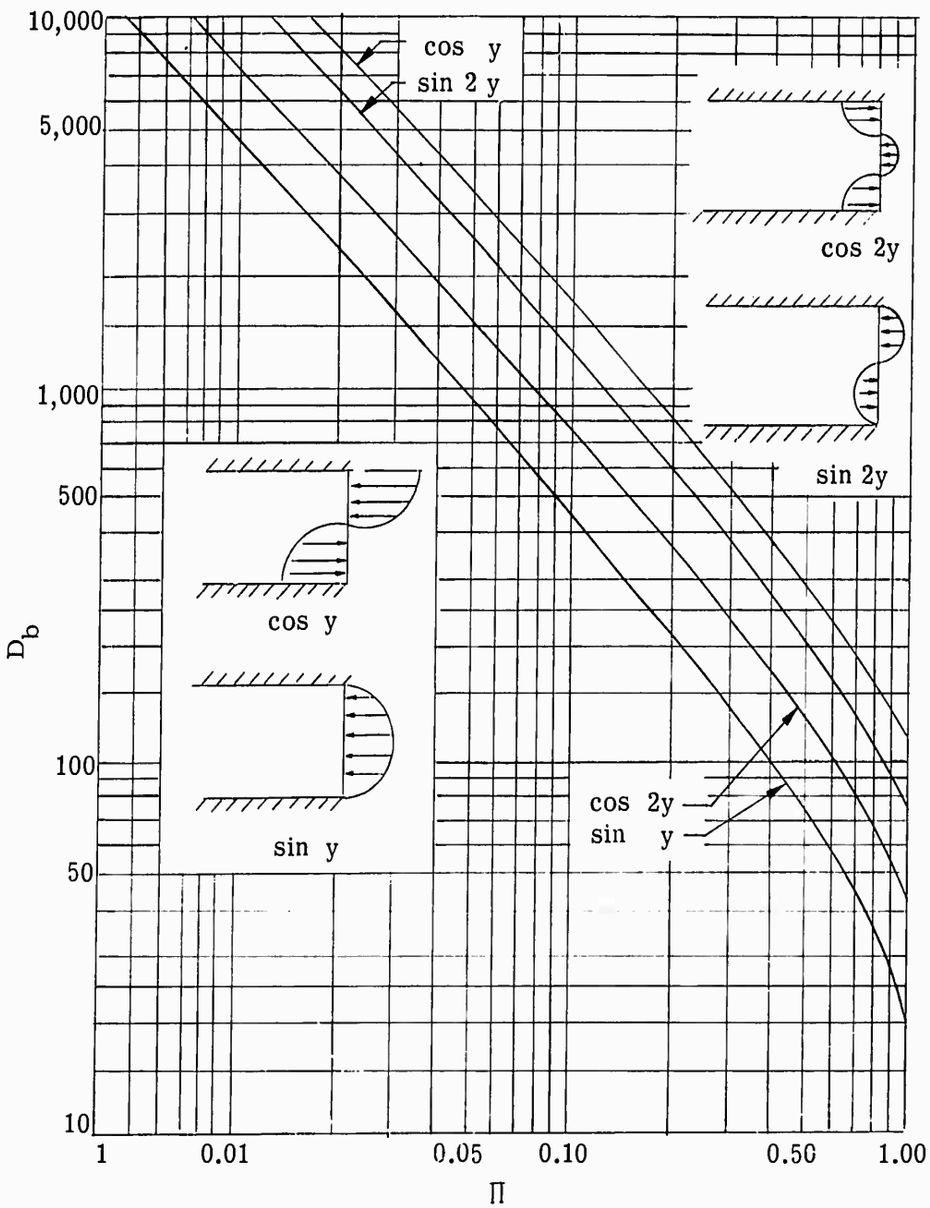

Figure II-4. Buckling Load of a Long Sandwich Panel Subjected to Trigonometric Edge Stresses (Long Edges Fully Fixed)

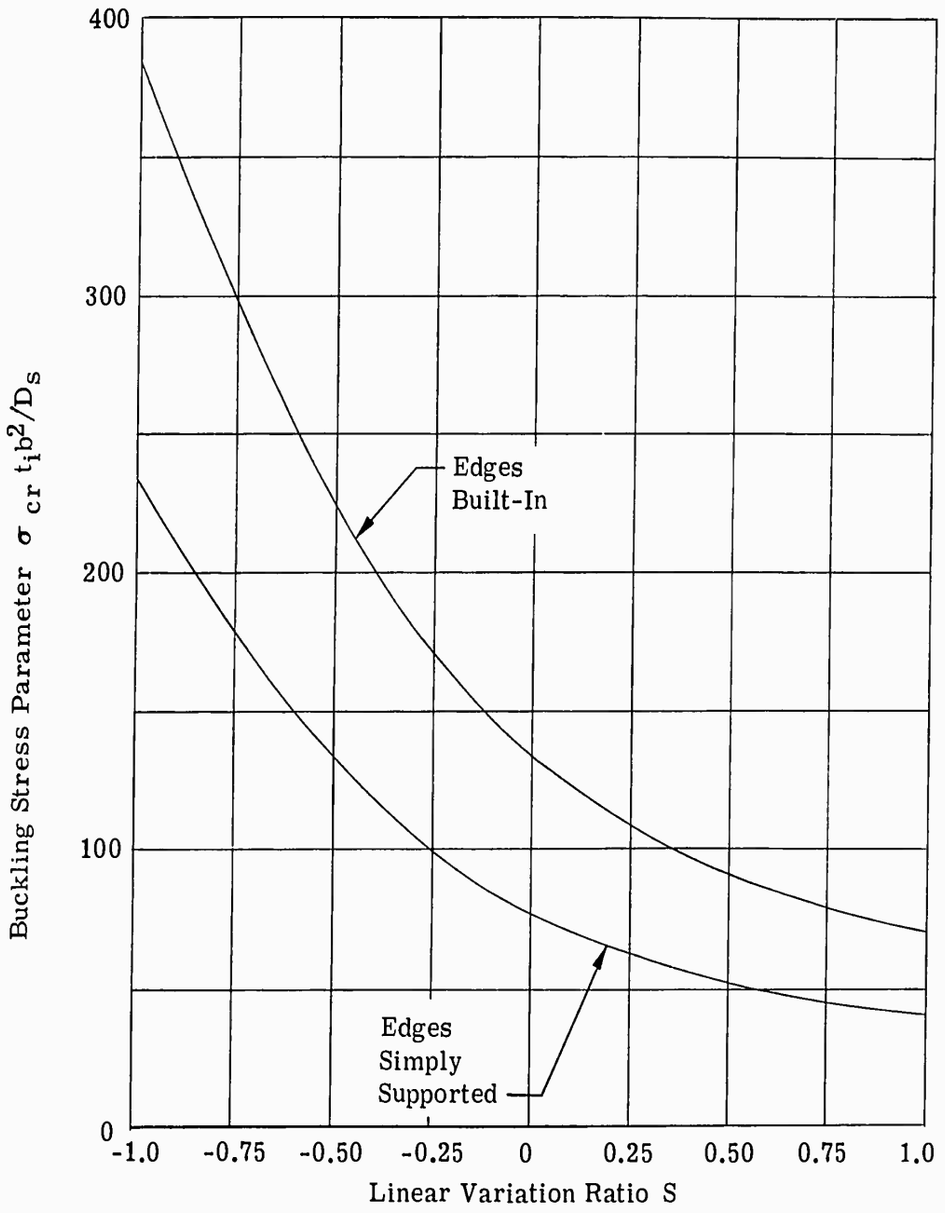

Figure II-5. Buckling Stress for Isotropic Plates Subject to Linearly Varying Compressive Loading

CHAPTER III

PROCEDURE FOR DETERMINING THE STRESSES AND DISPLACEMENTS FOR A RECTANGULAR SANDWICH PANEL

Design curves are presented in this chapter which permit the determination of the central deflection and maximum bending moments in a rectangular sandwich plate subjected to a uniform normal pressure and uniform temperature gradient through its thickness combined with an unaxial in-plane compression N_x. All edges of the panel are simply supported. In addition a limited number of curves is presented for the case of two opposing edges fully built-in and two edges simply supported. The sandwich panel consists of two isotropic faces of equal thickness t(Fig. III-1) and a core of thickness h. The core has the usual properties of zero in-plane stiffness and uniform transverse shear stiffnesses with a shear modulus G_c.

The type of loading combination considered here, consisting of mechanical and thermal loading, can occur, for example, in a wing panel of a high speed aircraft subjected to kinetic heating effects and cooled by the presence of fuel stored in integral tanks. The values of the mechanical and thermal loadings are assumed to have been determined from a general structural analysis.

The governing small deflection theory differential equations for a sandwich panel subjected to thermal as well as mechanical loading have been presented by Bijlaard[7] and Ebcioglu[8] but in neither paper design curves are presented. In Reference 22 a new formulation of the differential equations is developed and the equations are solved for a number of boundary conditions. An outline of the method of solution is given in Appendix B. The solution which involves the use of infinite Fourier series has been programmed in FORTRAN for evaluation on an IBM 7090 computer.

As in Chapter II the stiffness of the sandwich panel is described by single parameter

$$D_p' = \frac{D_p}{\pi^2} = \frac{b^2 D_q}{\pi^2 D_s}$$

In addition, however, since panels of finite proportions are now being considered, the aspect ratio

$$\Lambda = \frac{a}{b}$$

must also be introduced. Although both D_p' and Λ may both vary over very large ranges theoretically, practical considerations provide limitations, so that only values of D_p' between 1 and 100 and Λ between 0.4 and 2.5 have been considered.

Since there are three independent parameters, stiffness, aspect ratio and mid-plane loading, it is not possible to present all variations simultaneously on one graph. Thus Figures III-1 to III-4 present the variation of the maximum deflection per unit temperature gradient for four values of the mid-plane loading with all edges simply supported. Similarly Figures III-5 to III-8 show curves of the maximum deflection per unit normal pressure for the same four mid-plane loadings with all edges simply supported. Figures III-9 to III-16 depict the central bending moments per unit temperature difference or unit pressure for the four mid-plane loadings with all edges simply supported.

In Figures III-17 and III-18 the central deflections per unit temperature gradient and per unit normal pressure are plotted against the mid-plane loading for a panel having a stiffness $D_p' = 100$ (i.e. an equivalent isotropic plate). For values of the aspect ratio up to unity the buckled shape of such a plate consists of a single half-wave in each direction and thus buckling is represented by the maximum deflection increasing smoothly to infinity. On the other hand, for $a/b \geq 1.5$ the buckled shape has two or more half waves in the longitudinal direction and therefore does not conform to the deflection form generated by the thermal or normal loading. The curves for $a/b = 1.5$, 2.0 and 2.5 have been terminated at the true values of the critical stress as given by Timoshenko for an isotropic plate. At these values the buckling will be characterized by a sudden change in deflected shape of the panel. Similar curves may be generated by suitable cross plotting for other values of D_p'.

Figures III-19 to III-22 show central deflections and bending moments similar to Figures III-1, III-5, III-9 and III-13, but with two opposing edges fully built-in and two edges simply supported. The bending moments at the center of the built-in edge are given in Figure III-23.

Illustrative Examples

(1) A rectangular sandwich panel 20 in. by 30 in. is simply supported along each of its edges and is subjected to a uniform normal pressure of 1 psi. The dimensions of the sandwich are as follows:

Core thickness = 0.50 in.	$E = 10.5 \times 10^6$ psi
Face thickness = 0.020 in.	$G_c = 6.65 \times 10^4$ psi

Using the above data $D_s = 3.15 \times 10^4$ and $D_p' = 44.5$. By interpolation on Figure III-5 for $D_p' = 44.5$ and $\Lambda^s = 1.5$

$$\frac{w_{max}\ \pi^4 D_s}{pb^4} = 0.77$$

Hence maximum deflection $w_{max} = 0.0401$ in.

In Reference 23 a sandwich having the above dimensions has been subjected to normal pressure. The maximum deflection measured on this specimen was 0.0384 in., compared with a predicted maximum deflection, using the theory of Reference 23, of 0.0446 in.

(2) A rectangular sandwich panel 24 in. by 36 in. is simply supported along each edge and is subjected to a uniaxial compression of 1500 lb/in. The panel also carries a normal pressure of 10 psi acting downwards. The lower face is heated so that there is a constant temperature difference of 200°F between the lower and upper faces. It is required to find the maximum deflection at the center of the panel and also the maximum bending moments.

Core thickness = 0.97 in. $\quad E = 10.5 \times 10^6$ psi
Face thickness = 0.03 in. $\quad G = 3 \times 10^4$ psi
$\alpha = 1.2 \times 10^{-5} / °F$

Using the above dimensions $D_s = 1.73 \times 10^5, D_q = 3 \times 10^4, \Lambda = 1.5$

Thus $D_p' = 10.0$ and $\eta_x = \frac{N_x}{D_q} = -0.05$

From Figure III-2 for these values of D_p' and

$$\frac{w_{max_T} \pi^2 h}{b^2 (1+\mu) T} = 1.135$$

$$w_{max_T} = 0.2067 \text{ in. (downwards)}$$

From Figure III-6

$$\frac{w_{max_p} \pi^4 D_s}{Pb^4} = 0.97$$

$$w_{max_p} = 0.1910 \text{ (downwards)}$$

Total maximum deflection = 0.2067 + 0.1910 = 0.3977 in.

In a similar fashion using Figures III-10 and III-14 the maximum bending moments are found to be

$$M_x = M_{xp} + M_{xt} = 294.14 - 250.45 = 43.69 \text{ lb. in.}$$
$$M_y = M_{yp} + M_{yt} = 535.75 - 16.19 = 519.56 \text{ lb. in.}$$

These bending moments yield direct stresses in the facings $\sigma_x = \pm 1262$ psi and $\sigma_y = \pm 15015$ psi. In addition the compressive load N_x causes a compressive stress

$\sigma_x = 25000$ psi

i.e. σ_x total = 26262 psi.

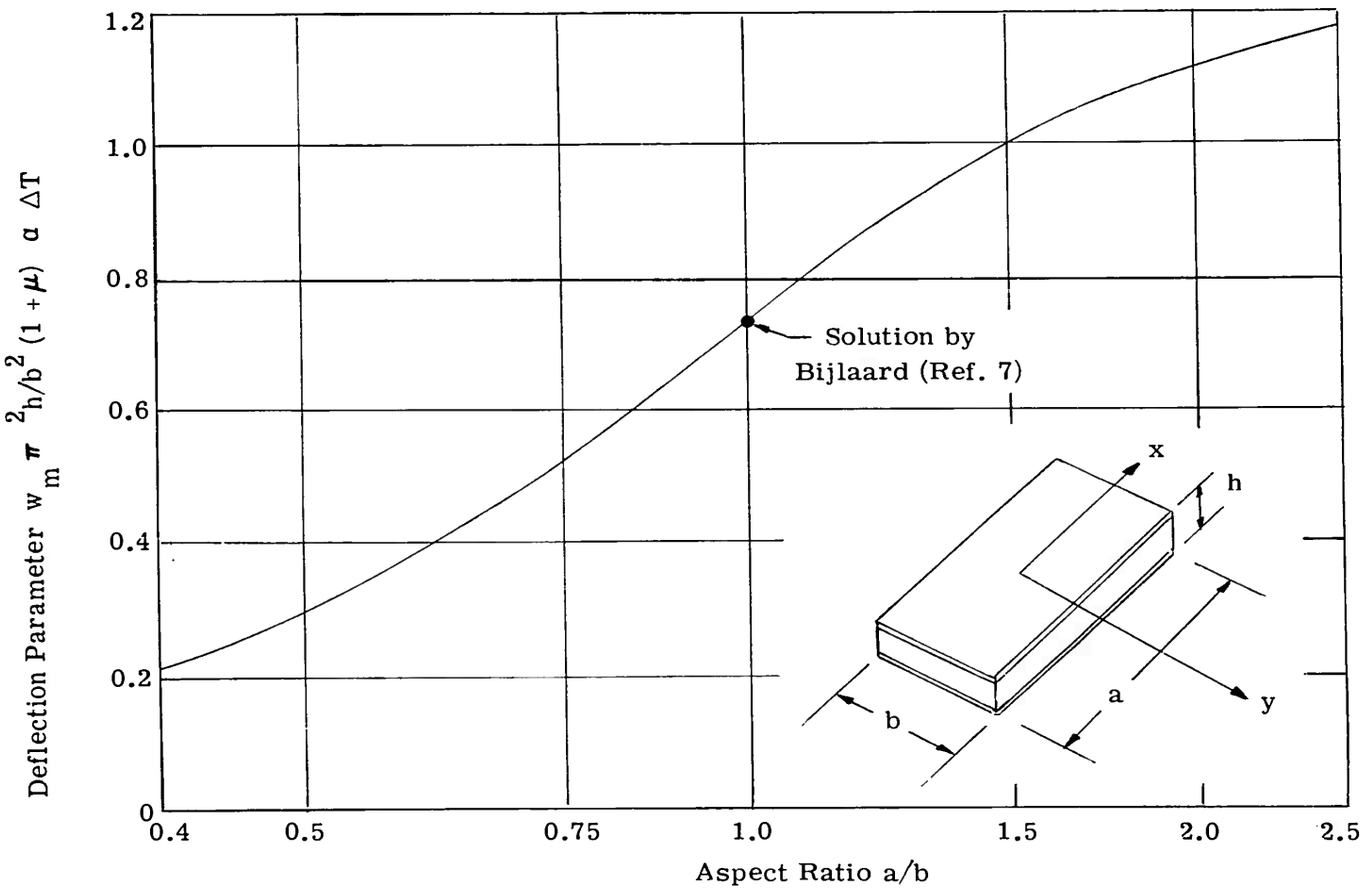

Figure III-1. Maximum Deflection (W_m) of a Rectangular Sandwich Panel Due to a Temperature Difference (Δ T) Between the Faces and Subjected to a Compression $\eta_x = 0.0$. All Edges Simply Supported

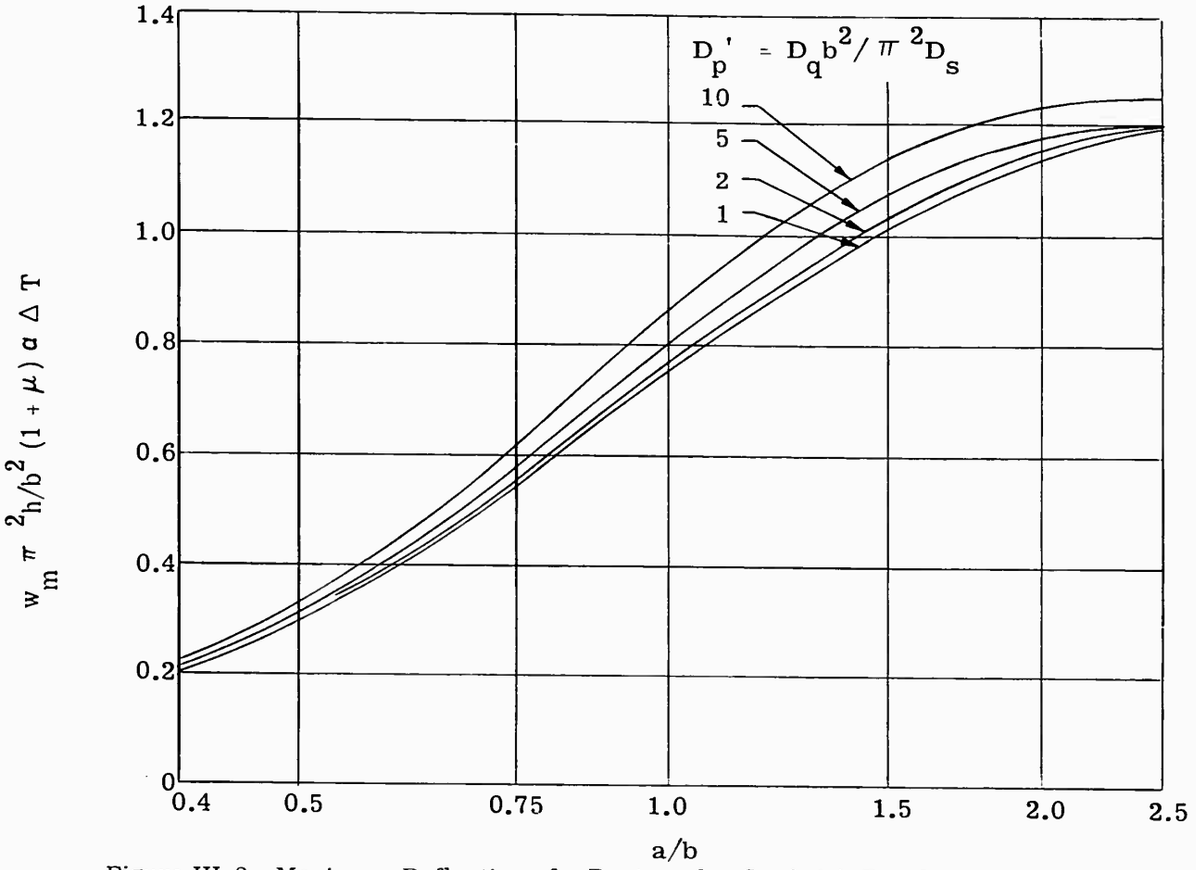

Figure III-2. Maximum Deflection of a Rectangular Sandwich Panel Due to a Temperature Difference (Δ T) Between the Faces and Subjected to a Compression $\eta_x = -0.05$ All Edges Simply Supported

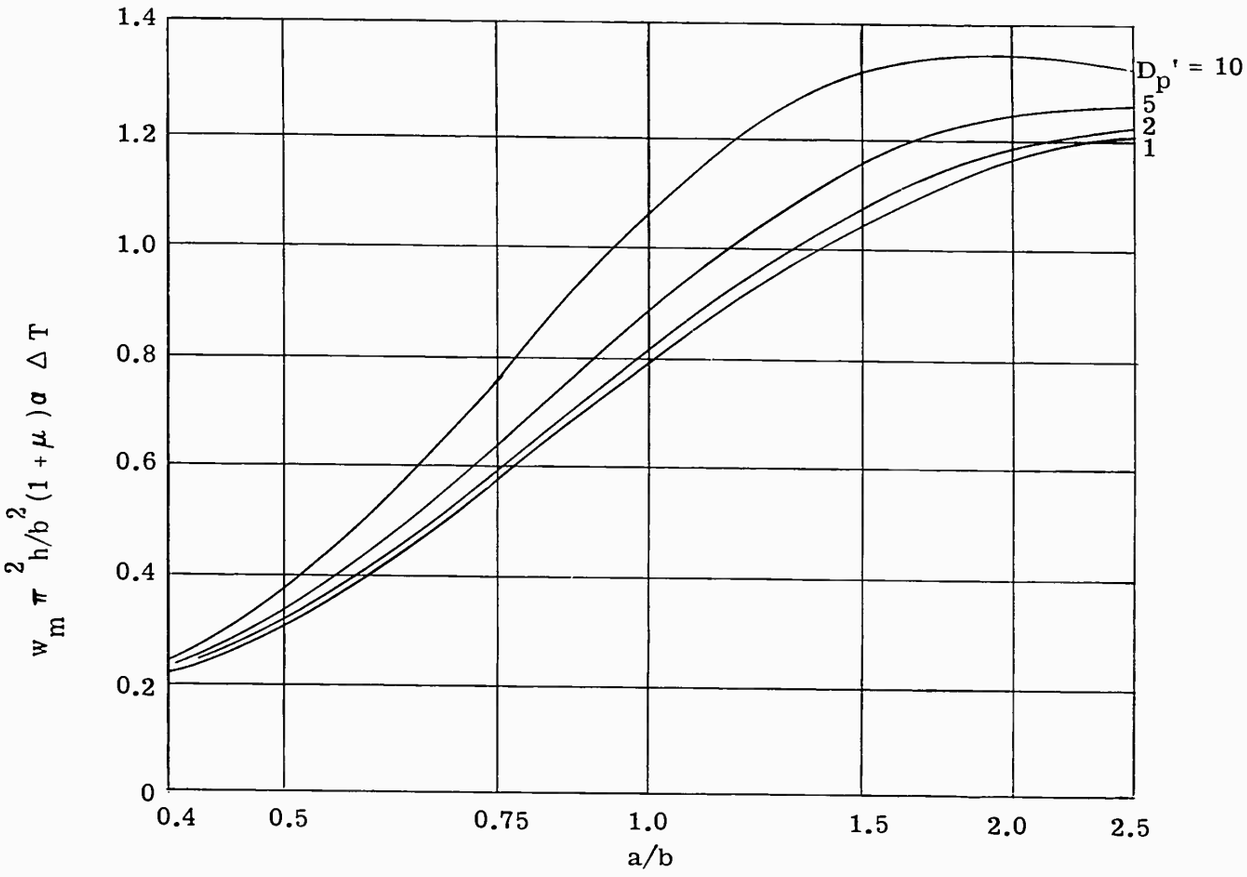

Figure III-3. Maximum Deflection of a Rectangular Sandwich Panel Due to a Temperature Difference (Δ T) Between the Faces and Subjected to a Compression $\eta_x = -0.10$ All Edges Simply Supported

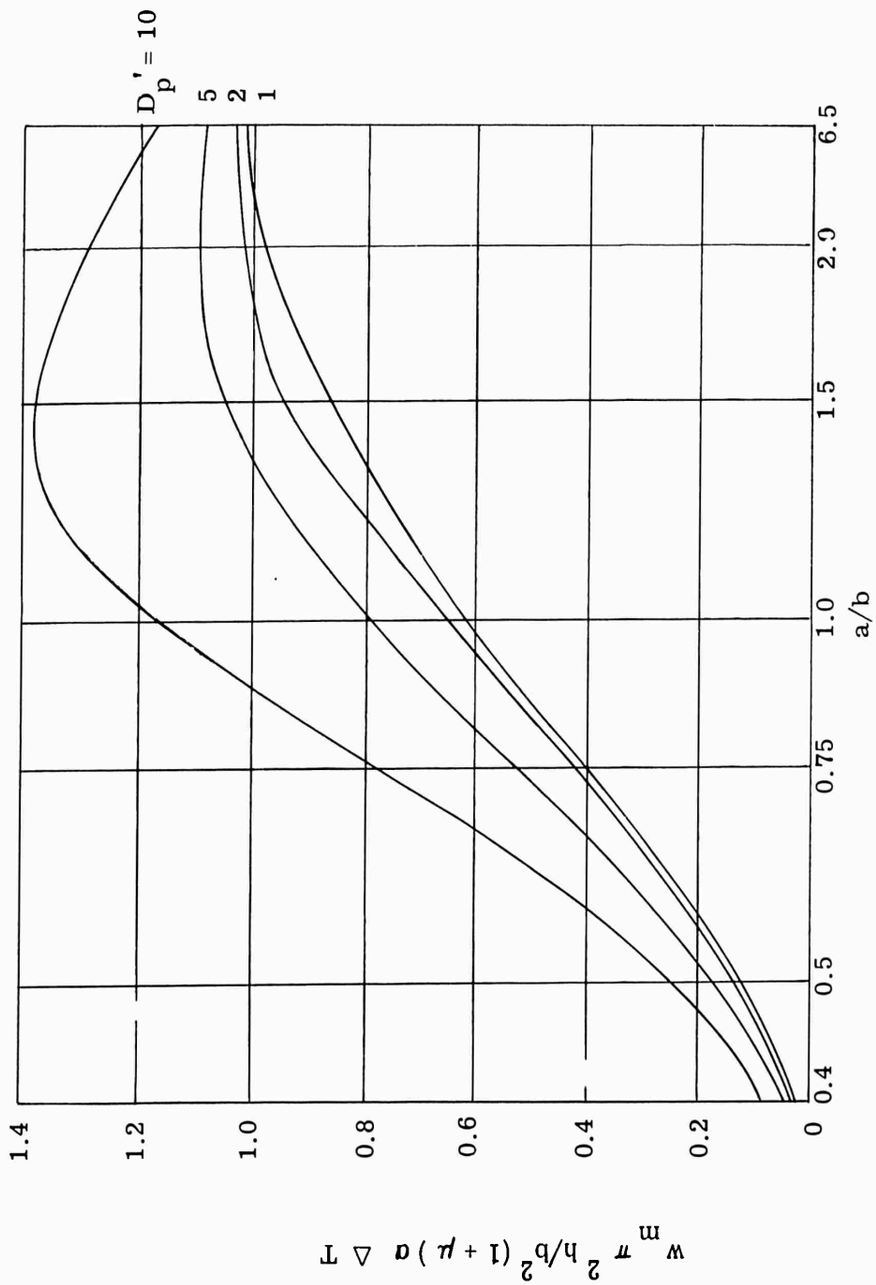

Figure III-4. Maximum Deflection of a Rectangular Sandwich Panel Due to a Temperature Difference (ΔT) Between the Faces and Subjected to a Compression $\eta_x = -0.15$ All Edges Simply Supported

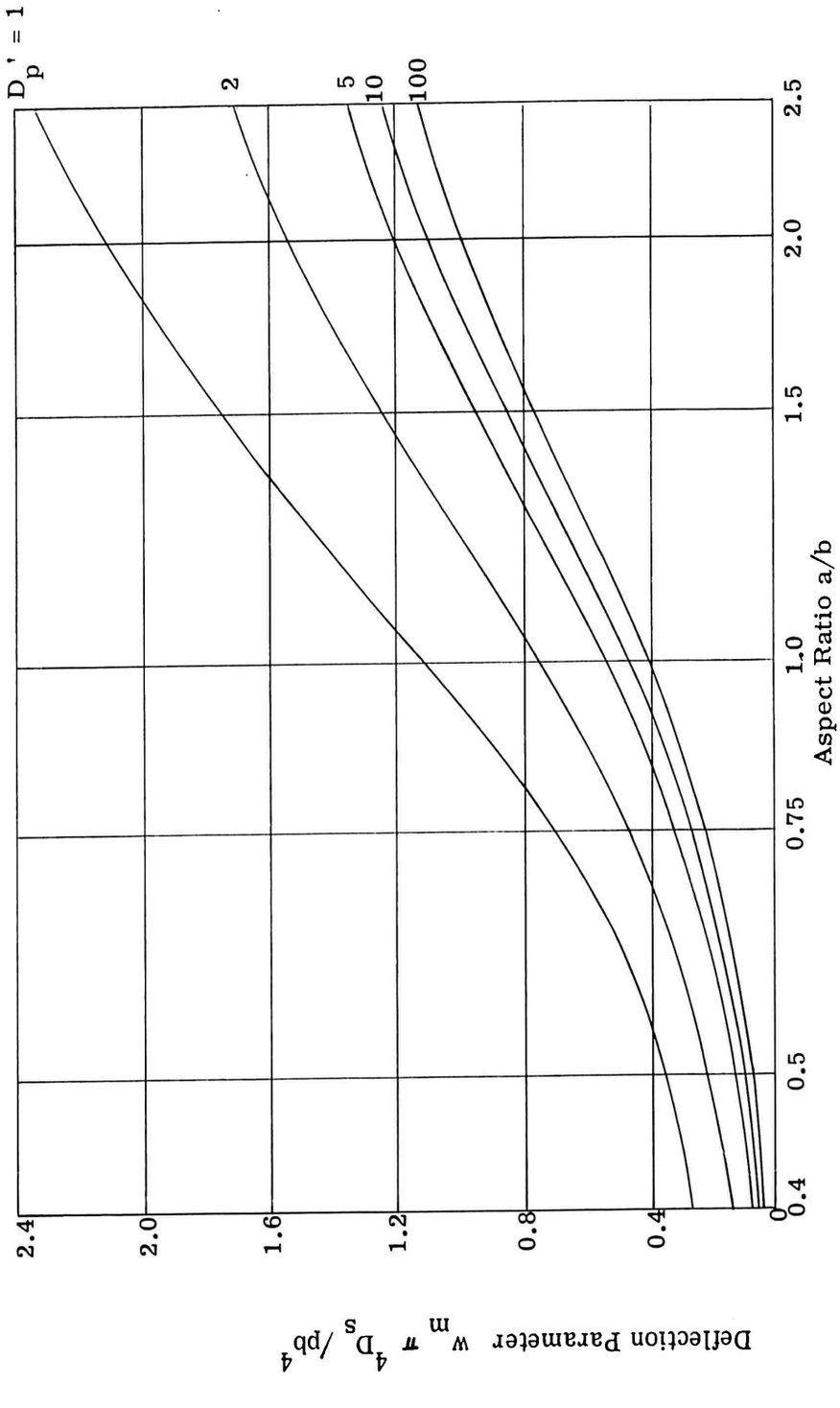

Figure III-5. Maximum Deflection (W_m) of a Rectangular Sandwich Panel Due to a Uniform Normal Pressure(p) and Subjected to a Compression $\eta_x = 0.0$ All Edges Simply Supported

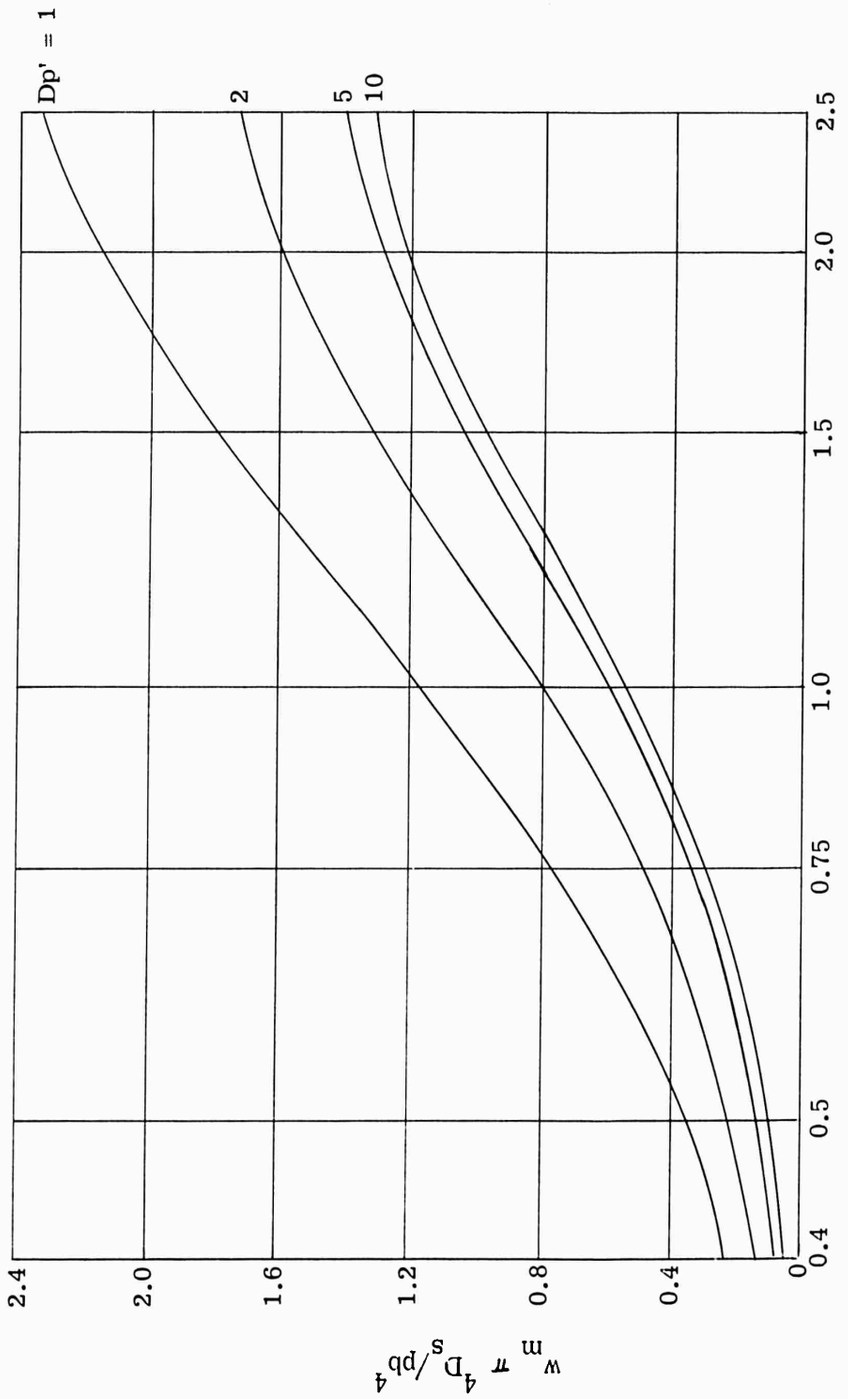

Figure III-6. Maximum Deflection (W_m) of a Rectangular Sandwich Panel Due to a Uniform Normal Pressure (p) and Subjected to a Compression $\eta_x = -0.05$. All Edges Simply Supported

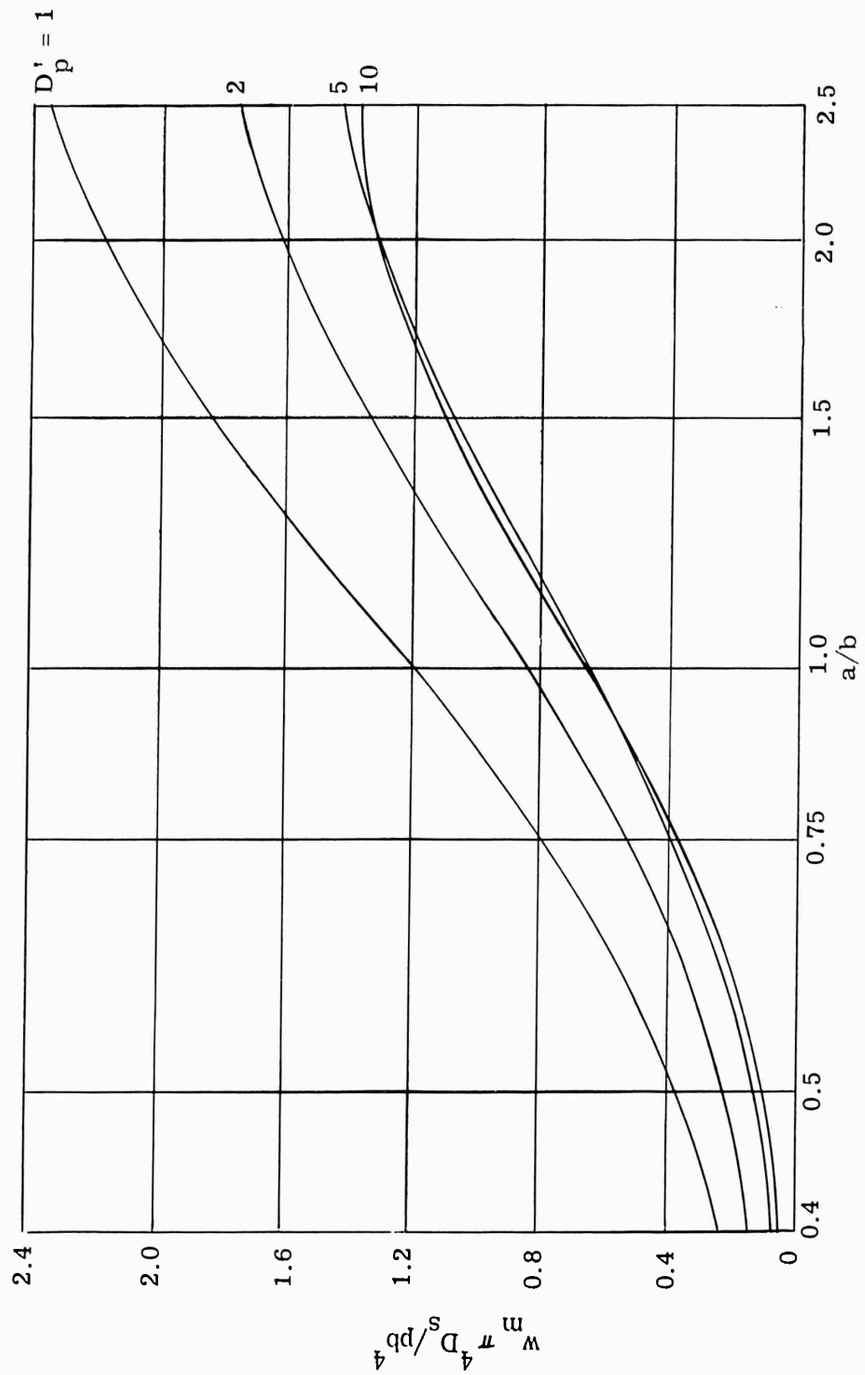

Figure III-7. Maximum Deflection (W_m) of a Rectangular Sandwich Panel Due to a Uniform Normal Pressure (p) and Subjected to a Compression $\eta_x = -0.10$. All Edges Simply Supported

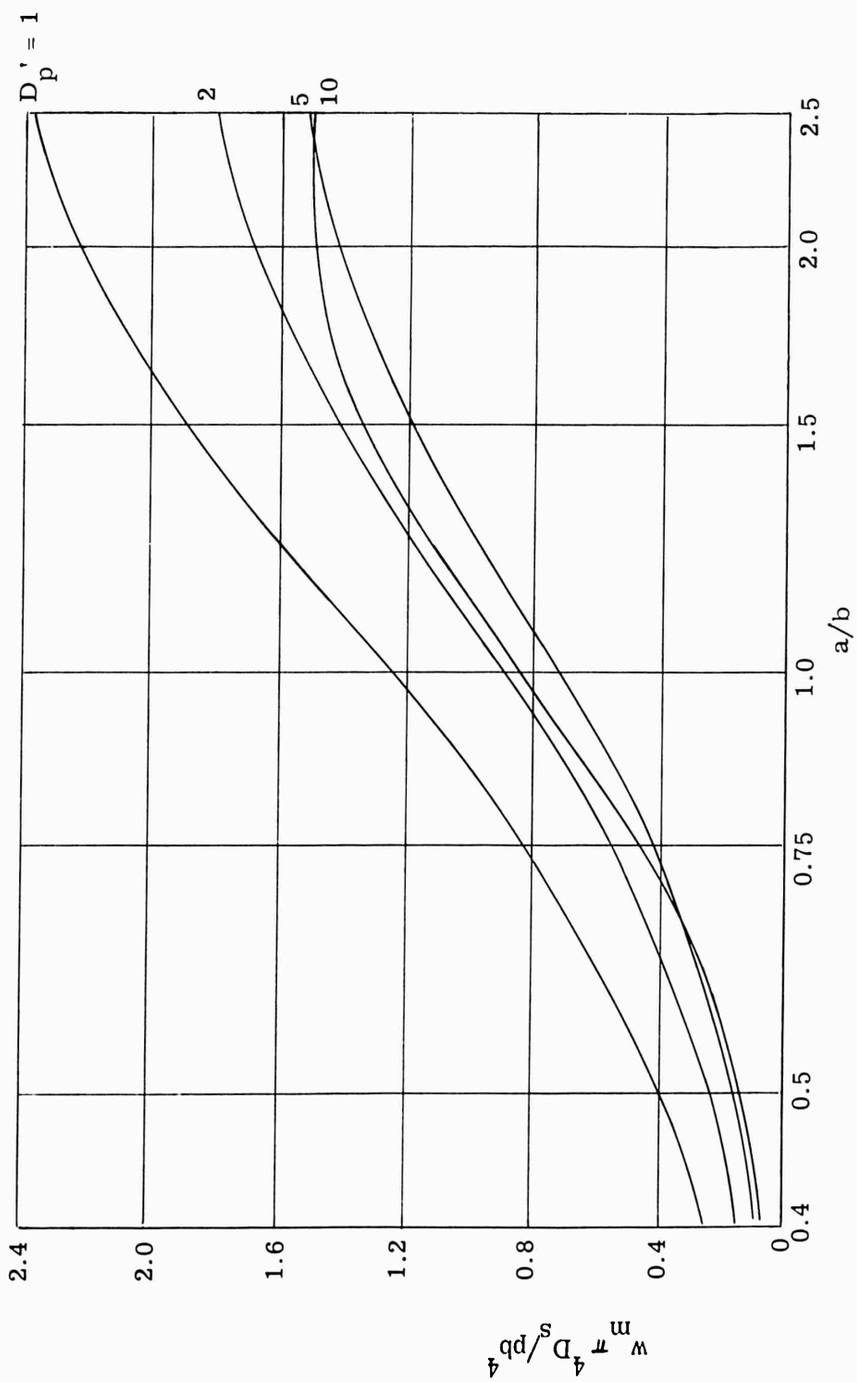

Figure III-8. Maximum Deflection (W_m) of a Rectangular Sandwich Panel Due to a Uniform Normal Pressure (p) and Subjected to a Compression $\eta_x = -0.15$. All Edges Simply Supported

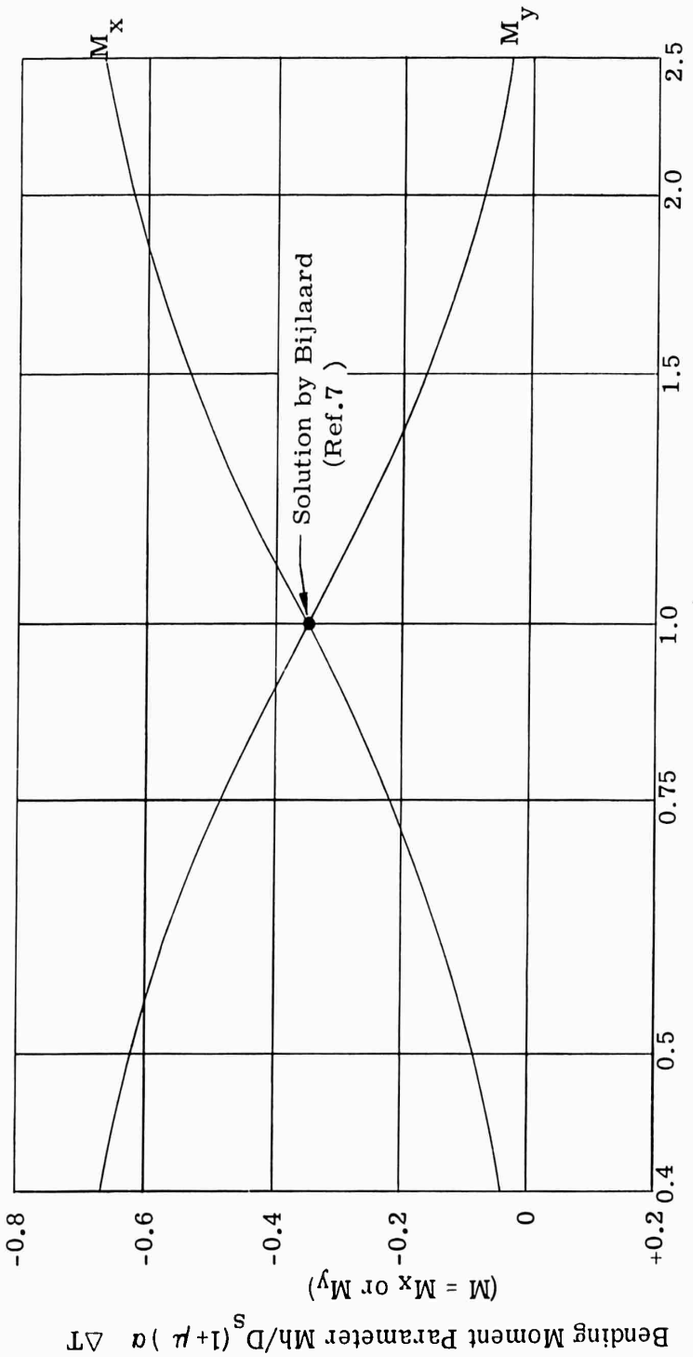

Figure III-9. Maximum Bending Moment In a Rectangular Sandwich Panel Due to a Temperature Difference (Δ T) Between the Faces and Subjected to a Compression $\eta_x = 0.0$. All Edges Simply Supported

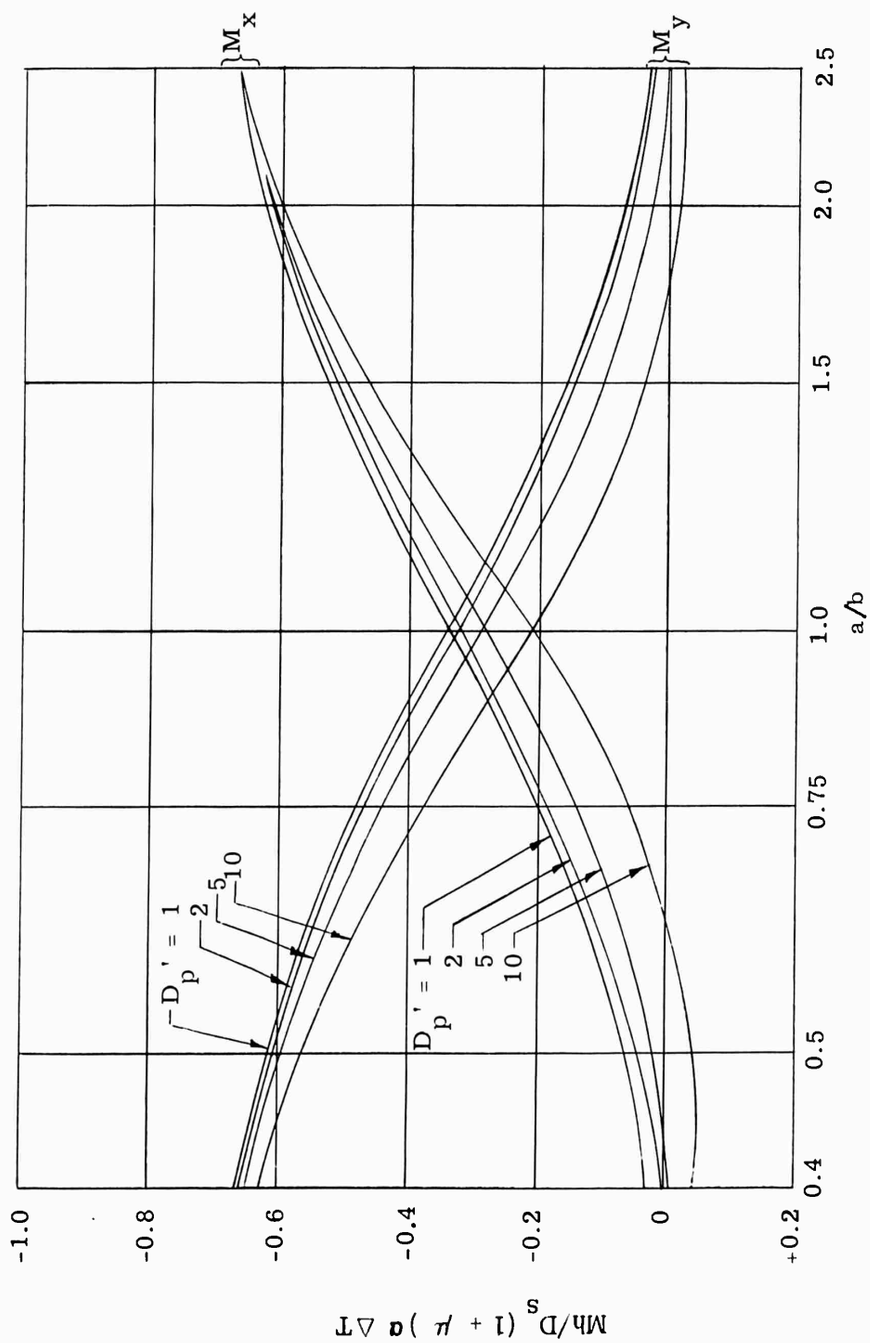

Figure III-10. Maximum Bending Moment In a Rectangular Sandwich Panel Due to a Temperature Difference (ΔT) Between the Faces and Subjected to a Compression $\eta_x = -0.05$
All Edges Simply Supported

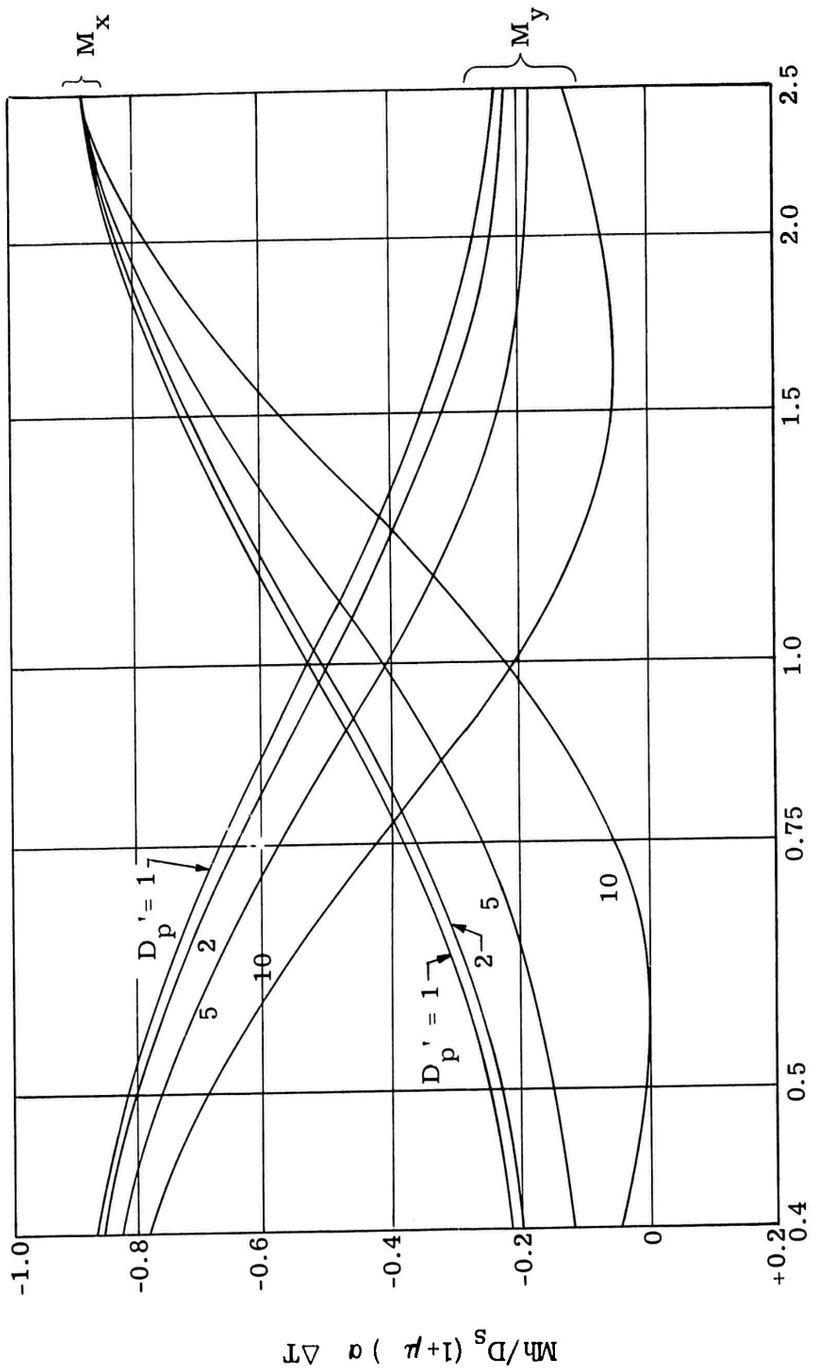

Figure III-11. Maximum Bending Moment in a Rectangular Sandwich Panel Due to a Temperature Difference (Δ T) Between the Faces and Subjected to a Compression $\eta_x = -0.10$. All Edges Simply Supported

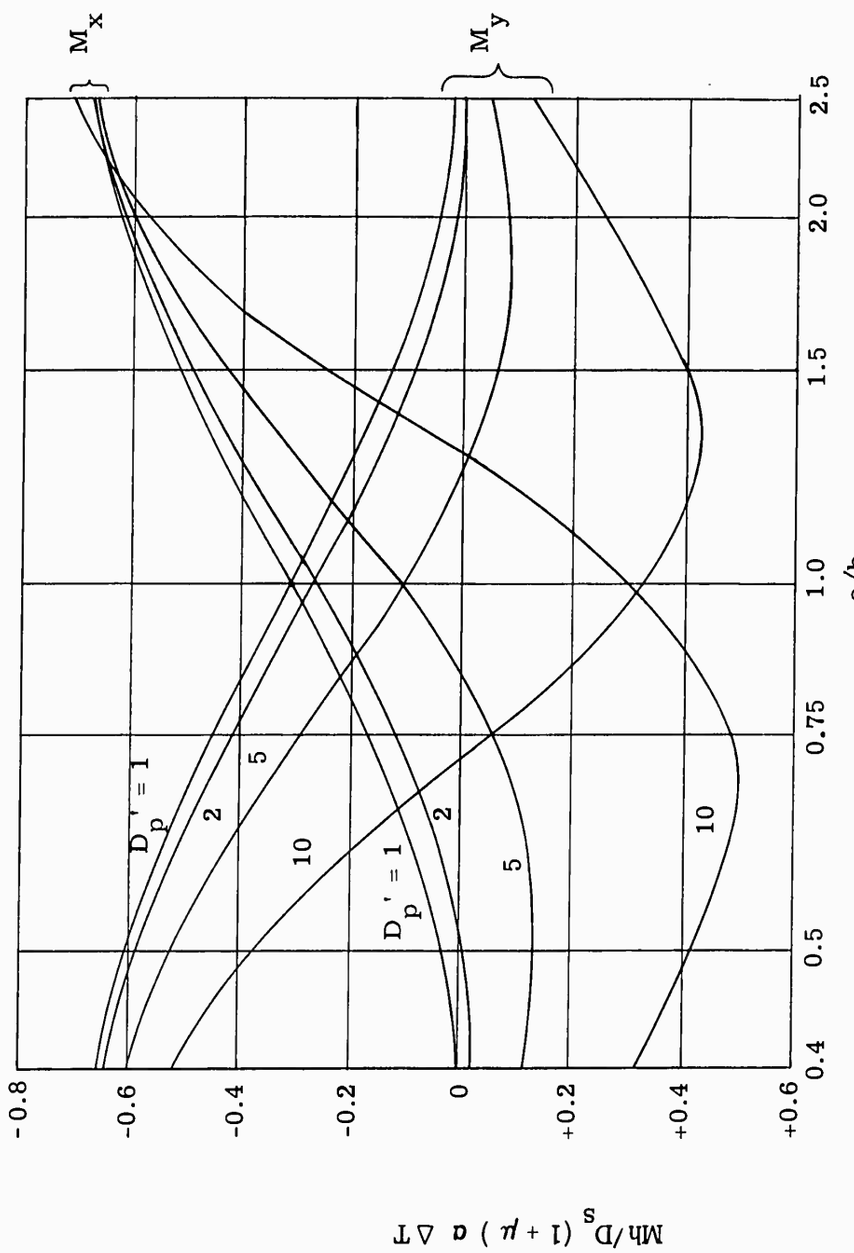

Figure III-12. Maximum Bending Moment in a Rectangular Sandwich Panel Due to a Temperature Difference (Δ T) Between the Faces and Subjected to a Compression $\eta_x = -0.15$. All Edges Simply Supported

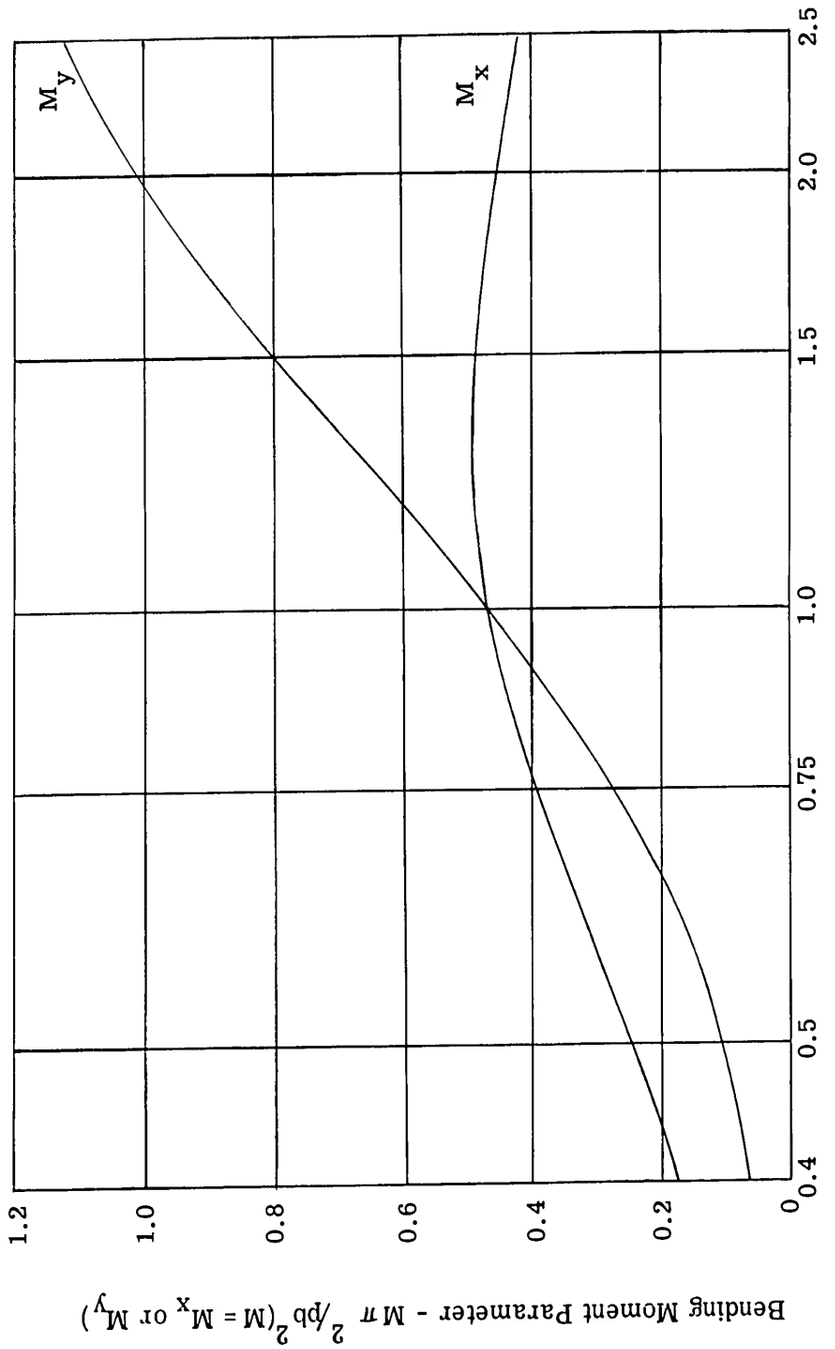

Figure III-13. Maximum Bending Moment in a Rectangular Sandwich Panel Due to a Uniform Normal Pressure (p) and Subjected to a Compression $\eta_x = 0.0$. All Edges Simply Supported

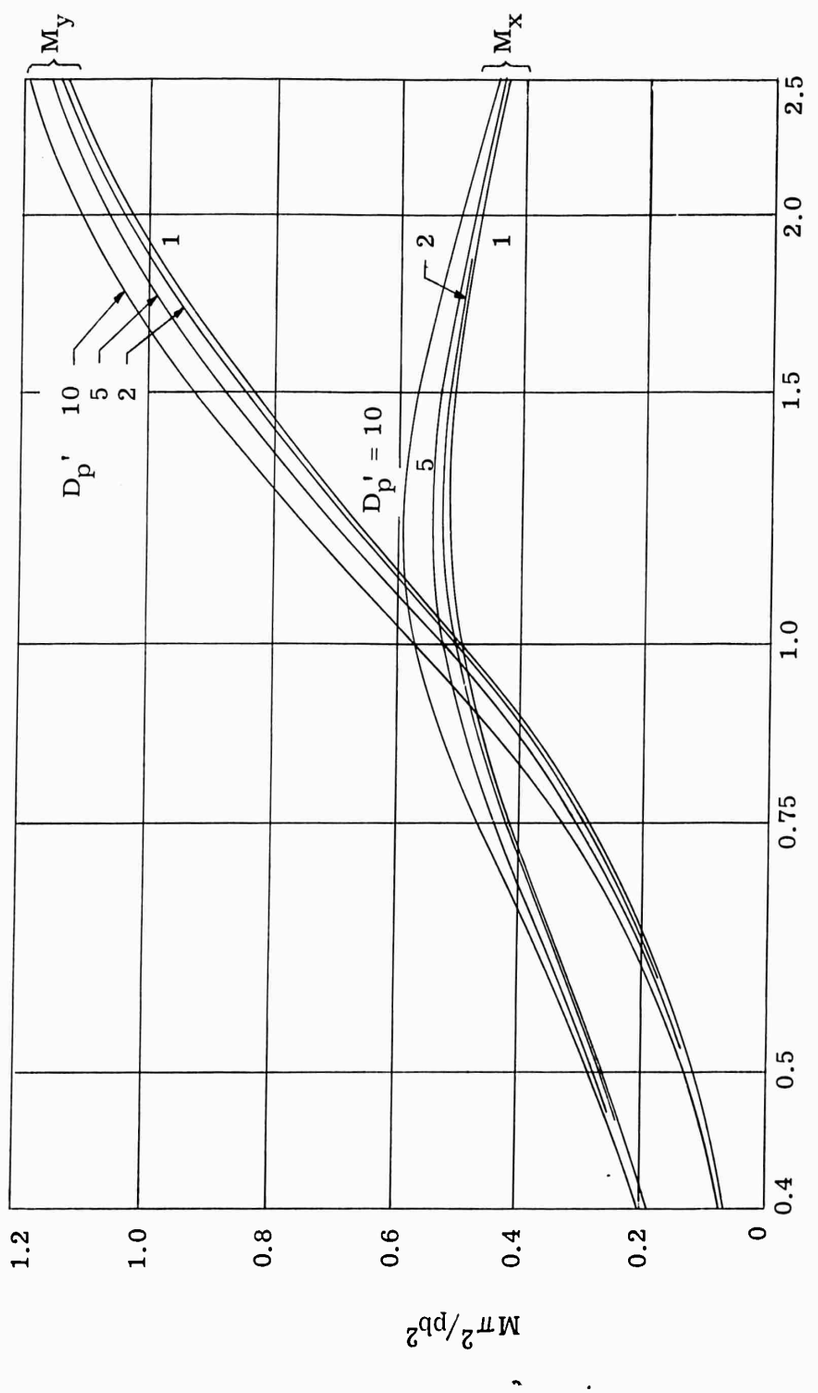

Figure III-14. Maximum Bending Moment in a Rectangular Sandwich Panel Due to a Uniform Normal Pressure (p) and Subjected to a Compression $\eta_x = -0.05$. All Edges Simply Supported

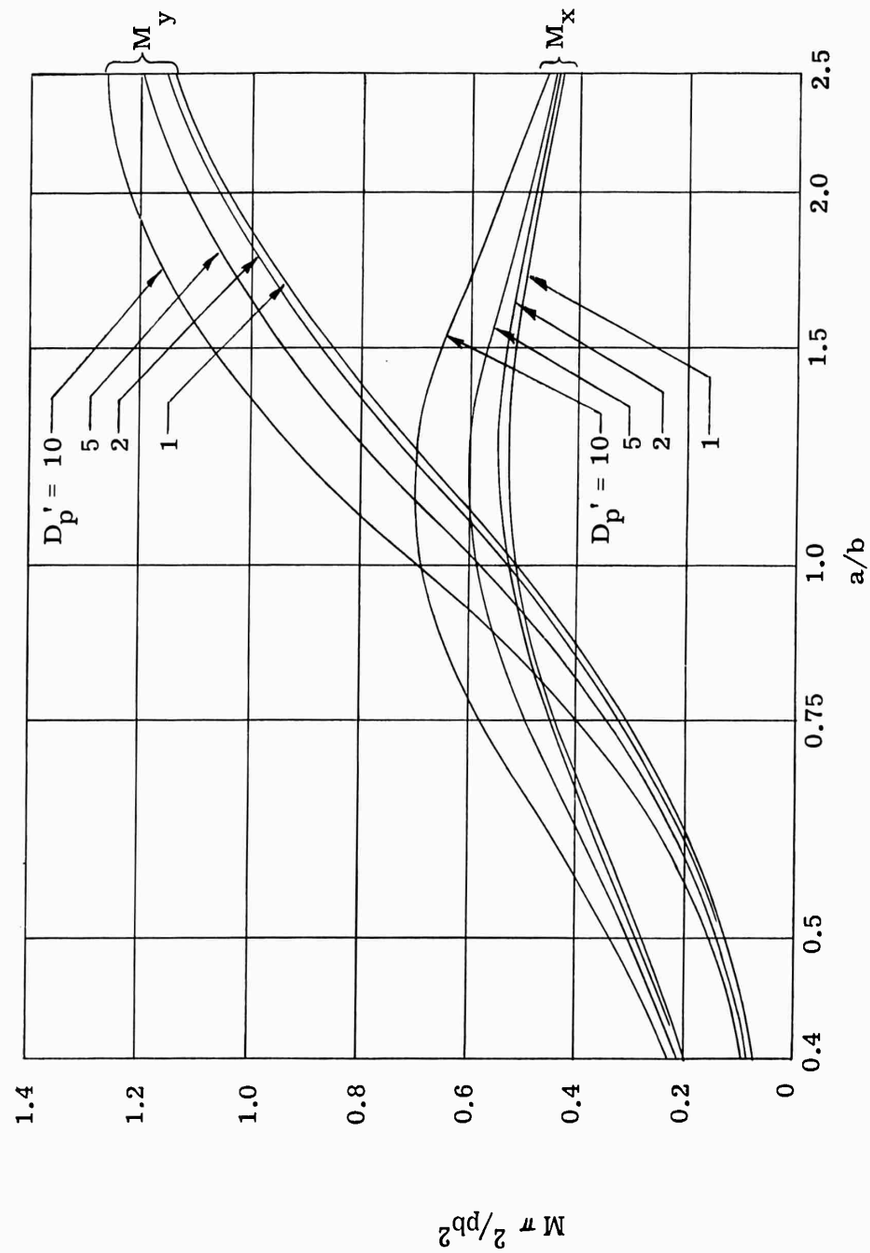

Figure III-15. Maximum Bending Moment in a Rectangular Sandwich Panel Due to a Uniform Normal Pressure (p) and Subjected to a Compression $\eta_x = -0.10$. All Edges Simply Supported

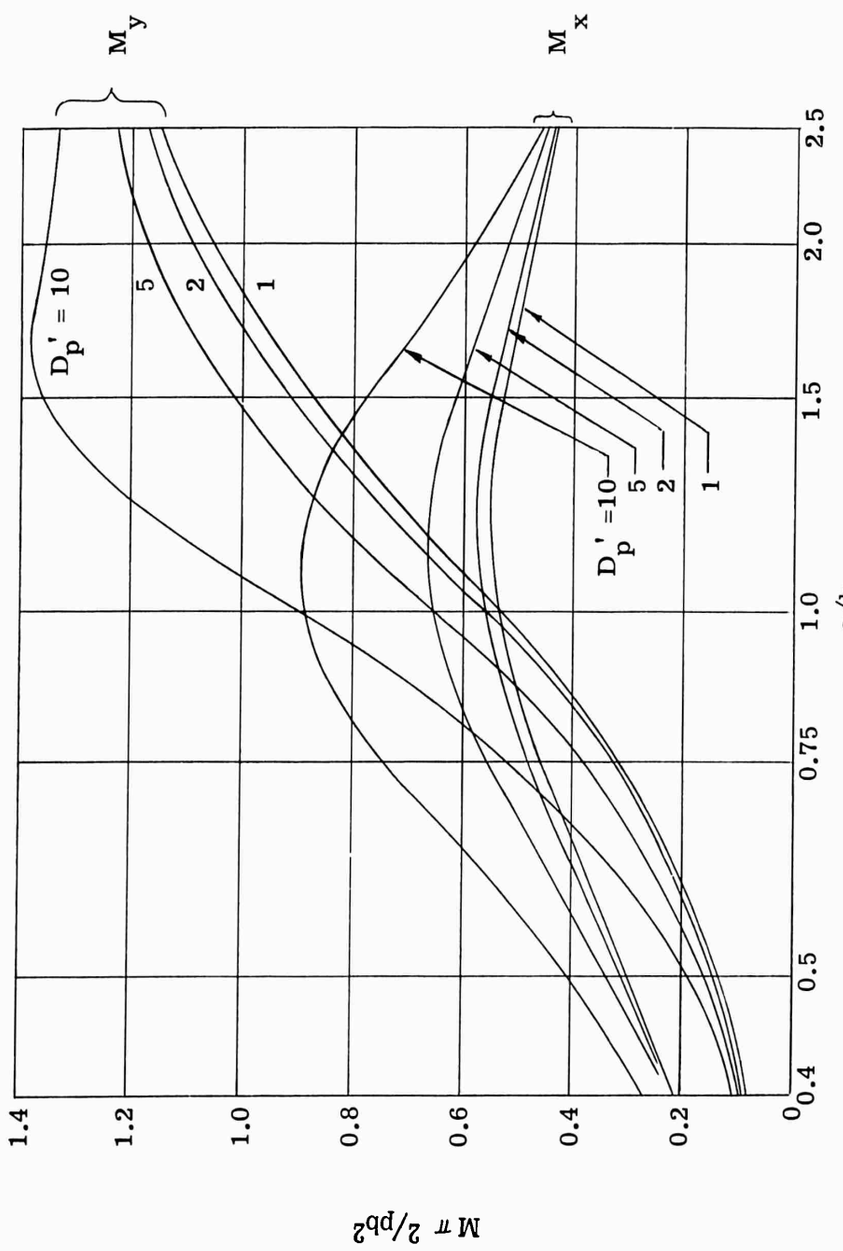

Figure III-16. Maximum Bending Moment in a Rectangular Sandwich Panel Due to a Uniform Normal Pressure (p) and Subjected to a Compression $\eta_x = -0.15$. All Edges Simply Supported

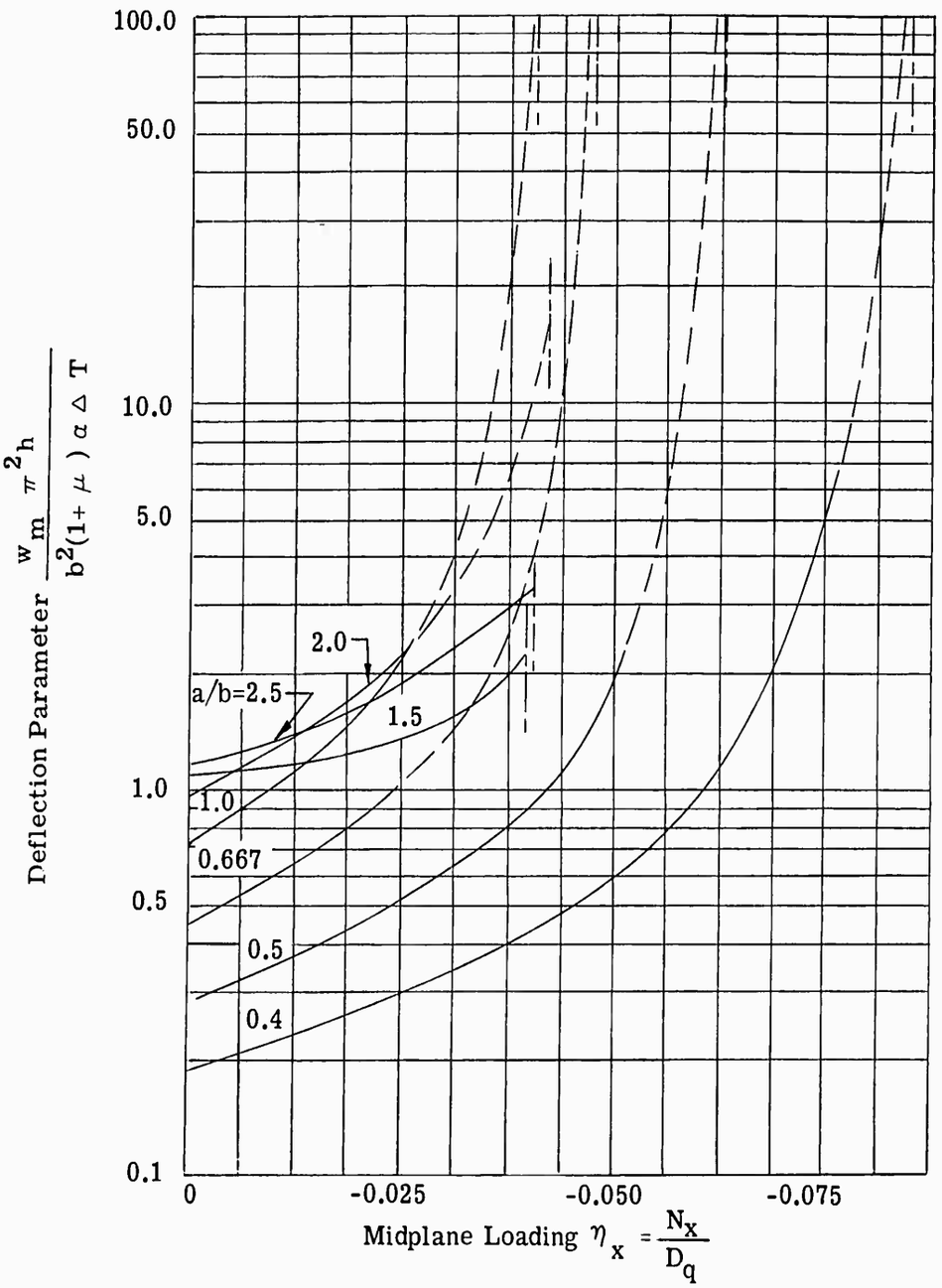

Figure III-17. Maximum Deflection of a Rectangular Sandwich Panel Due to a Temperature Difference (Δ T) Between the Faces and Subjected To Midplane Compression η_x. All Edges Simply Supported

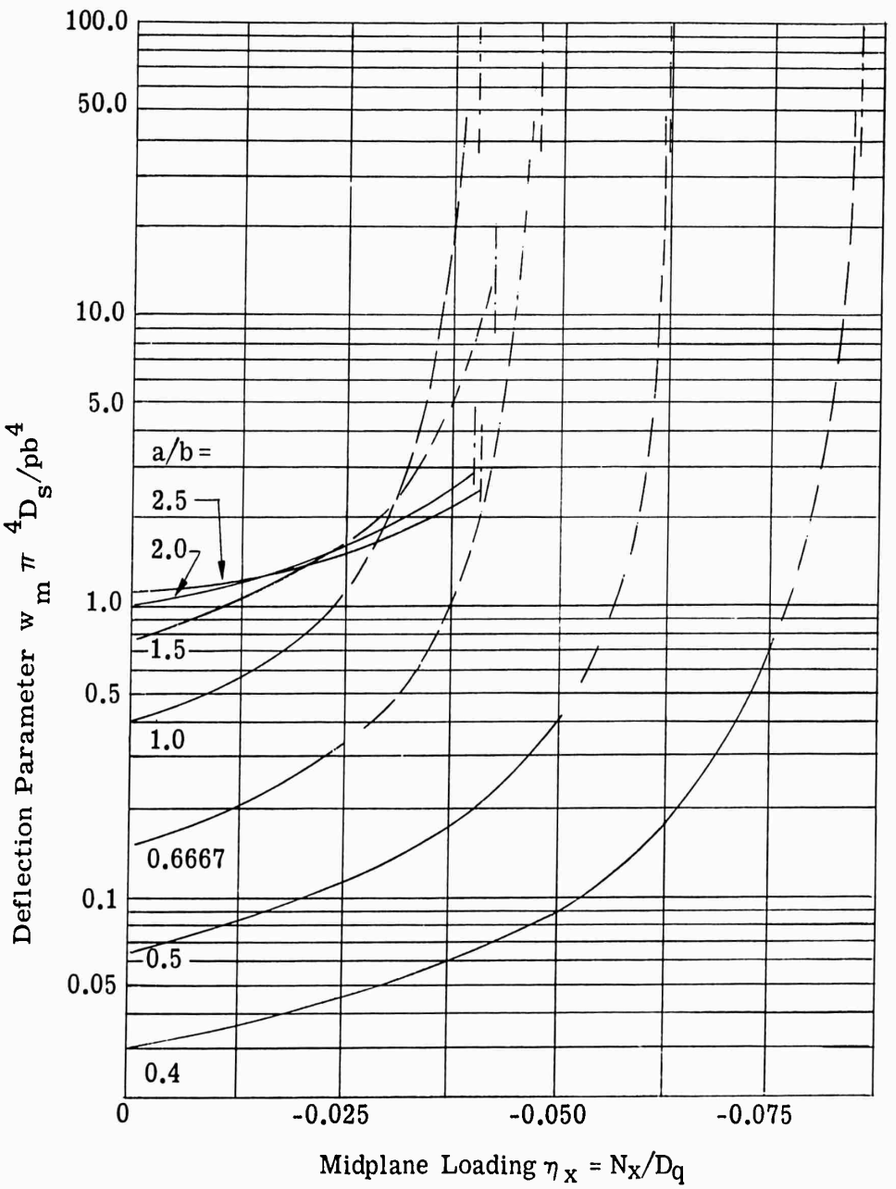

Figure III-18. Maximum Defleetion of a Rectangular Sandwieh Panel Due to a Uniform Normal Pressure(p) and Subjeeted to Midplane Compression η_x. All Edges Simply Supported.

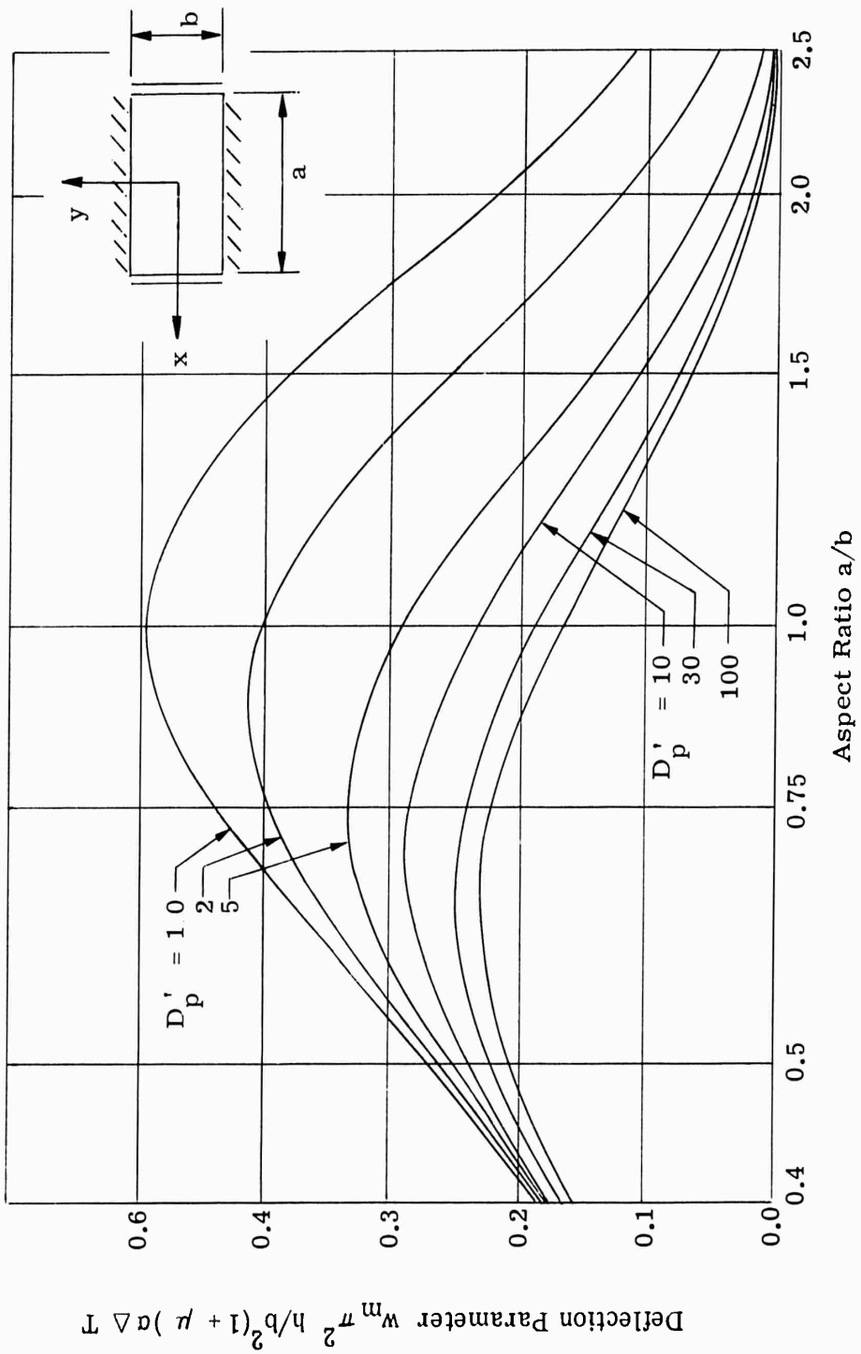

Figure III-19. Maximum Deflection (W_m) of a Rectangular Sandwich Panel Due to a Temperature Difference (ΔT) Between the Faces. Two Edges Simply Supported and Two Edges Built-In.

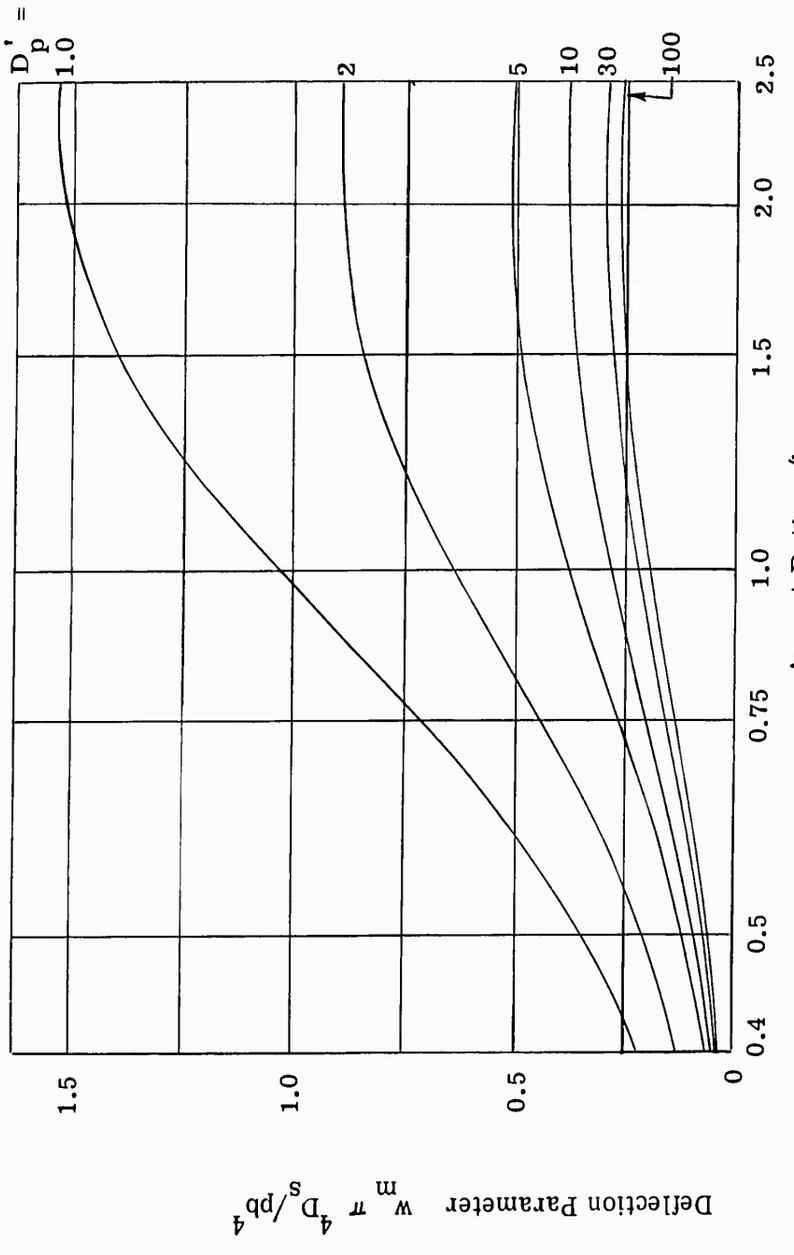

Figure III-20. Maximum Deflection (W_m) of a Rectangular Sandwich Panel Due to Uniform Normal Pressure(p). Two Edges Simply Supported and Two Edges Built-In

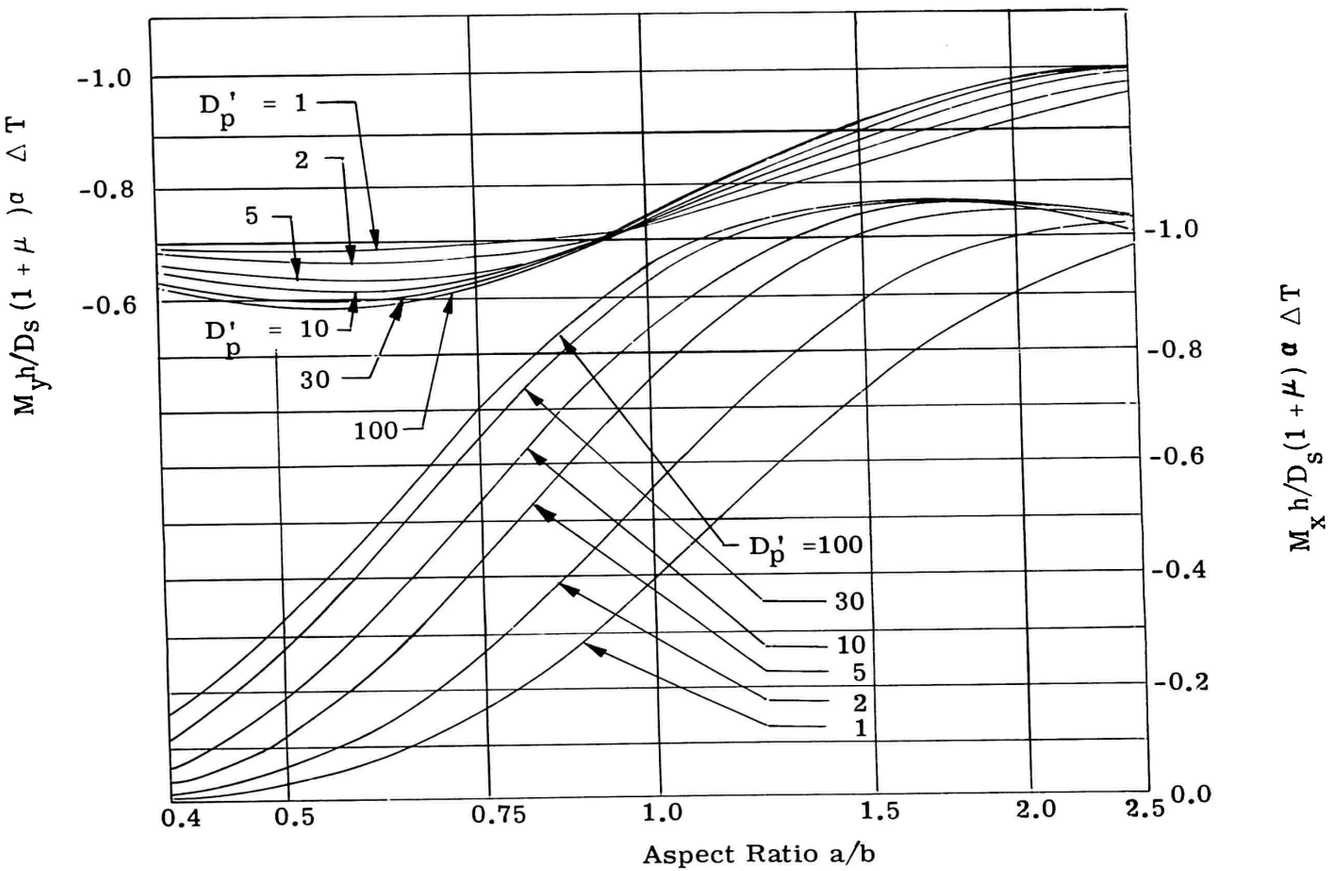

Figure III-21. Bending Moments at Center of a Rectangular Sandwich Panel Due to a Temperature Difference (ΔT) Between the Faces. Two Edges Simply Supported and Two Edges Built-In

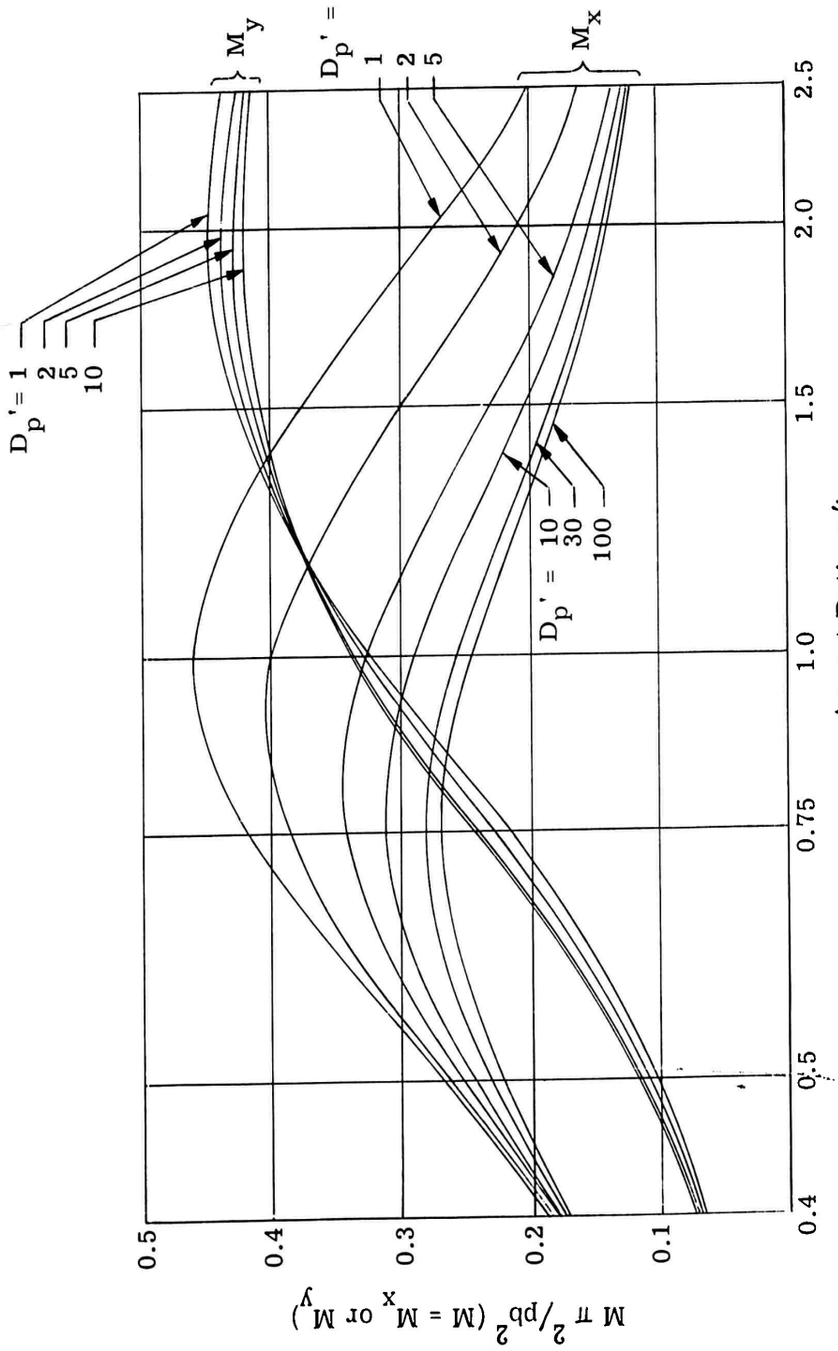

Figure III-22. Bending Moments at Center of a Rectangular Sandwich Panel Due to a Uniform Normal Pressure (p). Two Edges Simply Supported and Two Edges Built-In

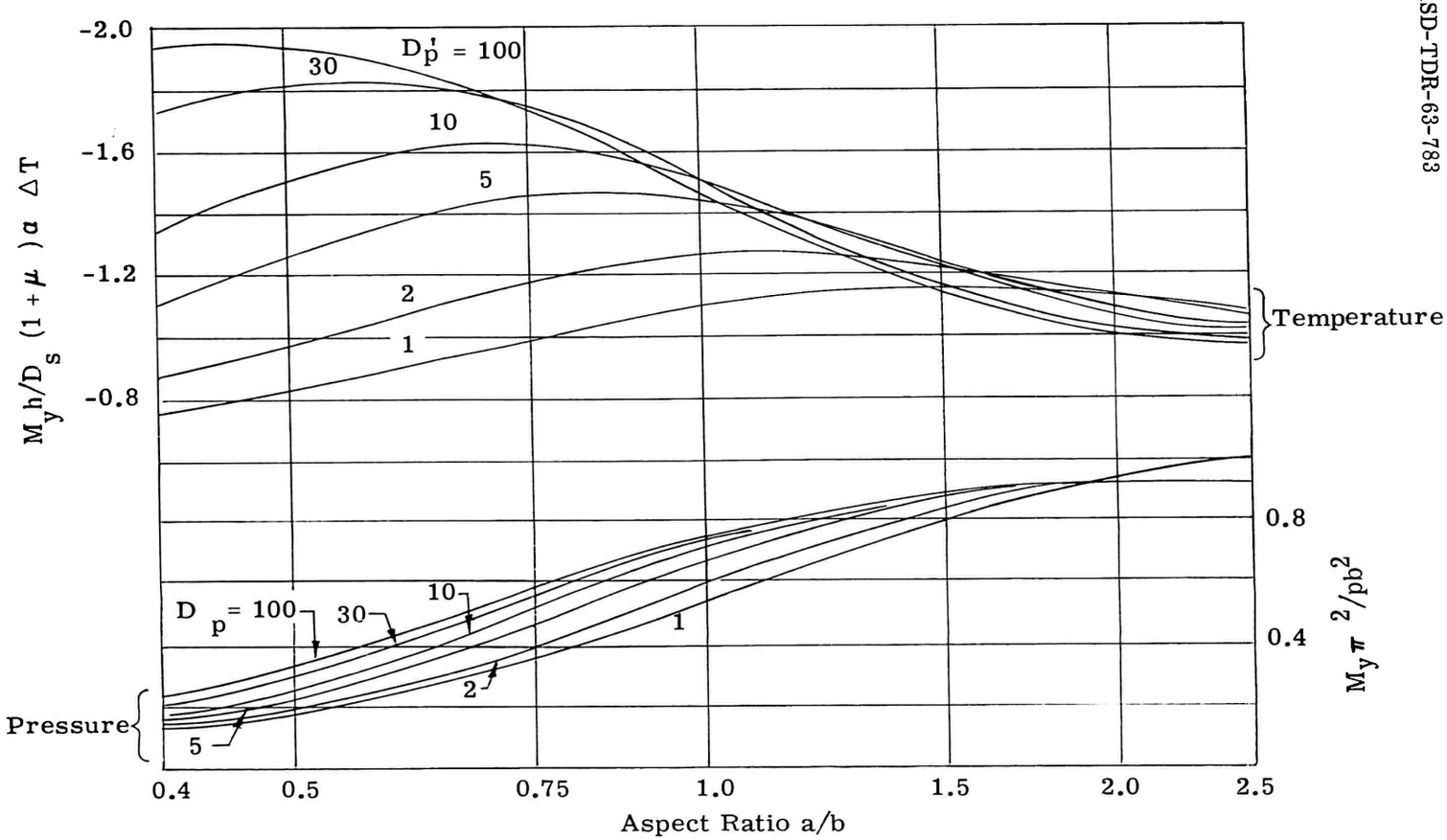

Figure III-23. Bending Moments M_y at Center of Built-In Edge of Rectangular Sandwich Panel Due to Temperature Difference ($\triangle T$) Between the Faces or Due to Uniform Normal Pressure (p). Two Edges Simply Supported and Two Edges Built-In

CHAPTER IV

SANDWICH CYLINDER INSTABILITY UNDER CIRCUMFERENTIALLY VARYING AXIAL STRESS

This chapter is concerned with the prediction of the elastic instability of an axially loaded sandwich cylinder of mean radius r and core thickness h, with isotropic faces of equal thickness t (Figure IV-1). The faces possess only inplane stiffness and have a modulus of elasticity E, while the core possesses only a transverse shear stiffness with a modulus of rigidity G_c. The axial load per unit circumferential length, N_x, varies in the circumferential (y) direction and at any point the stress in each of the two faces is assumed equal at a value $\sigma_x = \frac{N_x}{2t}$

Conditions of circumferentially varying stress, as shown here, may result from the combination of an applied axial load and bending moment, or as a result of temperatures which vary around the circumference at the cylinder. Transformation of the applied loads or temperature profile into the required stress distribution is assumed to have been accomplished by the user of the present data by means of the appropriate stress analysis technique.

The problem of the elastic instability of an isotropic thin-walled cylinder has been solved in References 9 and 10 on the basis of small deflection theory. Both references concluded that instability is reached when the maximum axial stress has the value

$$\sigma_{cr} \approx 0.6 \frac{E\bar{t}}{r} \qquad \text{(IV-1)}$$

regardless of the nature of the circumferential variation of σ_x. (The compression zone within which the maximum value σ_{cr} occurs must at least extend over the wavelength of a circumferential buckle, however). $\bar{t}$ is the wall thickness of the isotropic shell. The result of Equation IV-1 is,of course, the small deflection theory solution for uniform compression. In view of these results it would appear reasonable to expect that for the case of a sandwich cylinder the same conclusions would prevail, i.e., the instability stress is given by the solution for uniform axial compression, regardless of how nonuniformly the stress might vary.

Small deflection theory solutions for the instability at sandwich cylinders under uniform axial compression, based on infinite series techniques, have been presented in references 11, 12 and 13. These results are useful for comparison purposes but to develop solutions for nonuniform stress it has been found more convenient to extend the finite difference technique used in Reference 9 to the present case. Details of this extension are given in Appendix C.

Based on the theory described in Appendix C a computer program for the prediction of critical stress under the subject conditions was coded and employed in the development of parametric results. For sandwich cylinders, two stiffness parameters must be considered:

$$D_c = \frac{D_q r^2}{D_s} \tag{IV-2}$$

and $\left(\frac{Et}{G_c r}\right)$. The chosen values of D_c range from 66.7 to 2500, while $\frac{Et}{G_c r}$ ranges from 0 to approximately 0.95. The upper limits of both parameters are governed by a wrinkling failure characterized by a shear instability of the core. As in Chapter II, this instability is governed by the condition

$$\frac{2\ \sigma_{cr} t}{(h+t)G_c} = 1 \tag{IV-3}$$

The specific load conditions studied are those which produce a linear variation of stress, described by the ratio (S) of the crown stress (σ_{x_c}) to the stress at the bottom of the cylinder (σ_{x_b}), i.e.,

$$S = \frac{\sigma_{x_c}}{\sigma_{x_b}} \tag{IV-4}$$

Results were obtained for S = 1.0, 0.5, 0, -0.5 and -1.0 for various combinations, of the two governing parameters.

Selected results are presented in Table IV-1. As anticipated the critical stresses for nonuniform stress states are effectively equal to the critical stress for uniform axial compression (S = 1.0). The negligible differences between the results for a given stiffness condition may be the result of the differences in stress distribution, but it is also possible that the discrepancies are due entirely to numerical error. This question cannot be resolved by use of the method adopted for solution of the problem.

Results are plotted in Figures IV-1 through IV-3. Figure IV-1 is a carpet plot wherein both stiffness parameters play a role in the definition of the critical stress. If a conventional plotting procedure and slightly altered scales are adoped, as in Figure IV-2, the parameter D_c loses its significance and all results can be approximated by a single line. This manner of representation was also adopted in References 11, 12, and 13. The curve presented in Figure IV-2, based on an Equation from Reference 13, is given by

$$\sigma_{cr} = \frac{E(h+t)}{r}\left[1.05 - \frac{Et}{1.8\ rG_c}\right] \tag{IV-5}$$

TABLE IV-1

BUCKLING COEFFICIENTS - SANDWICH CYLINDER
UNDER NONUNIFORM AXIAL COMPRESSION

Stiffness Parameters		Critical Stress Parameter = $\frac{2t\ \sigma_{cr}}{D_q}$ (computed)				
D_c	$Et/G_c r$	S = -1.0	S = -0.5	S = 0	S = 0.5	S = 1.0*
1000	13.49	0.2672	0.2669	0.2665	0.2660	0.2630
200	30.17	0.5536	0.5511	0.5476	0.5433	0.5345
66.7	45.24	0.7699	0.7630	0.7555	0.7450	0.7243

* Uniform axial compression

The present results, as shown by individual points on Figure IV-2 are in very good agreement with the above curve.

For the isotropie cylinder, results obtained from small defleetion theory analyses are grossly in error except when a sufficiently high intcrnal pressurization is applied, the attainable critical stress being extremely sensitive to initial imperfections (e.g., out of roundness, etc). It is therefore to be expected that sandwich eylinder critieal stresses will be in closer agreement with small deflection theory predictions since the initial imperfeetion effeets, whieh are a function of the radial imperfection magnitude-to-total wall thickness ratio, will be very small in carefully fabrieated sandwich cylinder.

Experimental results presented by Cunningham and Jaeobson (Refercncc 24) lend eredenee to the above hypothesis. On the other hand thc test data of Norris and Kuenzi (Reference 25) support the view that largc-deflection formulations must bc used for the development of design data. A design curve from Reference 26, based on large deflection theory, is reproduced in Figure IV-2. Note the large differenees between the predictions based on large and small deflcetion theory. Unquestionably, a rational basis for the design of sandwich eylinders requires a corrclation and eritical evaluation of existing test data, with the pcrformanee of additional tests in regions of the governing parameter $\left(\frac{Et}{G_c r}\right)$ which have not yct becn examined. This work should be implemented by a thcoretieal study whieh treats instability under nonuniform stress on the basis of large deflection thcory. A study of this type is beyond the scope of the present effort.

As a final representation, the variation of the wavelength of the buekle in the axial direction is plotted parametrically in Figure IV-3. As in the case of the eigcn values, the eomputed wavelengths wcre found to bc esscntially indepcndcnt of the shapc of the stress distribution. Thc wavclength to radius ratios are relatively small; thus, thc present results should apply to short as well as to long eylinders. It should be noted that these eomputcd wavelengths are in elose agrccmcnt with results prescnted clsewhere (Refercnee 12).

Illustrative examples

(1) "Rigid eore"

Determine the maximum stress for buekling (σ_{er}) for an axially loaded sandwieh eylinder possessing thc following properties:

Radius (r) : 18 in.
Core Depth (h) : 0.125 in.
Faec Thiekness (t): 0.010 in.
Moduli $E = 10.5 \times 10^6$ psi
$G_e = 40{,}000$ psi
$\mu = 1/3$

$$\text{Thus, } D_c = \frac{D_q r^2}{D_s} = \frac{2(1-\mu^2)\, G_c r^2}{Et\,(h+t)} = 1660$$

$$\frac{Et}{G_c r} = 0.146$$

From Figure IV-1: k = 0.96

$$\text{Hence} \quad \sigma_{cr} = k\,E\,\frac{(h+t)}{r} = \frac{0.96 \times 10.5 \times 10^6 \times 0.135}{18} = 75{,}500 \text{ psi}$$

If the material in question is 7075-T6 aluminum, as was the case for uniformly compressed cylinders of the same proportions tested by Eakin (Reference 27) and discussed by Cunningham and Jacobson, this stress is well into the inelastic range. By using the dotted curve of Figure IV-2 and the appropriate plasticity reduction factor, Cunningham and Jacobson found a small-deflection theory critical stress of 57,000 psi. The test specimen failed at 61,000 psi.

(2) "Soft Core"

Assume all of the above properties and proportions remain the same except that the core now has a shear modulus G_c = 1450 psi and h = 0.1420 in. The parameter $Et/G_c r$ will then be equal to the value prevailing for tests described in Reference 12. Thus,

$$\frac{Et}{G_c r} = \frac{10.5 \times 10^6 \times 0.0100}{1450 \times 18} = 4.02$$

From Figure IV-2, it is seen that failure is governed by wrinkling associated with shear instability of the core. Hence

$$\sigma_{cr} = \frac{(h+t)G_c}{2t} = 10{,}300 \quad \text{psi}$$

This compares with a stress, computed from experimental data,of 11,300 psi. (Specimen 1424A, Reference 12).

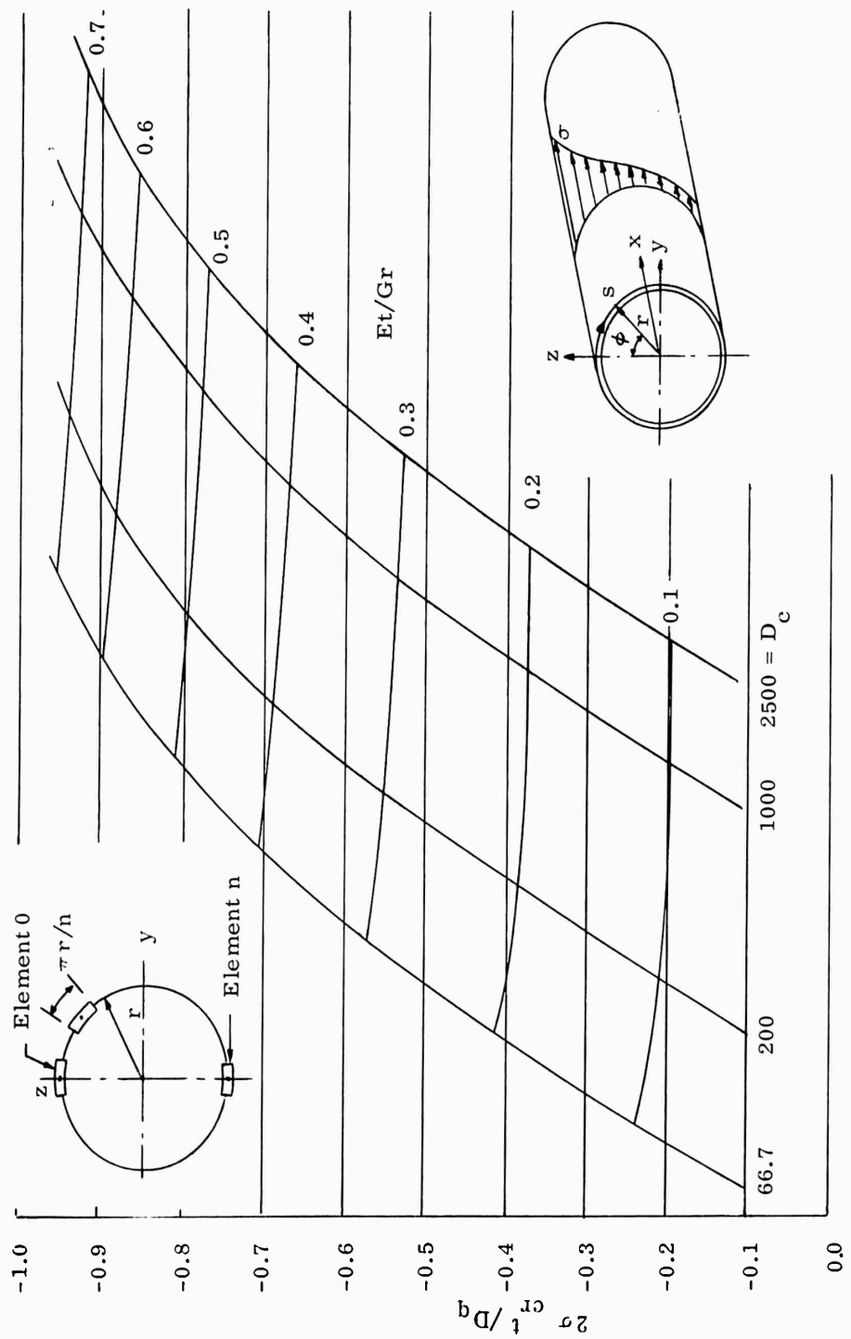

Figure IV-1. Variation of Critical Reference Stress with Two Stiffness Parameters

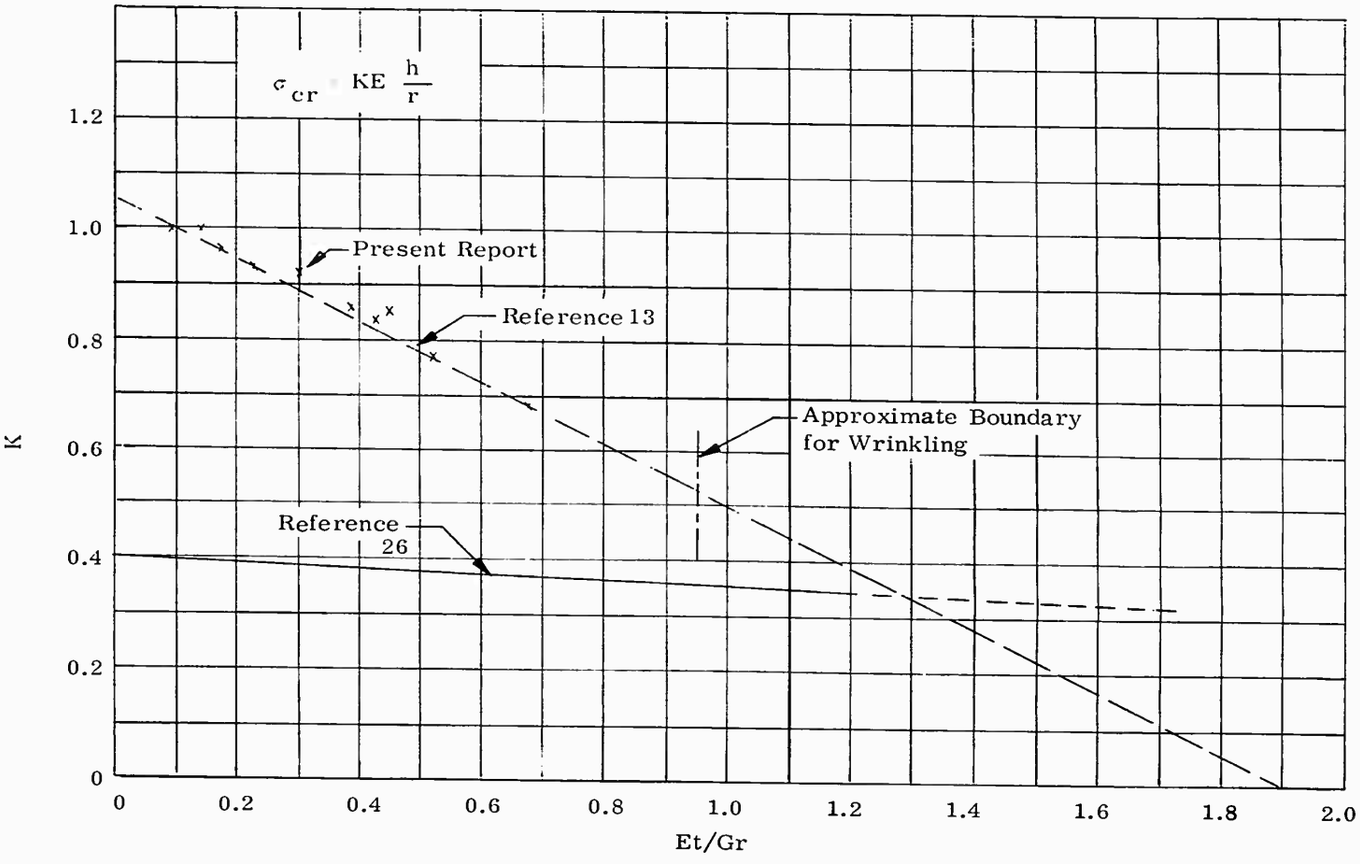

Figure IV-2. Variation of Critical Reference Stress with One Stiffness Parameter Supressed

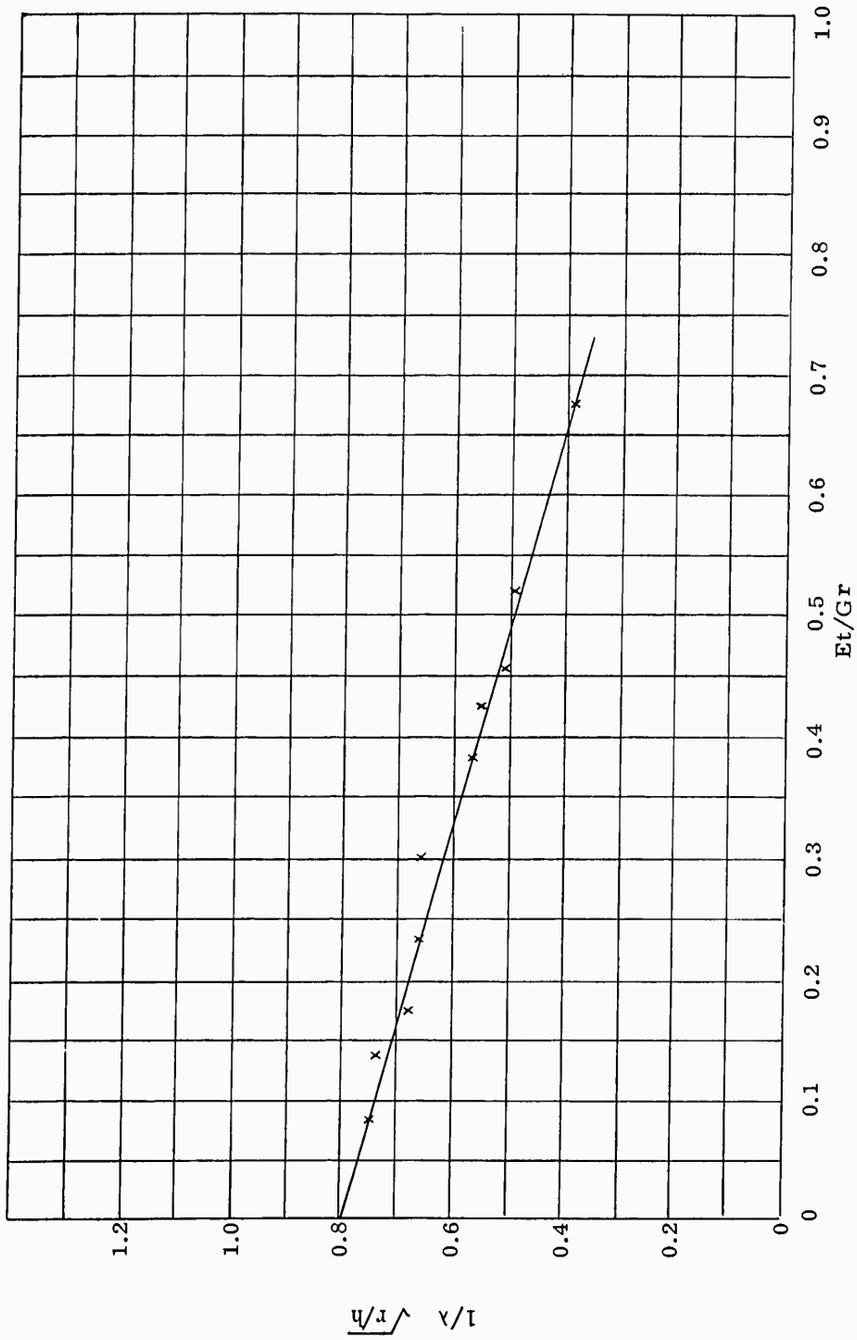

Figure IV-3. Variation of Critical Wavelength Parameter

CHAPTER V

THERMAL STRESSES AND BENDING MOMENTS IN A HEATED SANDWICH CYLINDER SUPPORTED BY RIGID BULKHEADS

This chapter presents data for the determination of the thermal stresses and displacements in a sandwich cylinder of length 2e supported at each end and subjected to a temperature change (Δ T) from the stress-free state. The cross-sectional properties and the material property characteristics are identical to those of the sandwich cylinder of the preceding chapter (see Figure V-1). Both fixed and simple support conditions are treated. The fixed support condition applies to a cylinder continuous over many supports, where, due to symmetry, each bay is effectively built-in at the bulkheads.

A detailed development of the pertinent formulations is presented in Appendix D. There, it is shown that the problem is similar to that of a beam on an elastic foundation. The radial displacements (w) for the simple support condition are found to be

$$w = \frac{r\alpha\ \Delta\ T}{(m_2^2 - m_1^2)} \left[(m_2^2 - 2)\ \frac{\text{eosh } m_1 H_x}{\text{eosh } m_1 H_l} - (m_1^2 - 2)\ \frac{\text{eosh } m_2 H_x}{\text{eosh } m_2 H_l} - (m_2^2 - m_1^2) \right] \tag{V-1}$$

where

$$m_1^2 = \left[1 + \sqrt{1 - \frac{2}{H_d}} \right] \tag{V-2}$$

$$m_2^2 = \left[1 - \sqrt{1 - \frac{2}{H_d}} \right] \tag{V-3}$$

$$H_d = \frac{EtD_s}{\nu^2 D_q^2} = \frac{Et}{D_c D_q} \tag{V-4}$$

$$H_x = \frac{x}{r} \sqrt{\frac{Et}{D_q}} \tag{V-5}$$

$$H_l = \frac{e}{r} \sqrt{\frac{Et}{D_q}} \tag{V-6}$$

The hoop stress (σ_ϕ) midway between the supports (at x = 0), which is a ring compression or tension (i.e., it has an equal value in both the inner and outer faces) is given by

$$\sigma_{\phi_e} = \frac{E\alpha\ \Delta T}{(m_2^2 - m_1^2)} \left[\frac{m_1^2 - 2}{\cosh m_2 H_l} - \frac{m_2^2 - 2}{\text{eosh } m_1 H_l} \right] \tag{V-7}$$

while the longitudinal bending moment (M_{x_e}) at x = 0 is calculable from

$$M_{x_c} = H_d D_q \, r \alpha \Delta T \, \frac{(m_1^2-2)\,(m_2^2-2)}{(m_2^2-m_1^2)} \left[\frac{1}{\cosh m_2 H_1} - \frac{1}{\cosh m_1 H_1} \right] \qquad \text{(V-8)}$$

Formulas for the center deflection, the hoop stress at the center, and for the longitudinal bending moments at the center and supports of the cylinder are given by Equations D-9 through D-12 of Appendix D.

The hoop stresses and bending moments for both support conditions were computed for realistic ranges of the pertinent parameters (H_1 and H_d) and are plotted in the form of nondimensionalized design charts in Figures V-1 through V-5. These figures show the characteristic reversal of stresses associated with the beam on an elastic foundation type of problem.

Illustrative Examples

(1) "Isotropic" cylinder

As a check on the accuracy of the plotted data the case of an isotropic cylinder with simply supported ends, examined by Hoff (Reference 3) will be treated (there are no alternative solutions published for the sandwich problem). In Hoff's paper, r = 10", C = 1.57", $\bar{t}$ = 0.0331" and E = 29 x 10^6 psi. To achieve a comparison with the present paper an equivalent sandwich must be defined. It has been suggested that a suitable criterion is that the radii of gyration of the sandwich and the isotropic plate shall be equal. Also the total cross sectional areas must be equal.

Thus, if $\bar{t}$ is the thickness of isotropic sheet, t is the thickness of each sandwich face and h' is the effective depth, (i.e. distance between centroid of the faces).

$$\text{then } 2t = \bar{t} \text{ and } \frac{\bar{t}^3}{12.\bar{t}} = \frac{th'^2}{2.2t}$$

$$\text{i.e. } t = \frac{\bar{t}}{2} \text{ and } h' = \frac{\bar{t}}{\sqrt{3}}$$

Also a core shear stiffness D_q must be defined. However, in the case of an isotropic plate the shear deformation has negligible influence and a large value for G_c may be chosen arbitrarily. Using the formula $D_q = h' G_c$ and with an arbitrary choice of $G_c = 1.1 \times 10^6$ psi one obtains $D_q = 2.1 \times 10^4$. The bending stiffness is computed as

$$D_s = \frac{E\bar{t}^3}{12(1-\mu^2)} = 96.307$$

$$\text{hence } H_d = \frac{EtD_s}{r^2 D_q^2} = 10^{-3} \text{ and } H_1 = \frac{c}{r}\sqrt{\frac{Et}{D_q}} = 0.742$$

From Figure V-2 at $H_d = 10^{-3}$ and $H_1 = 0.742$ the hoop stress at center

$$\sigma_\phi = 0.057\ E\ \alpha\ \Delta T$$

In Reference 3 the stress at the center of the cylinder is obtained from the expression

$$\sigma_\phi = \left[\frac{\cosh \beta \cos \beta}{\sinh^2 \beta + \cos^2 \beta} \right] E\ \alpha\ \Delta T$$

where $\beta = 0.643 \left(\frac{4c^2}{rt} \right)^{1/2} = 3.51$

The stress, as dcrvied from the above formula, is then

$$\sigma_\phi = 0.056\ E\ \alpha\ \Delta T$$

Thus, there is excellent agreement between the graphical and analytical rcsults.

(2) Sandwich Cylinder

A long sandwich cylinder of 70 inches mcan radius is ring stiffencd at intervals of 48 inches. The core thickness is 1.0 inch, the facc thicknesses 0.030 inch. Both the core and the faces are composed of 17-7PH stainless steel, $E = 27 \times 10^6$ psi, $\alpha = 6.1 \times 10^{-6}$ /°F, $G_c = 100{,}000$ psi. The cylinder is uniformly hcated to a tenıperature 600°F in excess of the ring temperature. Determine the resulting hoop stresses and longitudinal bending moments.

Assume the ring stiffencrs arc infinitcly rigid and that in any particular bay the cylinder can be assumed to bc fixed-supported at its ends.

$$D_c = \frac{2(1-\mu^2)\, G_c r^2}{Et(h+t)} = 1070 \qquad D_q = (h+t)\, G_c = 103{,}000$$

$$H_d = \frac{Et}{D_c D_q} = 7.35 \times 10^{-3} \qquad H_1 = \frac{c}{r}\sqrt{\frac{Et}{D_q}} = 0.961$$

From Figure V-3 by interpolation for H_d and H_1 thc hoop stress is given by

$$\sigma_\phi = 0.060\ E\ \alpha\ \Delta T = 5930 \text{ psi}$$

From Figures V-4 and V-5 the bending moments at thc ccntcr and cnds arc found to be

At ccnter $M_{xc} = 0.0152\ D_q r\ \alpha\ \Delta T = 401$ lb in./in.

At ends $M_{xe} = 0.12\ D_q r\ \alpha\ \Delta T = 3165$ lb in./in.

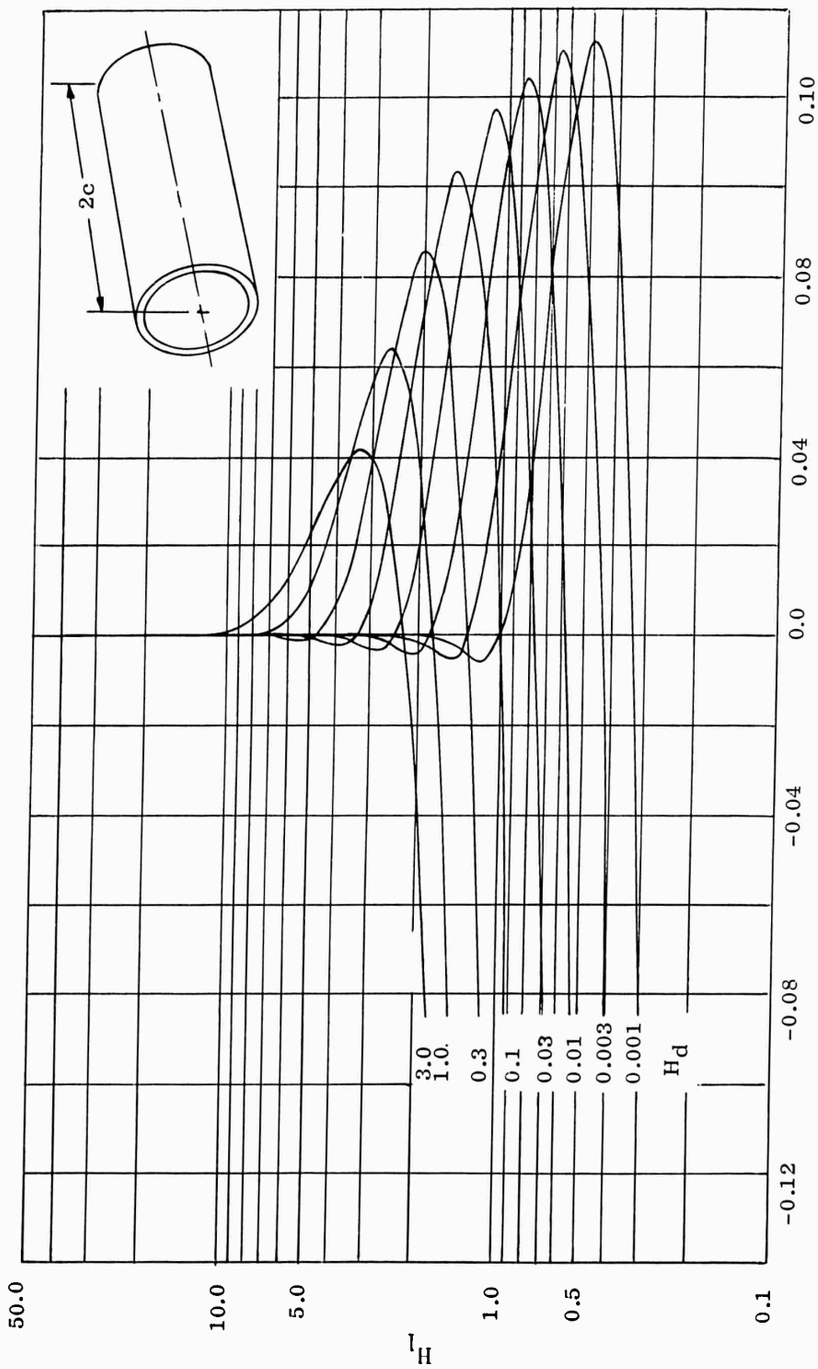

Figure V-1. Central Hoop Stress in Sandwich Cylinder Simply Supported at Each End with Rigid Bulkheads Subjected to Temperature Increase ΔT

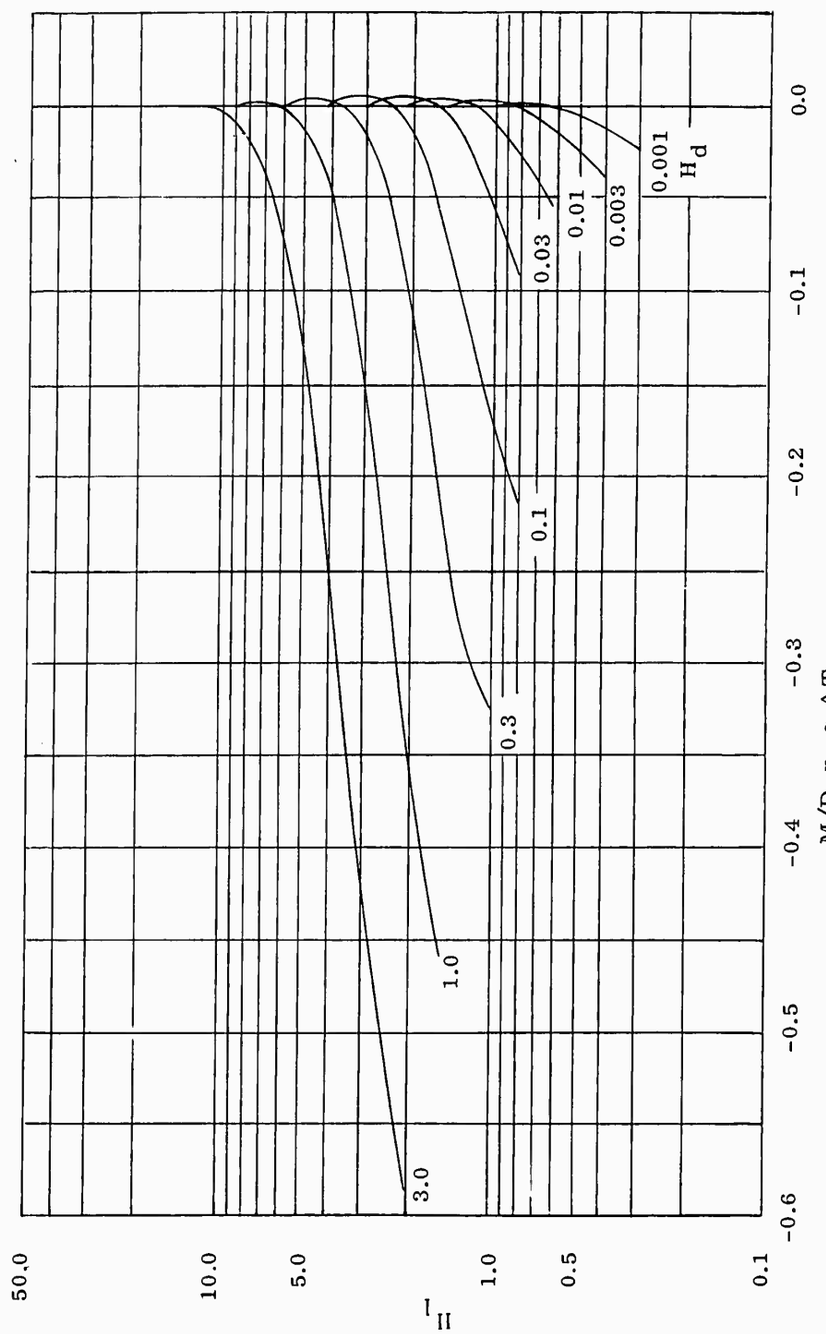

Figure V-2. Central Bending Moment in Sandwich Cylinder Simply Supported at Each End with Rigid Bulkheads Subjected to Temperature Increase ΔT

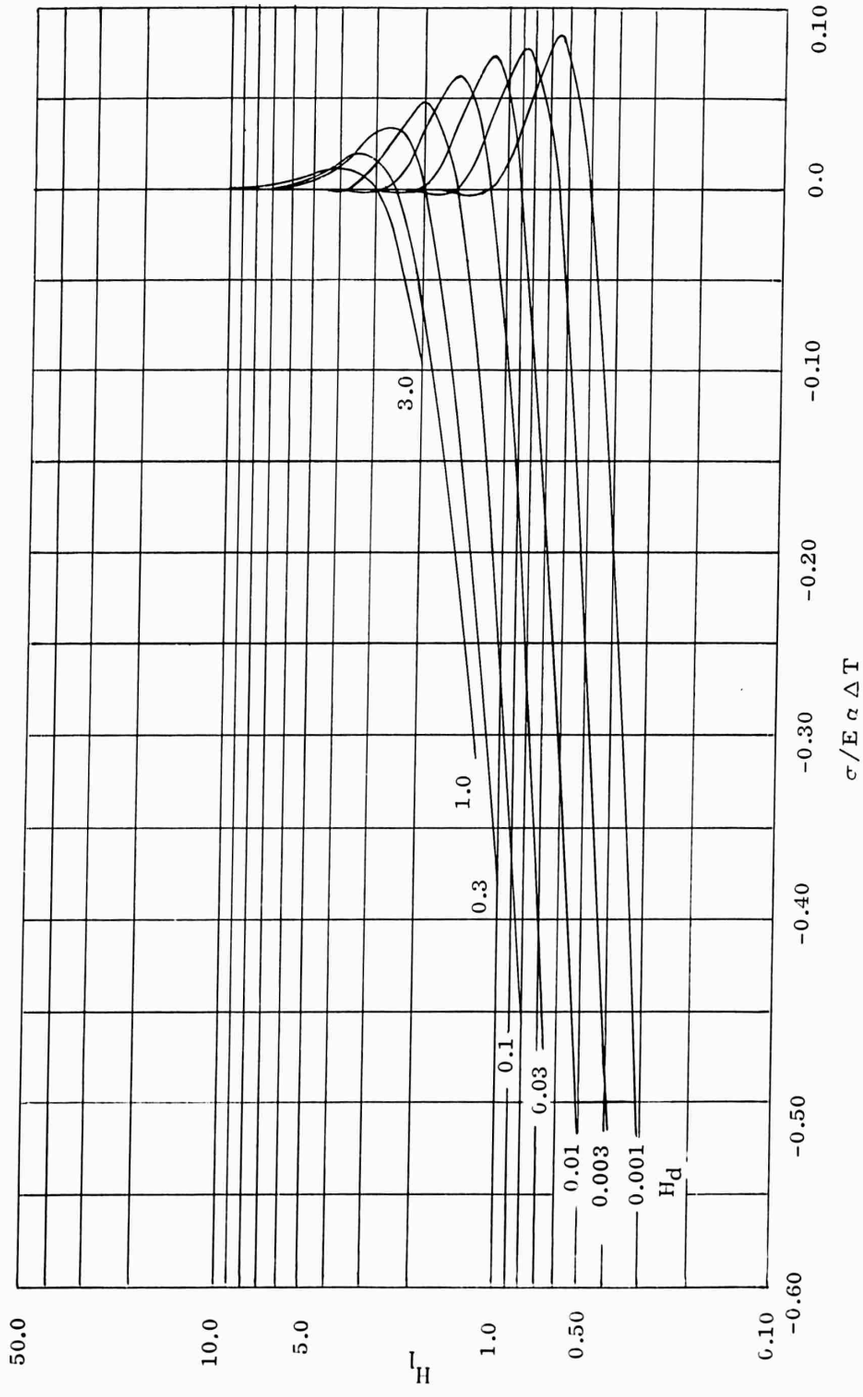

Figure V-3. Central Hoop Stress in Sandwich Cylinder Built in at Each End with Rigid Bulkheads Subjected to Temperature Increase ΔT

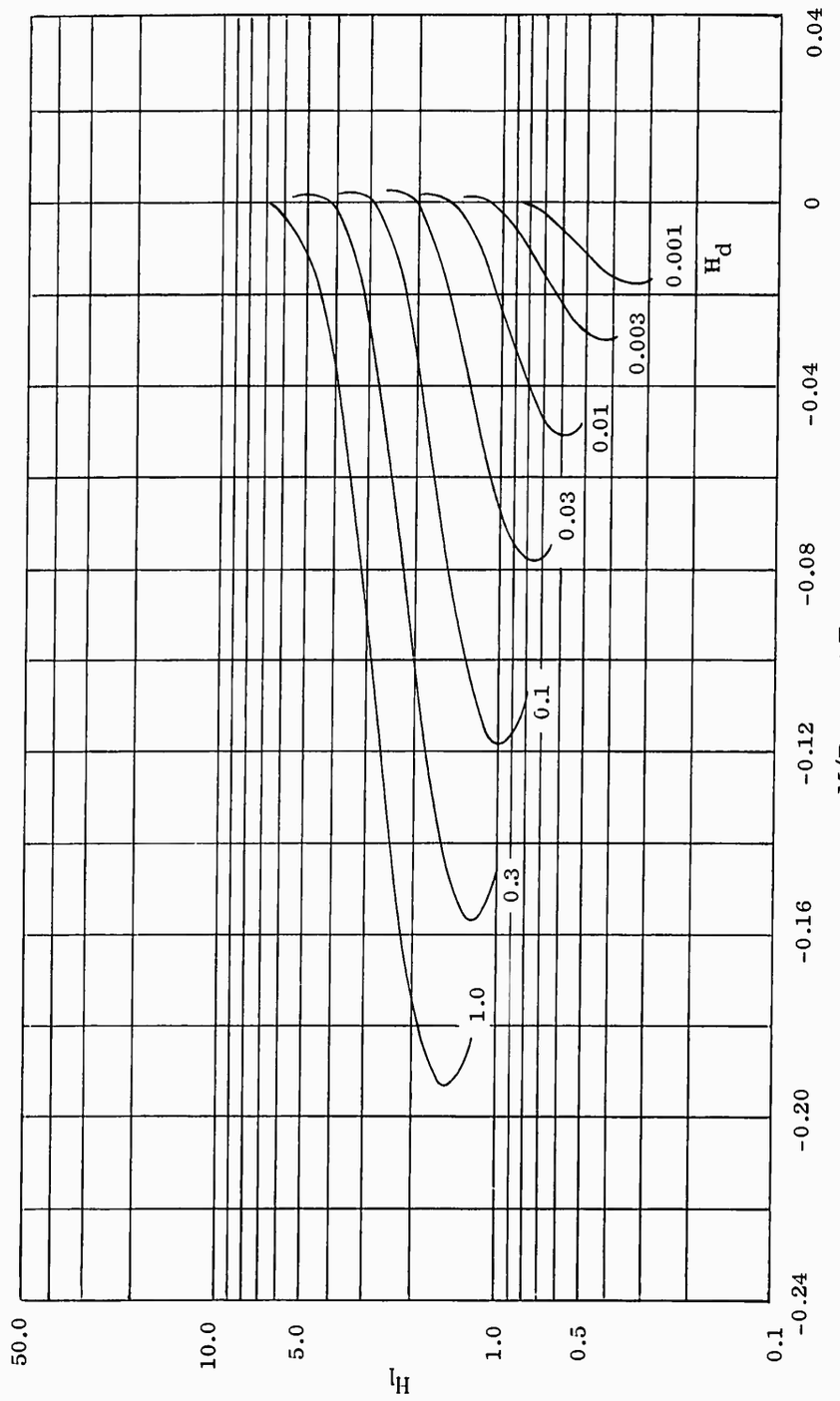

Figure V-4. Central Bending Moment in Sandwich Cylinder Built in at Each End with Rigid Bulkheads Subjected to Temperature Increase ΔT

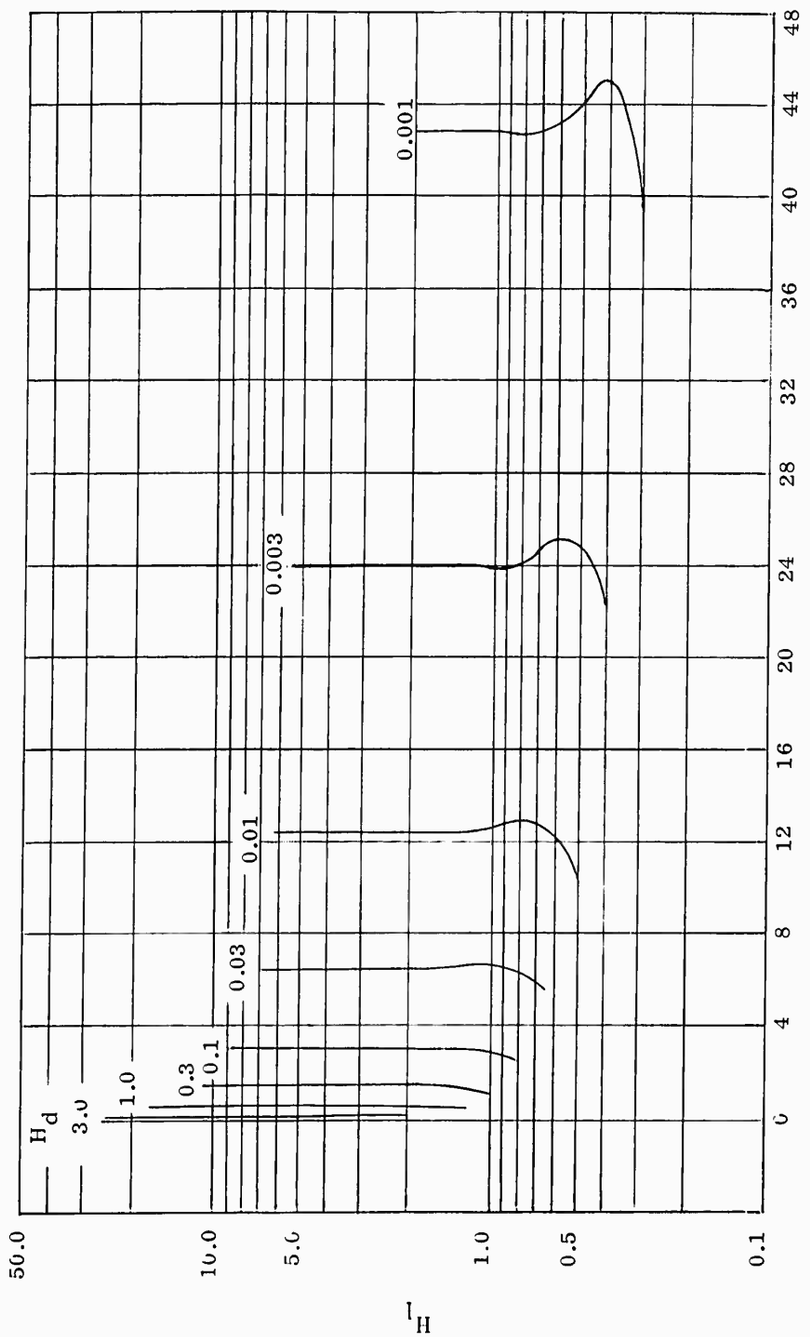

Figure V-5. End Fixing Moment in Sandwich Cylinder Built in at Each End with Rigid Bulkheads Subjected to Temperature Increase ΔT

CHAPTER VI

INSTABILITY OF HEATED SANDWICH CYLINDERS SUPPORTED BY RIGID BULKHEADS

The data presented in this Chapter permit the determination of the temperature change which will produce the elastic instability of sandwich cylinders supported by rigid bulkheads. The conditions of analysis are similar to those of the preceding Chapter, where the stresses introduced by the temperature change were determined. In determining the stresses only simply supported and fully fixed cylinders were considered. However, in considering the instability of the cylinders under hoop stress alone, it is necessary to define three conditions of analysis.

a) Fixed support condition. In this case the cylinder consists of a single bay fully fixed against rotation by a rigid bulkhead at each end.

b) Simple support condition--single bay. Again a single bay cylinder is considered but the rigid bulkheads no longer restrain the rotation of the ends.

c) Simple support condition--many bays. The cylinder is taken to be continuous over many bays, as in a fuselage. The bulkheads restrain radial displacement but provide no restriction against rotation.

In the case of a long multi-bay cylinder (Case c)) the thermal stress distribution in each bay corresponds to the fully fixed case. The fixing moment is produced by symmetry at the supports. Although one possible buckling mode could be the fully fixed one, as discussed in Section 2 of Appendix E, where each bay is fully fixed due to symmetry at the bulkheads, buckling could also occur in the simply supported mode as shown in the adjacent sketch. In this latter case each bay behaves as if it were simply supported at the bulkheads and since this mode will involve less bending of the faces than the fully fixed mode (see sketch), the simply supported mode will predominate.

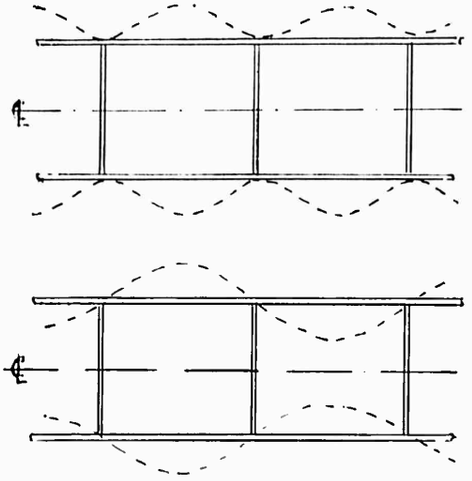

Thus, for a multi-bay cylinder of this type the stress distribution must be determined for the fully fixed case and this stress distribution used in the simply supported stability analysis to determine the critical temperature T_{cr}. This method has been used to develop curves for the determination of the critical temperature of a simply supported multi-bay sandwich cylinder. These curves are presented in Figure VI-2.

Figure VI-1 provides the means for determining the critical temperature for a simply supported single bay (case b)).

The pertinent parameters are in the same range of values as were employed for the design curves of Chapter V.

Both sets of curves have been terminated at an upper value $\frac{t E \alpha \Delta T_{cr}}{D_q} = 0.5$, corresponding to the shear instability failure of the core noted previously. This instability was characterized by the relationship

$$\frac{2t \sigma_\phi}{D_q} = 1.0$$

At the restrained ends of the cylinder the hoop stress (σ_ϕ) equals $E \alpha \Delta T_{cr}$. Thus

$$\frac{2t E \alpha \Delta T_{cr}}{D_q} = 1.0$$

or

$$\frac{t E \alpha \Delta T_{cr}}{D_q} = 0.5$$

The significance of the present data with respect to published isotropic cylinder solutions is discussed at length in the first of the two following illustrative examples.

(1) Isotropic Cylinder

A steel ($E = 29 \times 10^6$ psi, $\alpha = 6.1 \times 10^{-6}/°F$) isotropic cylinder of radius 15 in., wall thickness 0.022 in., is simply supported at rigid bulkheads at intervals of 5 in. The critical temperature is to be determined for each of two cases:

(a) Cylinder consists of a single bay only

(b) Cylinder is continuous over many bays

As in the illustrative example of Chapter V an equivalent sandwich must be defined. Using the relationships derived previously.

$$t = \frac{\bar{t}}{2} = 0.0110 \quad \text{and} \quad h' = \frac{\bar{t}}{3} = 0.0127$$

where $\bar{t}$ is the wall thickness of the isotropic cylinder. The shear modulus of the equivalent core is arbitrarily selected as

$$G_c = 1.576 \times 10^6 \text{ psi}$$

Thus $D_q = h'G_c = 2.002 \times 10^4$ and $D_s = \frac{E\,th'^2}{2(1-\mu^2)} = 28.27$

and $H_d = \frac{E\,t\,D_s}{r^2 D_q^2} = 10^{-4}$ and $H_l = \frac{E\,t\,c^2}{r^2\,D_q} = 0.665$

From Figures VI-1 and VI-2 for $H_d = 10^{-4}$ and $H_l = 0.663$

a) $\frac{t\,E\alpha\,\Delta T_{cr}}{D_q} = 0.121$ for a single bay cylinder

b) $\frac{t\,E\alpha\,\Delta T_{cr}}{D_q} = 0.049$ for a multi-bay cylinder

Since $\frac{t\,E\alpha\,\Delta T_{cr}}{D_q}\left[\frac{1}{2(1-\mu^2)\,H_d}\right]^{1/2} = (\alpha\,\Delta T_{cr})\left(\frac{r}{h'}\right)$ and $h' = \frac{\bar{t}}{3}$, then

a) $(\alpha\,\Delta T_{cr})\left(\frac{r}{\bar{t}}\right) = \frac{0.121}{\sqrt{3}\ \sqrt{1.82}} \times 10^2 = 5.18$

b) $(\alpha\,\Delta T_{cr})\left(\frac{r}{\bar{t}}\right) = \frac{0.049}{\sqrt{3}\ \sqrt{1.82}} \times 10^2 = 2.09$

For this cylinder $\frac{(2c)^2}{r\,t} = \frac{25}{15 \times 0.022} = 75$

In Figure 1 of Reference 18, Anderson presents the critical temperature for an isotropic cylinder $\frac{(2c)^2}{r\,t} = 75$. The corresponding values of $(\alpha\,\Delta T_{cr})\left(\frac{r}{t}\right)$ as taken from the curve, are 5.24 and 2.08 respectively. The actual critical temperatures are

a) $T_{cr} = \frac{0.121\,D_q}{t\,E\alpha} = 1245^\circ F$

b) $T_{cr} = \frac{0.049\,D_q}{t\,E\alpha} = 504^\circ F$

(2) Sandwich Cylinder

A sandwich cylinder of 95 in. mean radius is ring stiffened at intervals 48 in. The core thickness is 1.0 in., the face thicknesses 0.030 in. Both core and faces are composed of 17-7 PH stainless steel, $E = 30 \times 10^6$ psi, $\alpha = 6.1 \times 10^{-6}$ in./in.°F, $G_c = 70{,}000$ psi. The critical temperatures are again to be determined for the simply supported single and multi-bay cases.

Then $D_q = h' G_c = 7.21 \times 10^4$ and $D_s = \frac{E\,th'^2}{2(1-\mu^2)} = 5.246 \times 10^5$

and $H_d = \frac{E\,t\,D_s}{r^2 D_q^2} = 10^{-2}$ and $H_l = \left[\frac{E\,t\,c^2}{r^2 D_q}\right]^{1/2} = 0.893$

From Figure VI-1 for $H_d = 10^{-2}$ and $H_l = 0.893$ the point lies above the shear instability boundary. Thus the critical temperature for the single bay cylinder is given by

$$\frac{t\,E\alpha\,\Delta T_{cr}}{D_q} = 0.5$$

and $\Delta T_{cr} = \frac{0.5\,D_q}{t\,E\alpha} = 6566^\circ F$

From Figure VI-2 for the relevant H_q and H_l for a multi-bay cylinder

$$\frac{t E \alpha \Delta T_{cr}}{D_q} = 0.4$$

and $$\Delta T_{cr} = 5253^{\circ}F$$

It can be seen from the above examples that this type of instability is unlikely to occur in sandwich cylinders of normal proportions. It is, however, a possible mode of failure in cylinders of very large radii and low wall thickness.

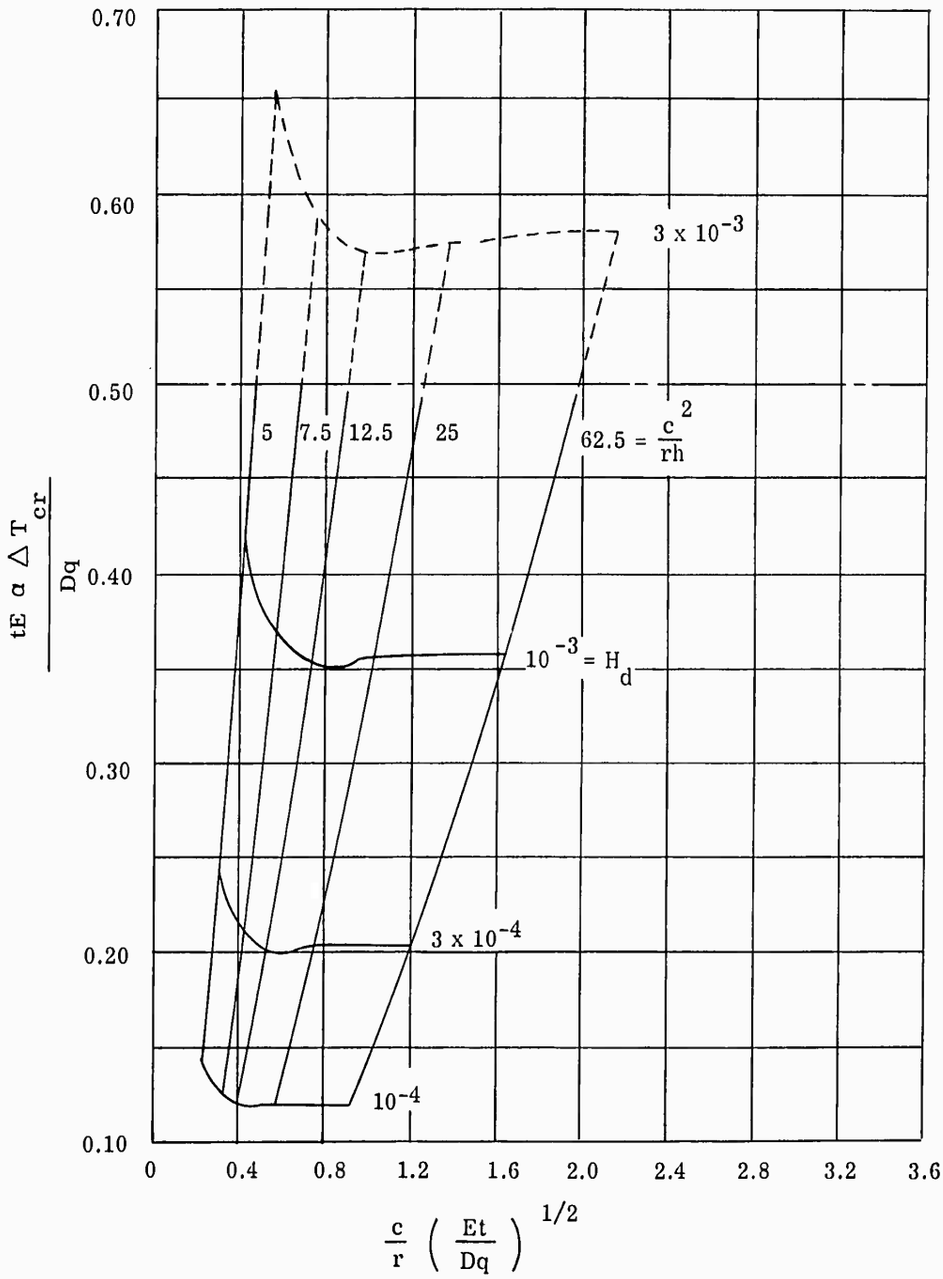

Figure VI-1. Critical Temperatures for the Instability of Simply Supported Single Bay Cylinders

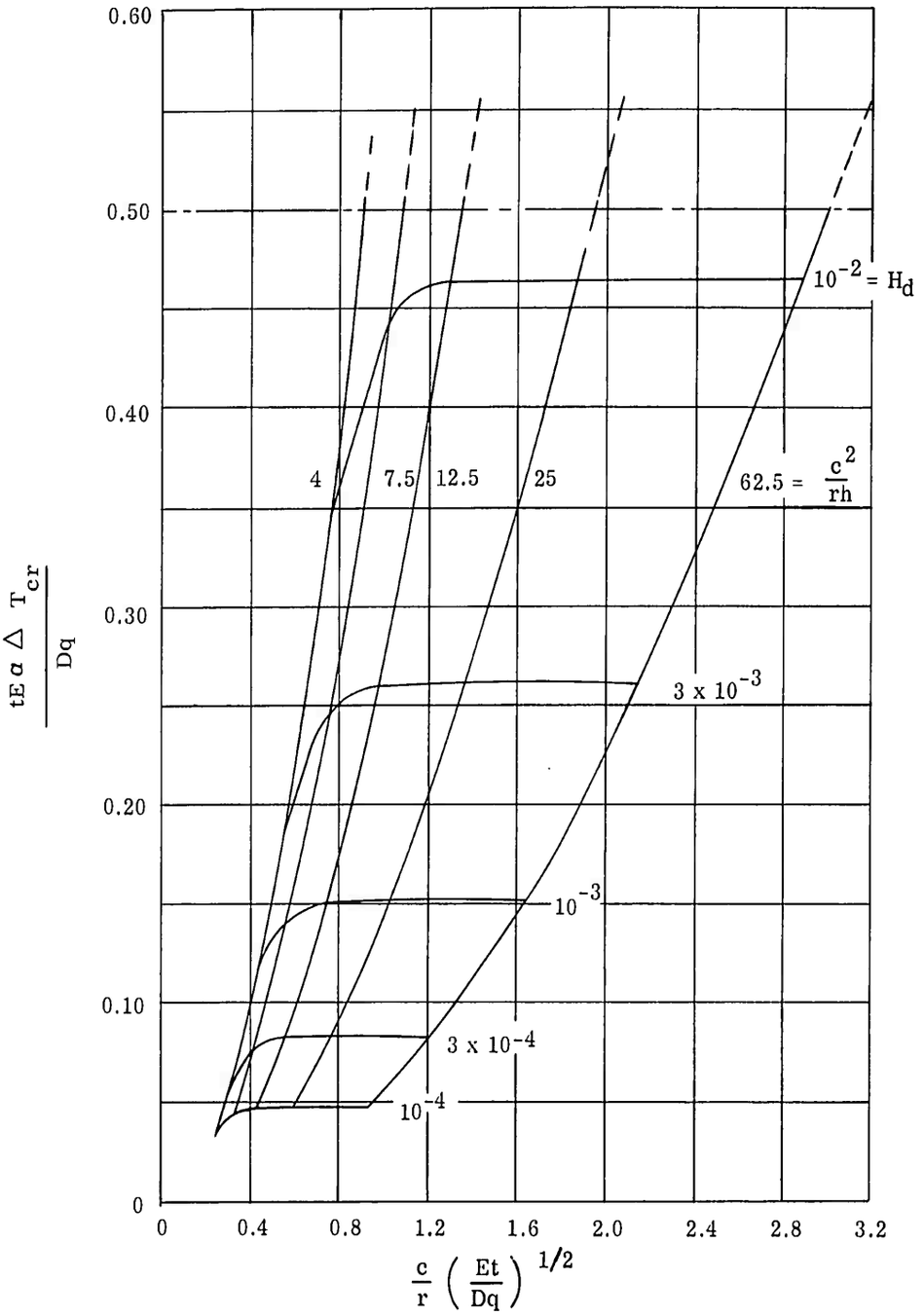

Figure VI-2. Critical Temperatures for the Instability of Cylinders Simply Supported Over Many Bays

CHAPTER VII

SANDWICH CYLINDER STRESSES DUE TO INTERNAL AND EXTERNAL PRESSURE AND RADIAL TEMPERATURE GRADIENTS

Design curves presented in this section permit the determination of the stresses in long sandwich cylinders subjected to radial temperature gradients and to internal and external pressure. As in the preceding chapter, the cylinder consists of two concentric thin cylinders of identical materials, with radii r_o and r_i and thicknesses t, separated by a honeycomb type core of thickness $h = r_o - r_i$ (see Figure VII-1). The cylinder is heated such that each skin has a constant temperature change from the stress-free state (T_o and T_i, respectively) with a linear variation across the core, while the internal and external pressures are p_o and p_i.

The theoretical basis of the present chapter is detailed in Appendix F, where the desired stress equations are derived by first considering the separate deformations of the three components - - the two skins and the core--under the actions of external and interface loading and by then applying the conditions of interface compatibility. The isotropic faces are analyzed using plane stress relationships. The core is assumed to possess a modulus of elasticity in the radial direction (E_r) and a coefficient of thermal expansion in the radial direction equal to that of the skins. Consistent with the common properties of honeycomb construction, the core has neither stiffness nor a coefficient of thermal expansion in the axial or circumferential directions. As shown in the illustrative example, however, homogeneous (rather than honeycomb) cores, of the type often employed in sandwich construction, can be analyzed with sufficient accuracy by use of the present curves.

It should be noted that the ends of the cylinder are assumed to be free to move in the axial direction and axial stresses due to end closure of the cylinder are not included. The latter, which are approximately equal to $\frac{p_i r_i}{4t}$, can be superimposed on the stresses obtained from the present curves. "End effect" stresses, if calculable, can also be superimposed.

Due to the imposed load and temperature conditions, axial and longitudinal stresses are produced in the faces and radial direct stresses are introduced into the core. There are no direct axial or circumferential stresses in the core due to the absence of core stiffness in these directions. Design curves for the axial and circumferential stresses at the outside surface due to external pressure, internal pressure, and temperature are presented in Figures VII-1 through VII-6. The related formulas for stress are shown in each figure; these formulas show that the dimensionless stress parameters (e.g. $\sigma_\theta^T / E\alpha\,(T_o - T_i)$) depend only upon $R = r_o/r_i$ and $Et/E_r r_i$. For shells of current interest and importance, appropriate values of R lie between 1.0025 and 1.10 while the ratio $Et/E_r r_i$ takes on values

in the range of 0.01 to 50.0. These ranges were employed in the development of the subject design curves.

Values for the inner surface and radial stresses are easily obtained from the corresponding outer surface stresses through simple algebraic operations and are therefore not plotted. The pertinent relationships are: (Equations VII-1 to VII-6 appear in Figures VII-1 to VII-6).

a. Stresses Due to Radial Temperature Gradient

$$\sigma_{\theta_i}^{T} = -\sigma_{\theta_o}^{T} \qquad \text{(VII-7)}$$

$$\sigma_{x_i}^{T} = -R\sigma_{x_o}^{T} \qquad \text{(VII-8)}$$

$$\sigma_{r}^{T} = -\left(\frac{t}{r_i}\right)\left(\frac{1+R}{2R}\right)\sigma_{\theta_o}^{T} \qquad \text{(VII-9)}$$

b. Stresses Due to Internal Pressure

$$\sigma_{\theta_i}^{p_i} = \left[\frac{p_i r_i}{t} - \sigma_{\theta_o}^{p_i}\right] \qquad \text{(VII-10)}$$

$$\sigma_{x_i}^{p_i} = -R\sigma_{x_o}^{p_i} \qquad \text{(VII-11)}$$

$$\sigma_{r}^{p_i} = -\left(\frac{t}{r_i}\right)\left(\frac{1+R}{2R}\right)\sigma_{\theta_o}^{p_i} \qquad \text{(VII-12)}$$

c. Stresses Due to External Pressure

$$\sigma_{\theta_i}^{p_o} = -\left[\frac{R\,p_o r_i}{t} + \sigma_{\theta_o}^{p_o}\right] \qquad \text{(VII-13)}$$

$$\sigma_{x_i}^{p_o} = -R\sigma_{x_o}^{p_o} \qquad \text{(VII-14)}$$

$$\sigma_{r}^{p_o} = \left(\frac{t}{r_i}\right)\left(\frac{1+R}{2R}\right)\sigma_{\theta_i}^{p_o} \qquad \text{(VII-15)}$$

Illustrative Example

Given a sandwich cylinder with r_i = 100.01 in., r_o = 101.03 in., t = 0.020 in., subjected to a radial temperature gradient $T_o - T_i$ = 100 °F, and pressures p_i = 10 psi and p_o = 5 psi. The skin material is aluminum alloy with $E = 10.5 \times 10^6$ psi and $\mu = 0.3$, while the core is aluminum honeycomb with $E_r = 1.5 \times 10^5$ psi. For

skin and core $\alpha = 12 \times 10^{-6}/^{\circ}F$. Determine the axial and hoop stresses in the outer skin and the radial stress in the core.

$$R = 1.0102 \quad , \qquad Et/E_r r_i = 0.014$$

By interpolation on Figures VII-1 to VII-6 the following stresses are found.

$$\frac{\sigma_{\theta_o}^{T}}{E\alpha(T_o-T_i)} = -0.714 \qquad \frac{\sigma_{x_o}^{T}}{E\alpha(T_o-T_i)} = -0.711 \qquad \frac{\sigma_{\theta_o}^{p_i} t}{p_i r_i} = 0.497$$

$$\frac{\sigma_{x_o}^{p_i} t}{p_i r_i} = -0.844 \times 10^{-3} \qquad \frac{\sigma_{\theta_o}^{p_o} t}{p_o r_i} = -0.492 \qquad \frac{\sigma_{x_o}^{p_o} t}{p_o r_i} = +0.829 \times 10^{-3}$$

Thus total hoop stress in outer skin

$$\sigma_{\theta_o} = \overset{T}{-9000} + \overset{p_i}{24850} - \overset{p_o}{12300} = 3550 \text{ psi}$$

Axial stress in outer skin

$$\sigma_{x_o} = \overset{T}{-8960} - \overset{p_i}{42} + \overset{p_o}{20} = -8980 \text{ psi}$$

Radial stress in core

$$\sigma_r = \overset{T}{+1.8} - \overset{p_i}{4.9} + \overset{p_o}{2.5} = -0.5 \text{ psi}$$

Similarly, the inner skin stresses are found to be

$$\sigma_{\theta_i} = -21{,}900 \text{ psi and } \sigma_{x_i} = +9010 \text{ psi.}$$

Yao[19] has analyzed the case of a sandwich cylinder under a radial thermal gradient alone, where the core possesses the properties of a homogeneous material. Otherwise, the problem data are identical to those given above. The stresses found by Yao are as follows:

$$\sigma_{\theta_o}^{T} = -0.730\, E\alpha\,(T_o-T_i) = -9200 \text{ psi}$$

$$\sigma_{\theta_i}^{T} = 0.685\, E\alpha\,(T_o-T_i) = 8630 \text{ psi}$$

$$\sigma_r^T = 1.37 \times 10^{-4} E \alpha (T_o - T_i) = 1.7 \text{ psi}$$

These values compare closely with the present results of -9000, 9000, and 1.8 psi, respectively.

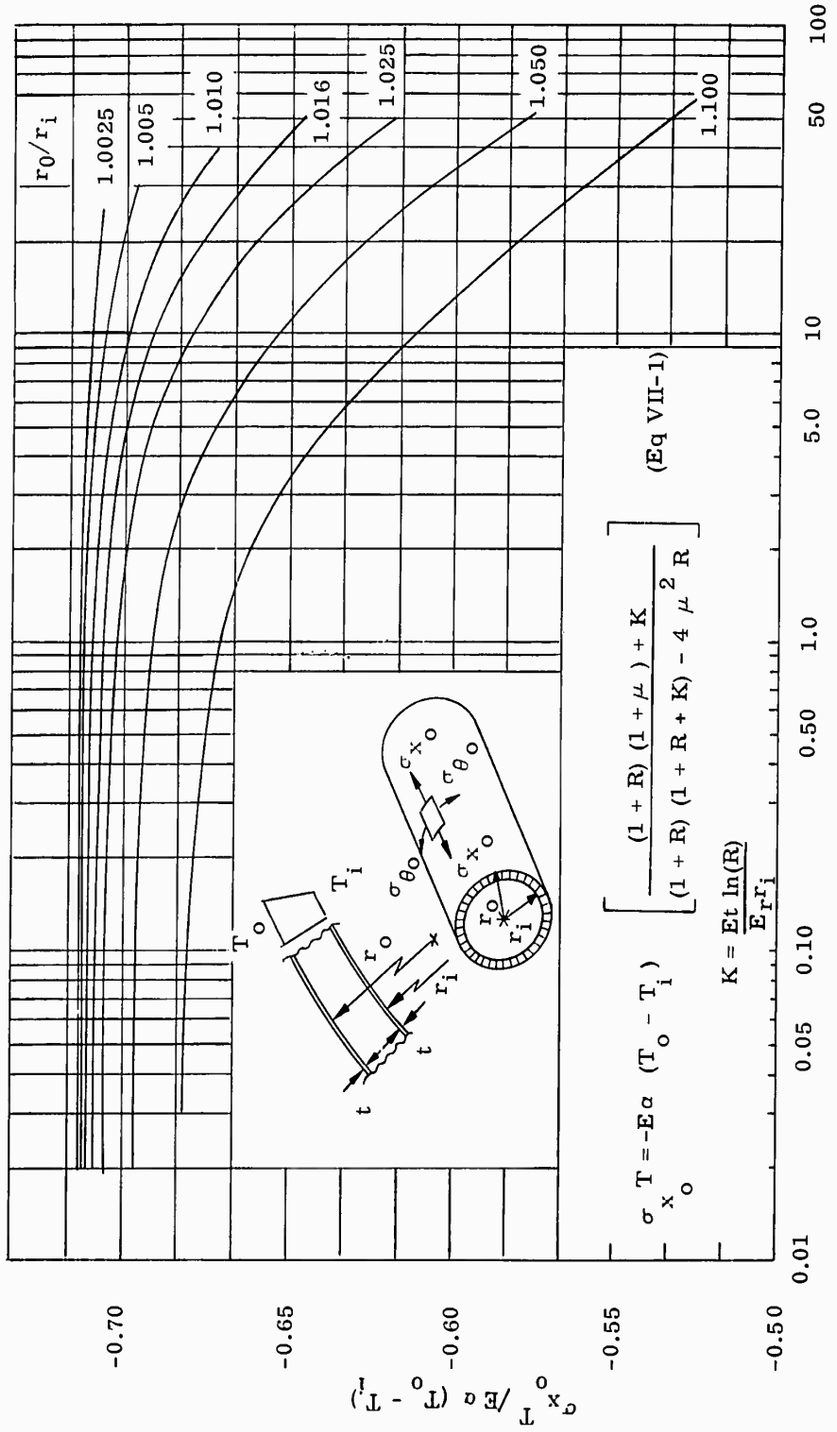

Figure VII-1. Axial Thermal Stress In Outer Face of a Sandwich Cylinder ($\sigma_{x_o}{}^T$)

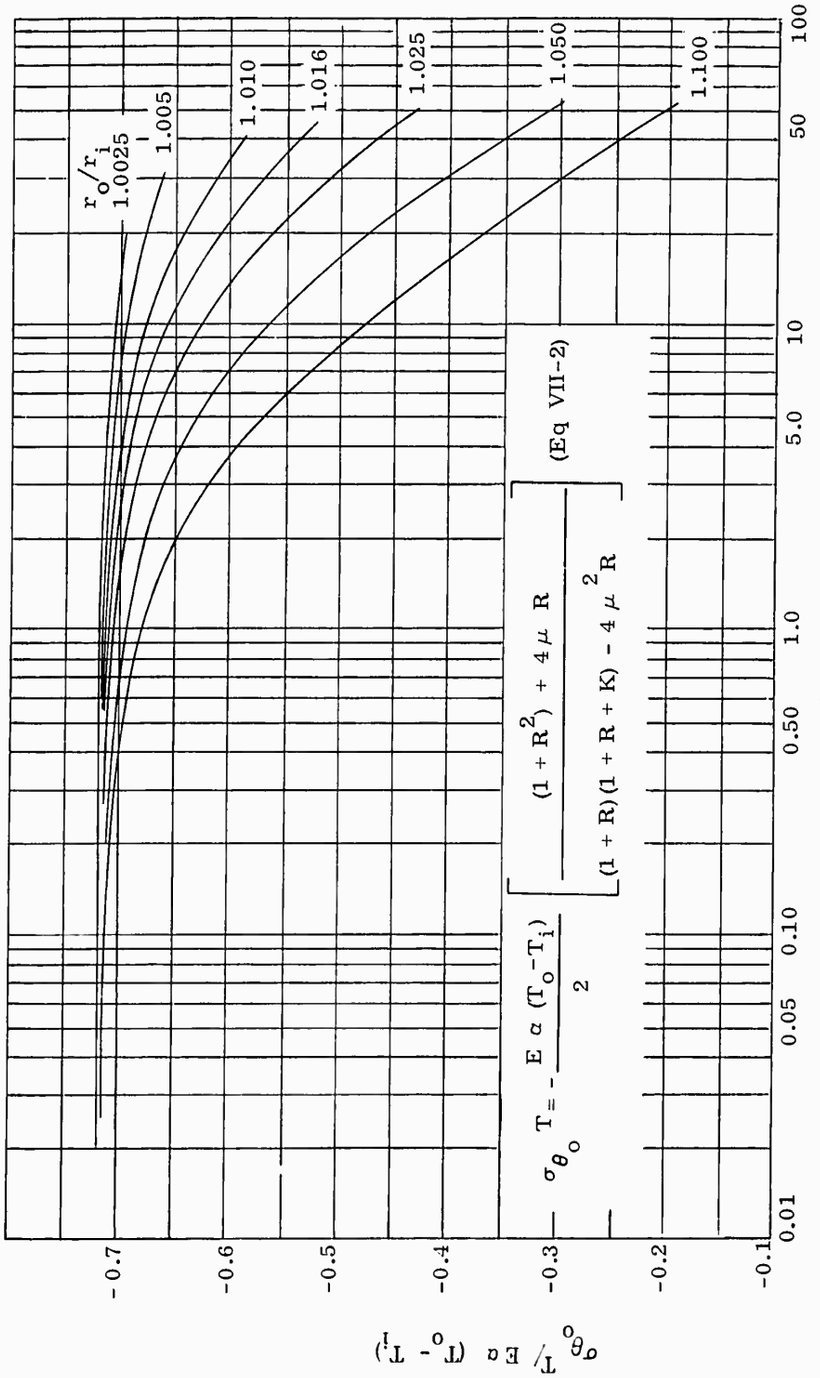

Figure VII-2. Hoop Thermal Stress in Outer Face ($\sigma_{\theta_o}{}^T$) of a Sandwich Cylinder

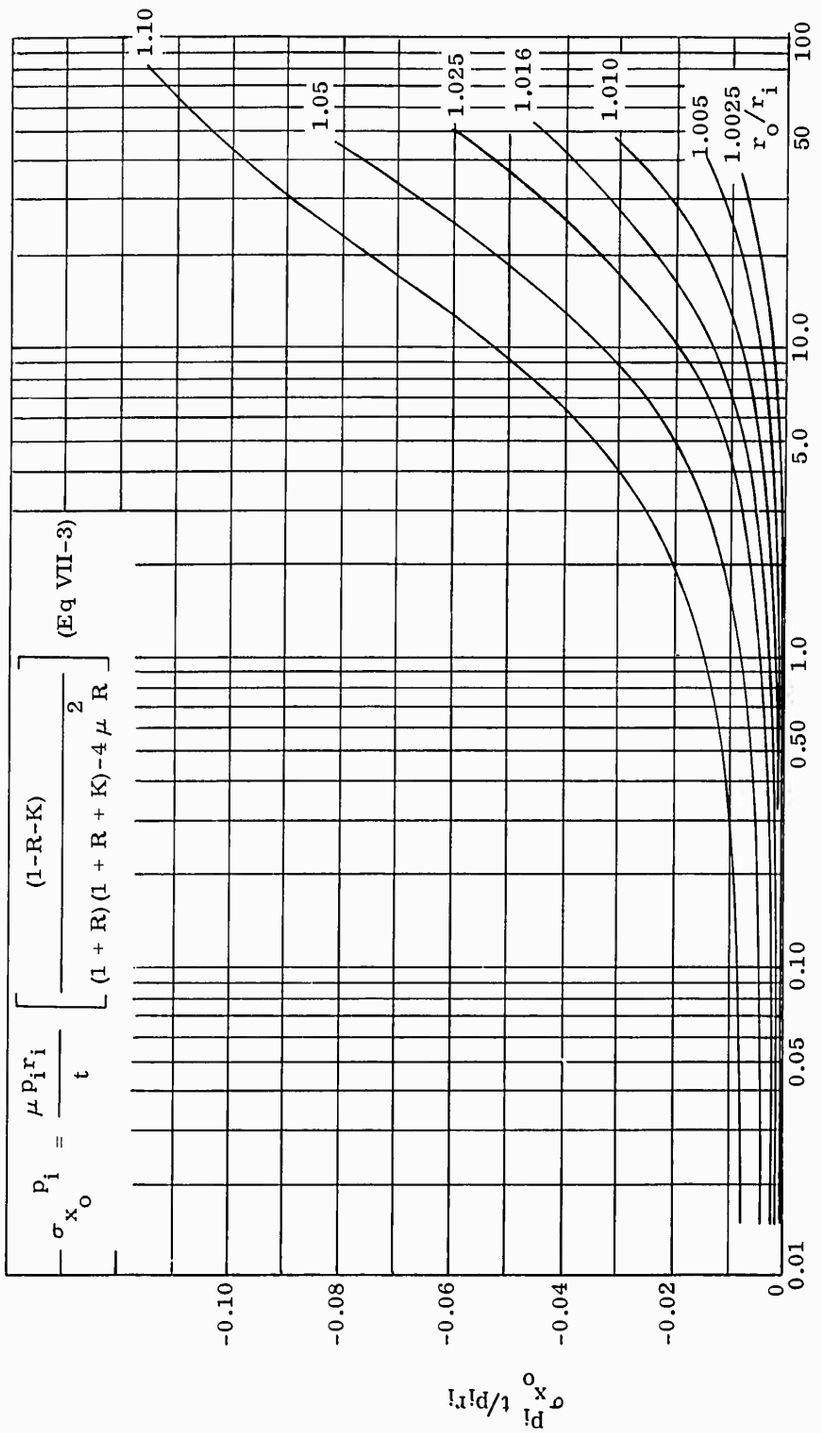

Figure VII-3. Axial Stress in Outer Face of Sandwich Cylinder Due to Internal Pressure ($\sigma_{x_o}^{p_i}$)

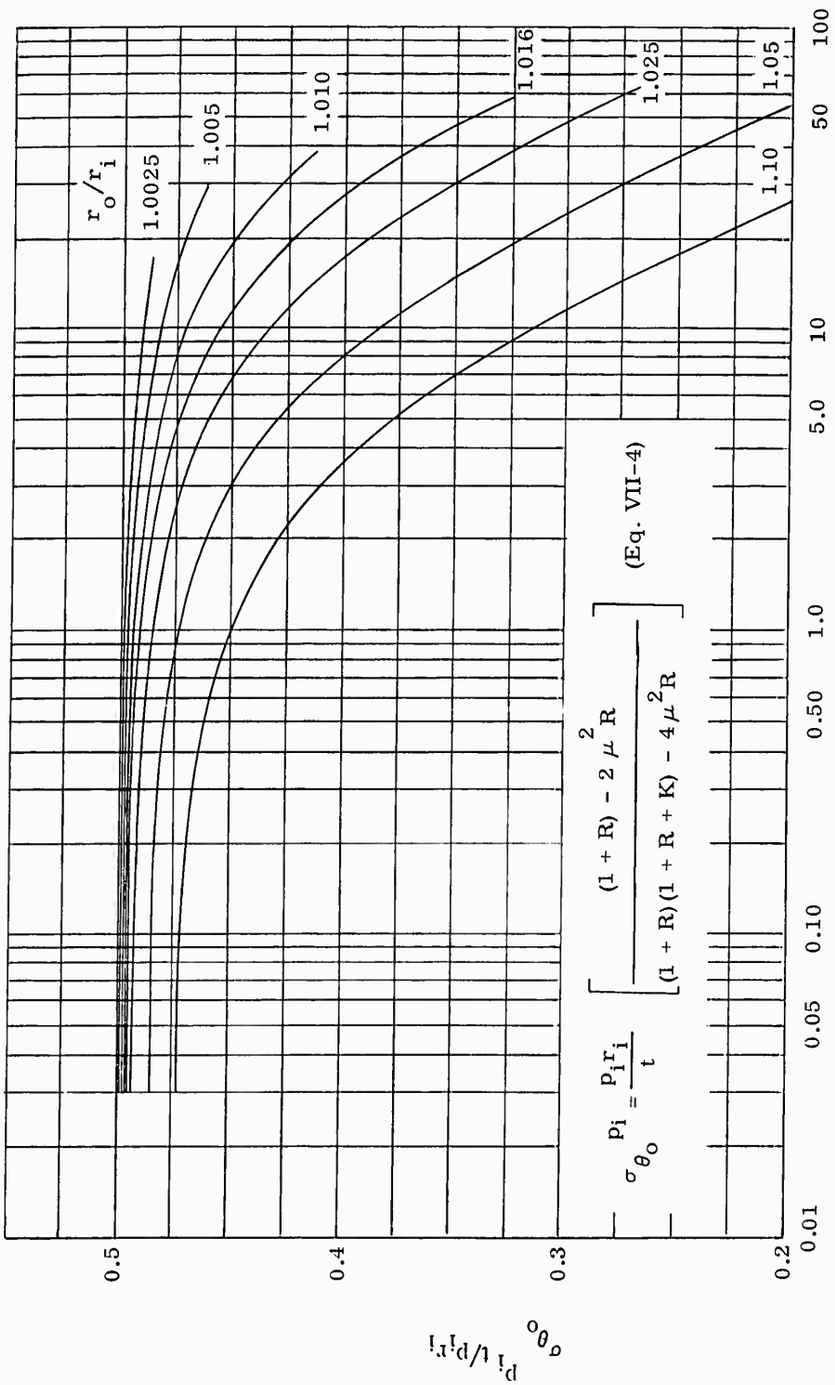

Figure VII-4. Hoop Stress in Outer Face of Sandwich Cylinder Due to Internal Pressure ($\sigma_{\theta_o}{}^{p_i}{}_{i}$)

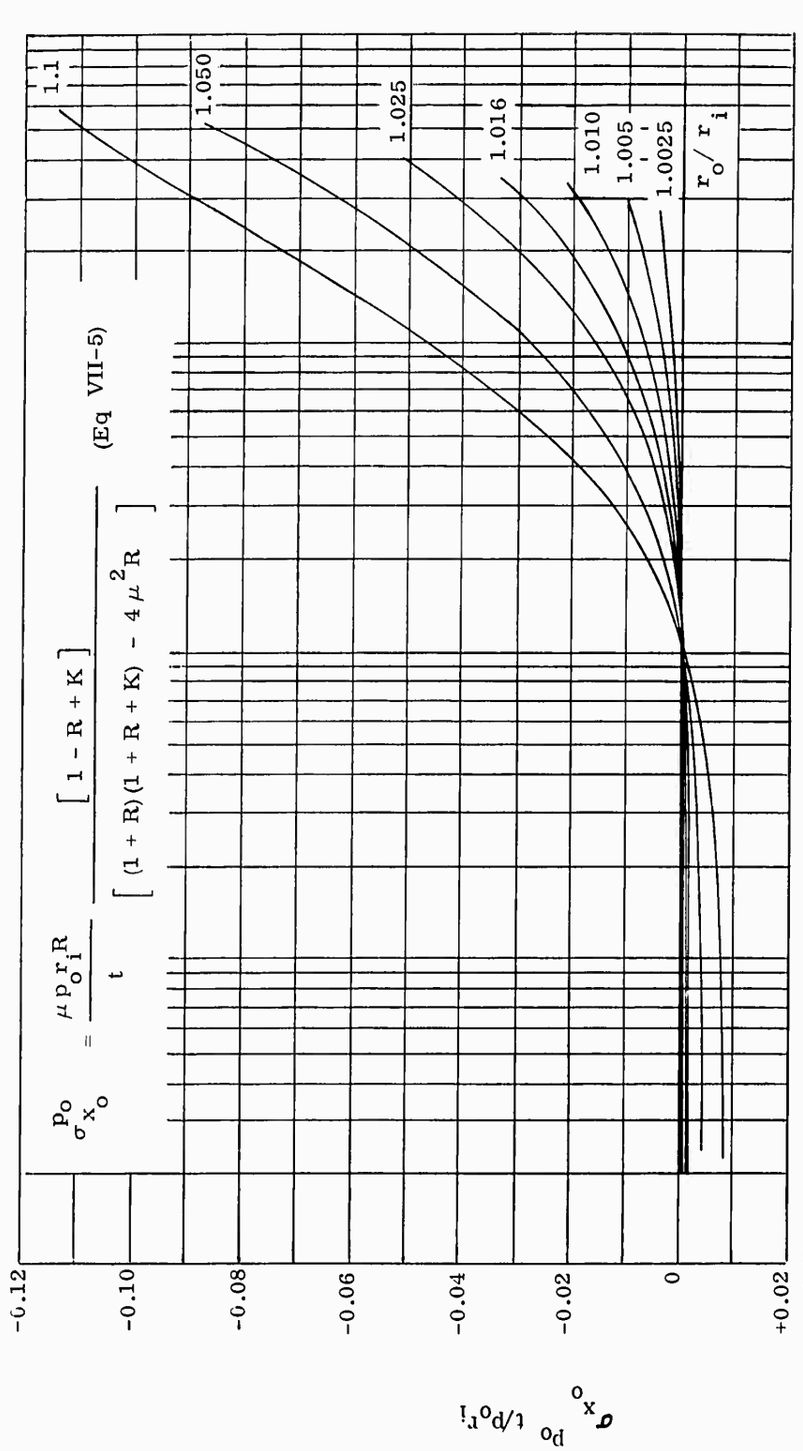

Figure VII-5. Axial Stress in Outer Face of Sandwich Cylinder Due to External Pressure (σ_{x_o} p_o)

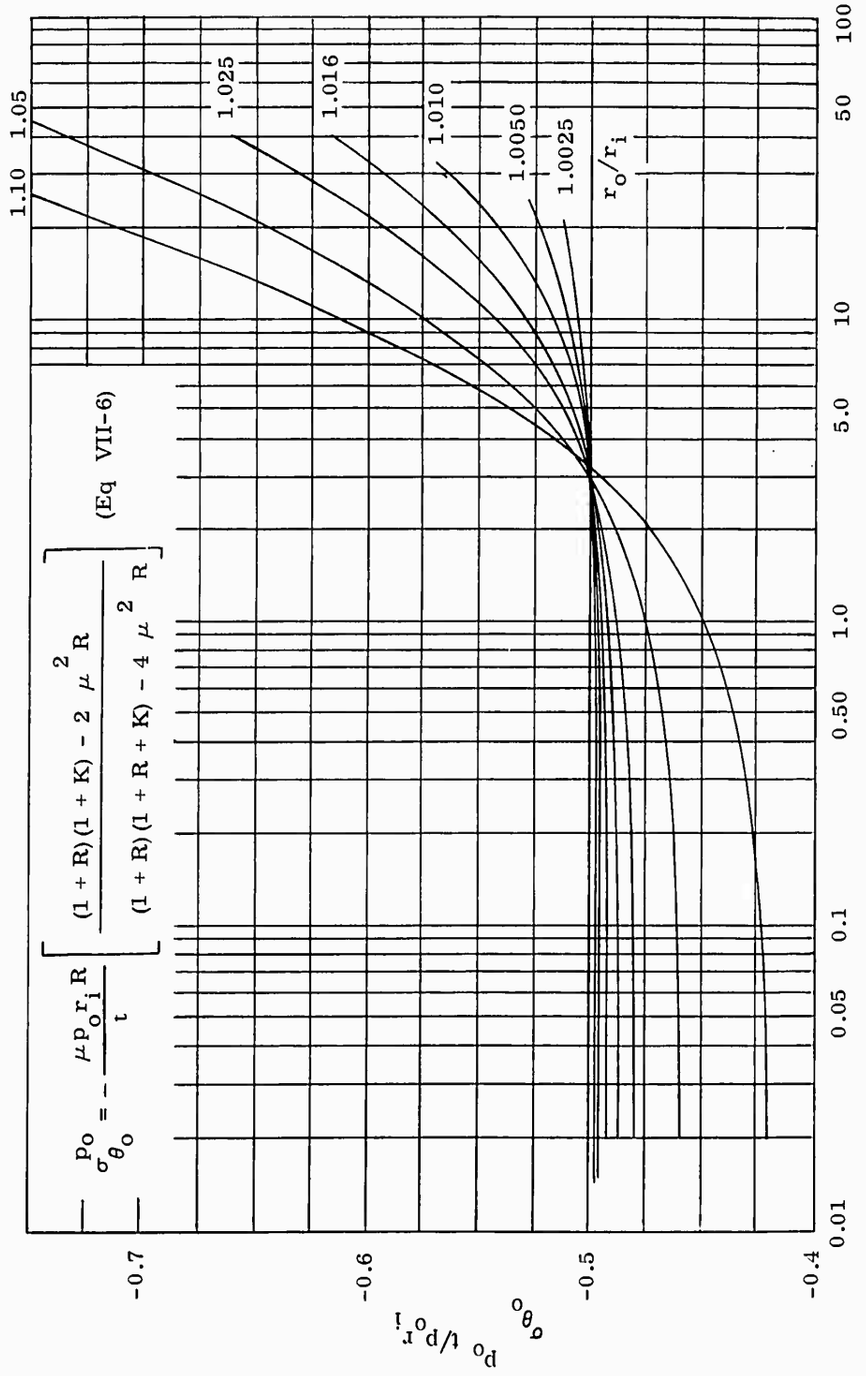

Figure VII-6 Hoop Stress in Outer Face of Sandwich Cylinder Due to External Pressure ($\sigma_{\theta_o}^{p_o}$)

APPENDIX A

BUCKLING OF SANDWICH PANELS UNDER NONUNIFORM STRESS

The governing differential equation for the stability of a sandwich plate composed of equal thickness isotropic faces possessing only stiffness in direct stress and an isotropic core which possesses only shear stiffness (see Figure II-1 in text) can be written in the form (Reference 20)

$$D_s \nabla^4 w + \left(1 - \frac{D_s}{D_q} \nabla^2\right) 2t \sigma_x \frac{\partial^2 w}{\partial x^2} = 0 \qquad \text{(A-1)}$$

where D_s is the panel bending stiffness

D_q is the core shear stiffness

$$\nabla^2 = \frac{\partial^2}{\partial x^2} + \frac{\partial^2}{\partial y^2}$$

and $$\nabla^4 = \nabla^2 \nabla^2$$

To solve Equation (A-1), the displacement is first assumed as

$$w = W \sin \lambda x \qquad \text{(A-2)}$$

where W is a function of y only and λ is a parameter involving the buckle wavelength in the longitudinal (x) direction. Using Equation (A-2) in (A-1) and introducing a nondimensionalization of the stress distribution through use of $\rho_y = \frac{\sigma_x}{\sigma_{cr}}$, one obtains

$$\left[\lambda^4 W - 2\lambda^2 W^{II} + W^{IV}\right] - \frac{2t\sigma_{cr}}{D_s} \lambda^2 \left[\left(1 + \frac{D_s \lambda^2}{D_q}\right) \rho_y W - \frac{D_s}{D_q} (\rho_y W)^{II}\right] = 0 \qquad \text{(A-3)}$$

where the primes on W and ($\rho_y W$) indicate derivatives with respect to y. Note that the introduction of ρ_y serves to establish a single parameter (σ_{cr}) which characterizes instability in the presence of nonuniformly distributed stresses.

Finite differences are used to reduce this equation to algebraic form. With 9 intervals (see Figure II-1) and second order finite differences one obtains the following evaluation of Equation (A-3) at an arbitrary point k

$$\left\{-2\left[W_{k-3}+W_{k+3}\right]+\left[W_{k-2}+W_{k+2}\right]\left(24+\frac{2}{81}\Lambda\right)\right.$$
$$\left.-\left[W_{k-1}+W_{k+1}\right]\left(78+\frac{32}{81}\Lambda\right)+W_k\left(12+\frac{20}{27}\Lambda+12\left(\frac{\Lambda}{81}\right)^2\right)\right\}$$
$$-\Pi\frac{\Lambda}{81}\left\{\rho_{k-2}W_{k-2}-16\rho_{k-1}W_{k-1}+\rho_k W_k\left(30+\frac{4}{27}\Lambda+\frac{4}{27}D_p\right)\right.$$
$$\left.-16\rho_{k+1}W_{k+1}+\rho_{k+2}W_{k+2}\right\}=0 \qquad \text{(A-4)}$$

where $\Pi=\frac{2t\sigma_{cr}}{D_q}$, $D_p=\frac{D_q b^2}{D_s}$ and $\Lambda=(\lambda b)^2$

The boundary conditions on W are:

For simple support

$W_0 = W_9 = 0$, $W_{-1} = -W_1$, $W_{-2} = -W_2$, $W_{10} = -W_8$ and $W_{11} = -W_7$

For fixed support

$W_0 = W_9 = 0$, $W_{-1} = W_1$, $W_{-2} = W_2$, $W_{10} = W_8$ and $W_{11} = W_7$

The boundary conditions on ρ must be based on an extrapolation of the stress distribution beyond the edges of the plate. (Although there is no loading outside of the edges of the plate (i.e., in actuality $\rho_i = 0$ for $i < 0$ and $i > 9$) the use of finite differences requires the introduction of fictitious exterior loadings if the stress variation in the intervals adjacent to the edges are to be represented properly).

With use of the boundary conditions, Equation (A-4) can be adapted to each of the eight internal points, obtaining thereby eight simultaneous equations with coefficients W_1, ---W_8. These equations can be written in matrix form as follows

$$\left[\left[A\right]-\Pi\Lambda\left[B\right]\right]\left\{W\right\}=0 \qquad \text{(A-5)}$$

The matrices $\left[A\right]$ and $\left[B\right]$ are presented in Figures A-1 and A-2, respectively. Both simply supported and fully fixed edges are included.

The condition for buckling is that the determinant of Equation (A-5) shall vanish. A more attractive solution procedure is through matrix iteration, however, since direct evaluation of the determinant would lead to a somewhat complex polynomial of eighth order in Π. To permit matrix iteration, Equation (A-5) is rearranged as follows:

$$\frac{1}{\Pi\Lambda}\left\{W\right\}=\left[A\right]^{-1}\left[B\right]\left\{W\right\} \qquad \text{(A-6)}$$

	W_1	W_2	W_3	W_4	W_5	W_6	W_7	W_8
1	$112+60\left(\frac{\Lambda}{81}\right)+12\left(\frac{\Lambda}{81}\right)^2 + \delta\left(24+2\left(\frac{\Lambda}{81}\right)\right)$							
2	$-78-32\left(\frac{\Lambda}{81}\right)-2\delta$	$112+60\left(\frac{\Lambda}{81}\right)+12\left(\frac{\Lambda}{81}\right)^2$			(SYMMETRIC)			
3	$24+2\left(\frac{\Lambda}{81}\right)$	$-78-32\left(\frac{\Lambda}{81}\right)$	$112+60\left(\frac{\Lambda}{81}\right)+12\left(\frac{\Lambda}{81}\right)^2$					
4	-2	$24+2\left(\frac{\Lambda}{81}\right)$	$-78-32\left(\frac{\Lambda}{81}\right)$	$112+60\left(\frac{\Lambda}{81}\right)+12\left(\frac{\Lambda}{81}\right)^2$				
5	0	-2	$24+2\left(\frac{\Lambda}{81}\right)$	$-78-32\left(\frac{\Lambda}{81}\right)$	$112+60\left(\frac{\Lambda}{81}\right)+12\left(\frac{\Lambda}{81}\right)^2$			
6	0	0	-2	$24+2\left(\frac{\Lambda}{81}\right)$	$-78-32\left(\frac{\Lambda}{81}\right)$	$112+60\left(\frac{\Lambda}{81}\right)+12\left(\frac{\Lambda}{81}\right)^2$		
7	0	0	0	-2	$24+2\left(\frac{\Lambda}{81}\right)$	$-78-32\left(\frac{\Lambda}{81}\right)$	$112+60\left(\frac{\Lambda}{81}\right)+12\left(\frac{\Lambda}{81}\right)^2$	
8	0	0	0	0	-2	$24+2\left(\frac{\Lambda}{81}\right)$	$-78-32\left(\frac{\Lambda}{81}\right)-2\delta$	$112+60\left(\frac{\Lambda}{81}\right)+12\left(\frac{\Lambda}{81}\right)^2 + \delta\left(24+2\left(\frac{\Lambda}{81}\right)\right)$

For Simply Supported Edges $\delta = -1$
For Fully Built-In Edges $\delta = +1$

Figure A-1. [A] Matrix

	W_1	W_2	W_3	W_4	W_5	W_6	W_7	W_8
1	$+L\,\rho_1 + \delta\rho_{-1}$	$-16\,\rho_2$	$+\,\rho_3$	0	0	0	0	0
2	$-16\,\rho_1$	$+L\,\rho_3$	$-16\,\rho_3$	$+\,\rho_4$	0	0	0	0
3	$+\,\rho_1$	$-16\,\rho_2$	$+L\,\rho_3$	$-16\,\rho_4$	$+\,\rho_5$	0	0	0
4	0	$+\,\rho_2$	$-16\,\rho_3$	$+L\,\rho_4$	$-16\,\rho_5$	$+\,\rho_6$	0	0
5	0	0	$+\,\rho_3$	$-16\,\rho_4$	$+L\,\rho_5$	$-16\,\rho_6$	$+\,\rho_7$	0
6	0	0	0	$+\,\rho_4$	$-16\,\rho_5$	$+L\,\rho_6$	$-16\,\rho_7$	$+\,\rho_8$
7	0	0	0	0	$+\,\rho_5$	$-16\,\rho_6$	$+L\,\rho_7$	$-16\,\rho_8$
8	0	0	0	0	0	$+\,\rho_6$	$-16\,\rho_7$	$+L\,\rho_8 + \delta\rho_{10}$

Where: $L = \left[\frac{12D_p}{81} + \frac{12\Lambda}{81} + 30 \right]$

Figure A-2. $[B]$ Matrix

Then, iteration of Equation (A-6) is performed, starting with an initially assumed vector $\{W\}$, until convergence on the eigenvector $\{W\}_{cr}$ and eigenvalue $\left(\frac{1}{\Pi\Lambda}\right)_{cr}$ is achieved.

For this type of problem it has been found, under certain conditions, that an oscillation will occur in the iterative process. The process converges on two different vectors such that the vectors $\{W\}_p$, $\{W\}_{p+2}$ are identical and $\{W\}_{p+1}$, $\{W\}_{p+3}$ are identical (the subscript p designates the p^{th} iterative cycle). This case occurs when the matrix being iterated upon has two roots equal in magnitude but differing in sign. The relevant eigenvalues are then the two square roots of the product of the two apparent eigenvalues, i.e.,

$$\left(\frac{1}{\Pi\Lambda}\right)_{cr} = \pm\sqrt{\left(\frac{1}{\Pi\Lambda}\right)_{p} \left(\frac{1}{\Pi\Lambda}\right)_{p+1}} \qquad \text{(A-7)}$$

The above condition occurs in practice when the applied loading is a bending moment across the width of the panel. It is obvious that the same value of moment will induce buckling independent of whether the moment acts in either of two opposing directions.

The analysis procedure, as described above, yields a critical stress that corresponds to one preselected value of λ, the buckling wavelength parameter. As λ is varied the critical stress will vary, reaching a minimum for an as-yet unknown value of λ. To establish this absolute minimum, one can first select a range of λ's, and calculate for each the corresponding critical stress parameter, Π. Next, employing these results, a polynominal Π versus λ relationship is established through use of a curve-fitting technique. The minimum Π is then obtained through solution of the equation resulting from the condition $\frac{d\Pi}{d\lambda} = 0$.

The value of the critical buckling stress parameter is a function of

(1) The panel stiffness (represented by the parameter D_p).

(2) The buckle wavelength (represented by the parameter λ), and

(3) The applied load distribution (described by the parameter ρ_y).

Wavelength considerations are taken into account by the scheme described above. Thus, it is only necessary to decide which ranges of the parameters D_p and ρ_y are of practical interest. A discussion of this question is given in Chapter II.

In order to establish effectively convergent results all computations were performed for two mesh sizes, the first being the 9-interval solution described here

and the second an 18-interval scheme. In general, the differences between the results for the two schemes were of the order of 0.4%. In view of the unavoidable inaccuracies in the graphical representations which have been made of the computed results, the usefulness of any improvement of the results through an extrapolation technique is negated.

APPENDIX B

PROCEDURE FOR DETERMINING THE STRESSES AND DISPLACEMENTS FOR A RECTANGULAR SANDWICH PANEL

The governing small deflection theory differential equation for rectangular sandwich panels subjected to normal pressure, uniform inplane loading, and a constant temperature gradient through its thickness has been developed in Reference 22. This equation, derived from elemcntary equilibrium, compatibility, and stress-strain relationships, is applicable to a sandwich panel having unequal shear stiffnesses but equal bending stiffnesses with respect to the two principal directions. For the purpose of developing the design curves described in Chapter III, it was deemed desirable to consider only rectangular sandwich plates having isotropic cores and subjected to uniaxial inplane compression and uniform normal pressure. In this case, the differential equation reduces to the form

$$\frac{(1-\mu)D_s}{\eta_x D_q}\left[(1+\eta_x)\frac{\partial^6 w}{\partial x^6} + 2(1+\eta_x)\frac{\partial^6 w}{\partial x^4 \partial y^2} + (3+\eta_x)\frac{\partial^6 w}{\partial x^2 \partial y^4} + \frac{\partial^6 w}{\partial y^6}\right]$$

$$- \frac{1}{\eta_x}\left[(2+(3-\mu)\eta_x)\frac{\partial^4 w}{\partial x^4} + (4+(3-\mu)\eta_x)\frac{\partial^4 w}{\partial x^2 \partial y^2} + 2\frac{\partial^4 w}{\partial y^4}\right]$$

$$+ \frac{2D_q}{D_s}\frac{\partial^2 w}{\partial x^2} = -\frac{2p}{D_s \eta_x} \qquad \text{(B-1)}$$

where $\eta_x = \frac{N_x}{D_q}$ and N_x is the inplane loading in the x - direction (see Figure III-1 in Chapter III), p is the uniform normal pressure.

Since, for the boundary conditions of present interest, an exact solution to (B-1) cannot be obtained, a series solution is effected. The complementary function portion of the solution (w_c) is taken to have the form

$$w_c = \sum_{n=1}^{\infty} X \cos\frac{n\pi y}{b} + \sum_{m=1}^{\infty} Y \cos\frac{m\pi x}{a} \qquad \text{(B-2)}$$

where X is a function of x only
and Y is a function of y only.

Substitution of Equation (B-2) into (B-1) yields two differential equations.

$$\frac{(1-\mu)D_s}{\eta_x D_q}(1+\eta_x)\frac{d^6X}{dx^6} - \left[\frac{2(1-\mu)D_s}{\eta_x D_q}\left(\frac{n\pi}{b}\right)^2(1+\eta_x)+\frac{1}{\eta_x}(2+(3-\mu)\eta_x)\right]\frac{d^4X}{dx^4}$$

$$+\left[\frac{(1+\mu)D_s}{\eta_x D_q}\left(\frac{n\pi}{b}\right)^4(3+\eta_x)+\frac{1}{\eta_x}\left(\frac{n\pi}{b}\right)^2(4+(3-\mu)\eta_x)+\frac{2D_q}{D_s}\right]\frac{d^2X}{dx^2}$$

$$-\left[\frac{(1-\mu)D_s}{\eta_x D_q}\left(\frac{n\pi}{b}\right)^6+\frac{2}{\eta_x}\left(\frac{n\pi}{b}\right)^4\right]X = 0 \qquad \text{(B-3)}$$

and,

$$\frac{(1-\mu)D_s}{\eta_x D_q}\frac{d^6Y}{dy^6} - \left[\frac{(1-\mu)D_s}{\eta_x D_q}\left(\frac{m\pi}{a}\right)^2(3+\eta_x)+\frac{2}{\eta_x}\right]\frac{d^4Y}{dy^4}$$

$$+\left[\frac{2(1-\mu)D_s}{\eta_x D_q}\left(\frac{m\pi}{a}\right)^4(1+\eta_x)+\frac{1}{\eta_x}\left(\frac{m\pi}{a}\right)^2(4+(3-\mu)\eta_x)\right]\frac{d^2Y}{dy^2}$$

$$-\left[\frac{(1-\mu)D_s}{\eta_x D_q}\left(\frac{m\pi}{a}\right)^6(1+\eta_x)+\frac{1}{\eta_x}\left(\frac{m\pi}{a}\right)^4(2+(3-\mu)\eta_x)+\frac{2D_q}{D_s}\left(\frac{m\pi}{a}\right)^2\right]Y$$

$$= 0 \qquad \text{(B-4)}$$

Equations (B-3) and (B-4) are ordinary linear differential equations and can be readily solved to yield expressions for X and Y. Also, the particular integral can be obtained, using procedures described in Reference 22, resulting in the following complete expression for the deflection

$$w = \frac{D_s}{\eta_x D_q} \left\{ \sum_{n(odd)}^{\infty} \left[K_1 \left(\frac{1-\phi_1^2}{\phi_1^2} \right) \cosh \phi_1 \frac{n\pi x}{b} + K_2 \left(\frac{1-\phi_2^2}{\phi_2^2} \right) \cosh \phi_2 \frac{n\pi x}{b} + K_3 \left(\frac{1-\phi_3^2}{\rho_3^2} \right) \cosh \phi_3 \frac{n\pi x}{b} \right] \cos \frac{n\pi y}{b} \right.$$

$$+ \sum_{m(odd)}^{\infty} \left[K_4 (\phi_4^2 - 1) \cosh \phi_4 \frac{m\pi y}{a} + K_5 (\phi_5^2 - 1) \cosh \phi_5 \frac{m\pi y}{a} + K_6 (\phi_6^2 - 1) \cosh \phi_6 \frac{m\pi y}{a} \right] \cos \frac{m\pi x}{a}$$

$$\left. + \frac{p}{2D_s} \left[\left(\frac{a^2}{4} - x^2 \right) - \left(\frac{b^2}{4} - y^2 \right) \right] \right\} \qquad \text{(B-5)}$$

where $\phi_1, \cdots \phi_6$ are the roots of the cubic auxiliary equations of Equations (B-3) and (B-4) and $K_1, \cdots K_6$ are the six constants required to satisfy the boundary conditions. It can occur for some combinations of dimensions etc. that the auxiliary equations have complex roots. In such cases ϕ_1 and ϕ_2 become complex conjugates and ϕ_5 is purely imaginary. In principle the hyperbolic functions with complex arguments should be transformed into the appropriate trigonometric and hyperbolic functions. However, if the complete computation is carried out using a complex mode, as is possible in FORTRAN-coded programs, it is not necessary to perform this transformation and the present algebraic form can be retained without loss of generality.

For the special case of $\eta_x = 0$ (no midplane force), equal roots occur in the two auxiliary equations, so that

$$\phi_1 = \phi_2 = 1 \qquad \text{and } \phi_4 = \phi_5 = 1$$

and the deflection function has the slightly different form

$$w = \sum_{n(odd)}^{\infty} \left[K_{01} \frac{n\pi x}{b} \sinh \frac{n\pi x}{b} + K_{01} \cosh \frac{n\pi x}{b} + K_{03} \cosh \phi_3 \frac{n\pi x}{b} \right] \cos \frac{n\pi y}{b}$$

$$+ \sum_{m(odd)}^{\infty} \left[K_{04} \frac{m\pi y}{a} \sinh \frac{m\pi x}{a} + K_{05} \cosh \frac{m\pi y}{a} + K_{06} \cosh \phi_6 \frac{m\pi y}{a} \right] \cos \frac{m\pi x}{a}$$

$$+ \frac{p}{48 D_s} \left[\left(x^4 - \frac{a^4}{16} \right) + \left(y^4 - \frac{b^4}{16} \right) \right] \qquad \text{(B-6)}$$

The solutions presented in Chapter III can be divided into the following three classes of problems:

(1) Simple support on all edges with a uniform normal pressure and a constant temperature difference between thefaces. ($\eta_x = 0$.)

(2) As in case (1) but with the addition of uniaxial uniformly distributed inplane compression. ($\eta_x \neq 0$).

(3) Simple support on two opposite edges and fixed support on the other two edges and with same loading as case (1).

The boundary conditions pertinent to these cases are as follows:

For Cases (1) and (2)

at $x = \pm \frac{a}{2}$: $w = 0$, $M_x = 0$, $V_y = 0$

at $y = \pm \frac{b}{2}$: $w = 0$, $M_y = 0$, $V_x = 0$

where V_x and V_y are vertical shear stress resultants in the core

For Case (3)

at $x = \pm \frac{a}{2}$: $w = 0$, $M_x = 0$, $M_{xy} = 0$

at $y = \pm \frac{b}{2}$: $w = 0$, $\beta_y = 0$, $M_{xy} = 0$

where M_{xy} is the twisting moment and β_y is the rotation of the vertical fibers of the core. Note that although the classic solution for an isotropic plate requires only two boundary conditions, three are required for a sandwich panel.

Substitution of the above conditions into the appropriate expressions for moment and shear leads to simultaneous equations from which the constants (K_1--K_6 or K_{01}---K_{06}) are extracted. The deflections and moments are then obtained by back substitution into the pertinent expressions.

In cases (1) and (2) the series involved are orthogonal while in case (3) they are non-orthogonal. Thus, in cases (1) and (2), the individual constants can be determined directly for any given term of the series, defined by m or n, independently of any other term of the series and the problem is reduced to the simple solution of two groups of three simultaneous equations in K_1, K_2, K_3 and K_4, K_5, K_6. In the computer program employed for solutions to case (1) and (2) problems, a convergence criterion is used to select the number of terms in the series.

In case (3) the values of K_1---K_6 for any term of the series depend on all other terms. For a series of n terms, 6n simultaneous equations must be solved. Here, since the computational time will be quite long for a series with many terms, both convergence and computational efficiency considerations have been used to govern the number of terms selected.

APPENDIX C

SANDWICH CYLINDER INSTABILITY UNDER CIRCUMFERENTIALLY VARYING AXIAL STRESS

This problem concerns the prediction of the elastic instability of a circular cylinder of sandwich construction subjected to axial stresses that vary in the circumferential direction. The geometric and load conditions for this problem have been detailed in Chapter IV (see Figure IV-1).

The solution approach is essentially the same as that employed for isotropic cylinder analysis in Reference 9. There, Donnell's partial differential equation has reduced to an ordinary differential equation by assuming the buckled shape to be sinusoidal in the axial direction. Then, the ordinary differential equation was reduced to a set of algebraic equations through use of second-order finite differences and matrix iteration was applied in determination of the eigenvalues and eigenvectors.

Now, Donnell's equation, modified to apply to a sandwich cylinder, becomes: (see Reference 13).

$$D_s \nabla^8 w + 2tr^2 \left(1 - \frac{D_s}{D_q r^2} \nabla^2 \right) \left(E \frac{\partial^4 w}{\partial x^4} + \nabla^4 \sigma_x \frac{\partial^2 w}{\partial x^2} \right) = 0 \quad \text{(C-1)}$$

where x in this case is a non-dimensionalized axial coordinate (the axial coordinate divided by the radius).

The displacement w is assumed to be of the form

$$w = W \sin \lambda x \quad \text{(C-2)}$$

where W is a function of the circumferential coordinate (y) only, and λ is a function of the wavelength in the axial direction.

Substituting Equation (C-2) into (C-1) and introducing a nondimensionalization of the stress distribution similar to that used for the flat panel in Chapter II and Appendix A, the differential equation reduces to

$$\left[\left(D_s \lambda^8 + 2 tr^2 E \lambda^4 + 2 tr^2 \frac{E \lambda^6}{D_c} \right) W - \left(4 D_s \lambda^6 + 2 tr^2 \frac{E \lambda^4}{D_c} \right) W^{II} \right.$$

$$\left. + 6 D_s \lambda^4 W^{IV} - 4 D_s \lambda^2 W^{VI} + D_s W^{VIII} \right]$$

$$- 2 tr^2 \sigma_{cr} \left[\lambda^6 \left(1 + \frac{\lambda^2}{D_c}\right) (\rho_s W) - \lambda^4 \left(2 + \frac{3\lambda^2}{D_c}\right) (\rho_s W)^{II} \right.$$

$$\left. + \lambda^2 \left(1 + \frac{3\lambda^2}{D_c}\right) (\rho_s W)^{IV} - \frac{\lambda^2}{D_c} (\rho_s W)^{VI} \right] = 0 \qquad \text{(C-3)}$$

where primes indicate derivatives with respect to y only and $D_c = \frac{D_q r^2}{D_s}$.

The conditions examined are limited to stress variations which are symmetric about the vertical (z) axis. In order to write Equation C-3 in terms of finite differences, the circumference of the cylinder is divided into 2n spacings, each of length $r\pi/n$, as shown in Figure IV-1. Note that elements 0 and n lie on the axis of symmetry. With use of second order finite differences, C-2 reduces to

$$\left[- \left(W_{k-5} + W_{k+5} \right) A_1 + \left(W_{k-4} + W_{k+4} \right) A_2 - \left(W_{k-3} + W_{k+3} \right) A_3 \right.$$

$$\left. + \left(W_{k-2} + W_{k+2} \right) A_4 - \left(W_{k-1} + W_{k+1} \right) A_5 + W_k A_6 \right]$$

$$- \Pi \left[\left(\rho_{k-4} W_{k-4} + \rho_{k+4} W_{k+4} \right) B_1 - \left(\rho_{k-3} W_{k-3} + \rho_{k+3} W_{k+3} \right) B_2 \right.$$

$$\left. + \left(\rho_{k-2} W_{k-2} + \rho_{k+2} W_{k+2} \right) B_3 - \left(\rho_{k-1} W_{k-1} + \rho_{k+1} W_{k+1} \right) B_4 \right.$$

$$\left. + \rho_k W_k B_5 \right] = 0 \qquad \text{(C-4)}$$

where

$$A_1 = \frac{\Lambda^4}{3} \qquad A_2 = \Lambda^3 \left(\frac{13\Lambda}{3} + 1 \right)$$

$$A_3 = \Lambda^2 (23\Lambda^2 + 12\Lambda + 1)$$

$$A_4 = \Lambda \left(68\Lambda^3 + 52\Lambda^2 + 12\Lambda + \frac{1}{3} + \frac{\pi^2 K \Lambda}{6n^2 D_c}\right)$$

$$A_5 = \Lambda \left(126\Lambda^3 + 116\Lambda^2 + 39\Lambda + \frac{16}{3} + \frac{8\pi K\Lambda}{3n^2 D_c}\right)$$

$$A_6 = (154\Lambda^4 + 150\Lambda^3 + 56\Lambda^2 + 10\Lambda + 1 + \frac{\pi^2 K\Lambda}{n^2 D_c}(5\Lambda + 2) + \frac{2\pi^4 K\Lambda^2}{n^4})$$

$$B_1 = \frac{K\Lambda^3}{2D_c} \qquad B_2 = \frac{K\Lambda^2}{D_c}(6\Lambda + 1 + \frac{D_c \Lambda \pi^2}{3n^2})$$

$$B_3 = \frac{K\Lambda}{D_c}\left(26\Lambda^2 + 12\Lambda + \frac{1}{2} + \frac{\Lambda D_c \pi^2}{3n^2}(12\Lambda + 1)\right)$$

$$B_4 = \frac{K\Lambda}{D_c}\left(58\Lambda^2 + 39\Lambda + 8 + \frac{\Lambda D_c \pi^2}{3n^2}(39\Lambda + 16)\right)$$

$$B_5 = \frac{K}{D_c}\left(75.\Lambda^3 + 56\Lambda^2 + 15\Lambda + 2 + \frac{2\Lambda D_c \pi^2}{3n^2}(28\Lambda^2 + 15\Lambda + 3)\right)$$

$$\Lambda = \frac{n^2}{\pi^2 \lambda^2}$$

$$K = \frac{2(1-\mu^2)r^2}{(h+t)^2}$$

$$\Pi = \frac{\sigma_{cr}}{E}$$

Equation (C-4) can be written for each pivotal point, resulting in (n + 1) simultaneous equations in the W's for one-half of the cylinder (as noted above, symmetry permits the analysis to proceed on the basis of one-half of the cylinder). For points affected by the boundaries at the top and bottom of the cylinder, the following boundary conditions are applicable:

$$W_{-p} = W_p \qquad \text{and } W_{n-p} = W_{n+p} \qquad (p \leq 5)$$

As in Appendix A, the resulting algebraic equations can be cast in the matrix form

$$\left[\left[A\right] + \Pi\left[B\right]\right]\left\{W\right\} = 0 \qquad \text{(C-5)}$$

The matrices $[A]$ and $[B]$ are presented in Figures C-1 and C-2, respectively. The dominant eigenvalue, $\frac{1}{\Pi}$, corresponding to the lowest critical stress, can be extracted from Equation C-5 in the manner outlined in Appendix A.

	W_o	W_1	W_2	W_3	W_4	W_5								
0	A_6	$-2A_5$	$2A_4$	$-2A_3$	$2A_2$	$-2A_1$	0	0	0	0				
1	$-A_5$	(A_4+A_6)	$-(A_3+A_5)$	(A_2+A_4)	$-(A_1+A_3)$	A_2	$-A_1$	0	0	0				
2	A_4	$-(A_3+A_5)$	(A_2+A_6)	$-(A_1+A_5)$	A_4	$-A_3$	A_2	$-A_1$	0	0				
3	$-A_3$	(A_2+A_4)	$-(A_1+A_5)$	A_6	$-A_5$	A_4	$-A_3$	A_2	$-A_1$				0	
4	A_2	$-(A_1+A_3)$	A_4	$-A_5$	A_6	$-A_5$	A_4	$-A_3$				0	0	
	$-A_1$	A_2	$-A_3$	A_4	$-A_5$	A_6	$-A_5$				$-A_1$	0	0	
	0	$-A_1$	A_2	$-A_3$	A_4					$-A_3$	A_2	$-A_1$	0	
	0	0	$-A_1$	A_2				A_6	$-A_5$	A_4	$-A_3$	A_2	$-A_1$	
	0	0	0				A_4	$-A_5$	A_6	$-A_5$	A_4	$-(A_1+A_3)$	A_2	
	0	0				A_2	$-A_3$	A_4	$-A_5$	A_6	$-(A_1+A_5)$	(A_2+A_4)	$-A_3$	n-3
						$-A_1$	A_2	$-A_3$	A_4	$-(A_1+A_5)$	(A_2+A_6)	$-(A_3+A_5)$	A_4	n-2
					0	0	$-A_1$	A_2	$-(A_1+A_3)$	(A_2+A_4)	$-(A_3+A_5)$	(A_4+A_6)	$-A_5$	n-1
				0	0	0	0	$-2A_1$	$2A_2$	$-2A_3$	$2A_4$	$-2A_5$	A_6	n
								W_{n-5}	W_{n-4}	W_{n-3}	W_{n-2}	W_{n-1}	W_n	

Figure C-1 $\left[A\right]$ Matrix

$\rho_o B_5$	$-2\rho_1 B_4$	$2\rho_2 B_3$	$-2\rho_3 B_2$	$2\rho_4 B_1$	0	0	0					
$-\rho_o B_4$	$\rho_1(B_3 \cdot B_5)$	$-\rho_2(B_2 \cdot B_4)$	$\rho_3(B_1 \cdot B_3)$	$-\rho_4 B_2$	$\rho_5 B_1$	0	0					
$\rho_o B_3$	$-\rho_1(B_2 \cdot B_4)$	$\rho_2(B_1 \cdot B_5)$	$-\rho_3 B_4$	$\rho_4 B_3$	$-\rho_5 B_2$	$\rho_6 B_1$	0					
$-\rho_o B_2$	$\rho_1(B_1 \cdot B_3)$	$-\rho_2 B_4$	$\rho_3 B_5$	$-\rho_4 B_4$	$\rho_5 B_3$	$-\rho_6 B_2$	$\rho_7 B_1$					
$\rho_o B_1$	$-\rho_1 B_2$	$\rho_2 B_3$	$-\rho_3 B_4$	$\rho_4 B_5$	$-\rho_5 B_4$							
0	$\rho_1 B_1$	$-\rho_2 B_2$	$\rho_3 B_3$	$-\rho_4 B_4$							0	0
0	0	$\rho_2 B_1$							$-\rho_{n-3} B_2$	$\rho_{n-2} B_1$	0	0
0	0						$\rho_{n-5} B_5$	$-\rho_{n-4} B_4$	$\rho_{n-3} B_3$	$-\rho_{n-2} B_2$	$\rho_{n-1} B_1$	0
						$\rho_{n-6} B_3$	$-\rho_{n-5} B_4$	$\rho_{n-4} B_5$	$-\rho_{n-3} B_4$	$\rho_{n-2} B_3$	$-\rho_{n-1} B_2$	$\rho_n B_1$
					$\rho_{n-7} B_1$	$-\rho_{n-6} B_2$	$\rho_{n-5} B_3$	$-\rho_{n-4} B_4$	$\rho_{n-3} B_5$	$-\rho_{n-2} B_4$	$\rho_{n-1}(B_1 \cdot B_3)$	$-\rho_n B_2$
					0	$\rho_{n-6} B_1$	$-\rho_{n-5} B_2$	$\rho_{n-4} B_3$	$-\rho_{n-3} B_4$	$\rho_{n-2}(B_1 \cdot B_5)$	$\rho_{n-1}(B_2 \cdot B_4)$	$\rho_n B_3$
					0	0	$\rho_{n-5} B_1$	$-\rho_{n-4} B_2$	$\rho_{n-3}(B_1 \cdot B_3)$	$-\rho_{n-2}(B_2 \cdot B_4)$	$\rho_{n-1}(B_3 \cdot B_5)$	$-\rho_n B_4$
					0	0	0	$2\rho_{n-4} B_1$	$-2\rho_{n-3} B_2$	$2\rho_{n-2} B_3$	$-2\rho_{n-1} B_4$	$\rho_n B_5$

Figure C-2. $[B]$ Matrix

APPENDIX D

THERMAL STRESSES AND BENDING MOMENTS IN A HEATED SANDWICH CYLINDER SUPPORTED BY RIGID BULKHEADS

A sandwich cylinder of cross-sectional properties identical to those assigned to the sandwich cylinder of Appendix C, but of finite length 2c, is supported at each end by a rigid bulkhead. The cylinder may be continuous over several bays, so that each bay is effectively built-in at the rigid bulkheads due to symmetry, or one bay alone may be considered with simply supported ends. The cylinder is uniformly heated so that a temperature change from the stress-free state (Δ T) is sustained, while the bulkheads are unheated.

The subject problem is similar to that of a beam on an elastic foundation. Using this concept, the basic differential equation for the radial deflection (w) is

$$\frac{d^4w}{dx^4} - \frac{2tE}{r^2D_q}\frac{d^2w}{dx^2} + \frac{2tE}{r^2D_s}(w + r\,\alpha\,\Delta T) = 0 \qquad \text{(D-1)}$$

where α is the coefficient of thermal expansion. A general solution for this equation is

$$w = C_1 \cosh m_1\left(\frac{Et}{r^2D_q}\right)^{1/2} x + C_2 \cosh m_2\left(\frac{Et}{r^2D_q}\right)^{1/2} x - r\alpha\Delta T \qquad \text{(D-2)}$$

where m_1 and m_2, the roots of the auxiliary equation, are given (in nondimensional form) by

$$m_1^2 = \left[1 + \sqrt{1 - \frac{2}{H_d}}\right] \quad \text{and,} \quad m_2^2 = \left[1 - \sqrt{1 - \frac{2}{H_d}}\right] \qquad \text{(D-3)}$$

with $$H_d = \frac{EtD_s}{r^2D_q^2} = \frac{Et}{D_cD_q}$$

The roots m_1 and m_2 may be real ($H_d > 2$) or complex ($H_d < 2$). In the latter case, the hyperbolic functions of Equation (D-2) should be modified as follows:

$$\cosh(a + i\,b) = \cosh a \cosh b + i \sinh a \sin b$$

but, as in Appendix B, provided all computations are carried out in a complex mode, it is not necessary to transform the hyperbolic functions.

As noted above, two support conditions - simple and fixed support--are of present interest. Consider first the simple support condition, where the boundary conditions are

$$\text{at } x = \pm c, \quad w = 0 \quad \text{and} \quad M_x = -D_s \left[\frac{d^2w}{dx^2} - \frac{2tE}{r^2 D_q} (w + r\,\alpha\,\Delta T) \right] = 0$$

Using these conditions, the constants C_1 and C_2 are determined and the deflected form becomes

$$w = \frac{r\,\alpha\,\Delta T}{(m_2^2 - m_1^2)} \left[(m_2^2 - 2) \frac{\cosh m_1 H_x}{\cosh m_1 H_1} - (m_1^2 - 2) \frac{\cosh m_2 H_x}{\cosh m_2 H_1} - (m_2^2 - m_1^2) \right] \tag{D-4}$$

where $$H_x = \left(\frac{Et}{D_q} \right)^{1/2} \frac{x}{r} \quad \text{and} \quad H_1 = \left(\frac{Et}{D_q} \right)^{1/2} \frac{c}{r} \tag{D-4a}$$

The formula for hoop stress is

$$\sigma_\phi = - \frac{E}{r} \left[w + r\,\alpha\,\Delta T \right] \tag{D-5}$$

Thus, the hoop stress at the center (at x = 0) is given by

$$\sigma_{\phi_c} = \frac{E\,\alpha\,\Delta T}{(m_1^2 - m_2^2)} \left[\frac{m_2^2 - 2}{\cosh m_1 H_1} - \frac{m_1^2 - 2}{\cosh m_2 H_1} \right] \tag{D-5a}$$

Also, the expression for longitudinal bending moment is

$$M_x = - D_s \left[\frac{d^2w}{dx^2} - \frac{2tE}{r^2 D_q} (w + r\,\alpha\,\Delta T) \right] \tag{D-6}$$

Hence, the maximum bending moment in the cylinder (at the center, x = 0) is

$$M_{x_c} = H_d\, D_q\, r\,\alpha\,\Delta T \frac{(m_1^2 - 2)(m_2^2 - 2)}{(m_1^2 - m_2^2)} \left[\frac{1}{\cosh m_1 H_1} - \frac{1}{\cosh m_2 H_1} \right] \tag{D-6a}$$

With built-in ends, the boundary conditions are

$$\text{at } x = \pm c, \quad w = 0 \quad \text{and} \quad \frac{dw}{dx} = \frac{Q_x}{D_q}$$

where Q_x is the transverse shear force and is given by

$$Q_x = -D_s \left[\frac{d^3w}{dx^3} - \frac{2tE}{r^2 D_q} \frac{dw}{dx} \right] \tag{D-7}$$

so that the second boundary condition becomes

$$\frac{dw}{dx}\ (1-2\,H_d) + \frac{D_s}{D_q}\ \frac{d^3w}{dx^3} = 0 \qquad \text{(D-8)}$$

Use of the above boundary conditions with Equation (D-2) and its derivatives yields the constants C_1 and C_2 for built-in support conditions and leads to the following expression for the radial displacement

$$w = r\alpha\,\Delta T\left[\frac{\left[1-H_d(2-m_2^2)\right]\sinh m_2H_1\cosh m_1H_x - \left[1-H_d(2-m_1^2)\right]\frac{m_1}{m_2}\sinh m_1H_1\cosh m_2H_x}{\left[1-H_d(2-m_2^2)\right]\sinh m_2H_1\cosh m_1H_1 - \left[1-H_d(2-m_1^2)\right]\frac{m_1}{m_2}\sinh m_1H_1\cosh m_2H_1} - 1\right] \qquad \text{(D-9)}$$

The hoop stress at the center is now

$$\sigma_{\phi_c} = -E\alpha\,\Delta T\left[\frac{\left[1-H_d(2-m_2^2)\right]\sinh m_2H_1 - \left[1-H_d(2-m_1^2)\right]\frac{m_1}{m_2}\sinh m_1H_1}{\left[1-H_d(2-m_2^2)\right]\sinh m_2H_1\cosh m_1H_1 - \left[1-H_d(2-m_1^2)\right]\frac{m_1}{m_2}\sinh m_1H_1\cosh m_2H_1}\right] \qquad \text{(D-10)}$$

while the bending moment at the center is given by

$$M_{x_c} = -H_dD_q\,r\alpha\,\Delta T\left[\frac{\left[1-H_d(2-m_2^2)\right](m_1^2-2)\sinh m_2H_1 - \left[1-H_d(2-m_1^2)\right](m_2^2-2)\frac{m_1}{m_2}\sinh m_1H_1}{\left[1-H_d(2-m_2^2)\right]\sinh m_2H_1\cosh m_1H_1 - \left[1-H_d(2-m_1^2)\right]\frac{m_1}{m_2}\sinh m_1H_1\cosh m_2H_1}\right] \qquad \text{(D-11)}$$

Of additional interest is the bending moment at the built-in ends

$$M_{x_c} = -H_dD_q\,r\alpha\,\Delta T\left[\frac{\left[1-H_d(2-m_2^2)\right](m_1^2-2)\sinh m_2H_1\cosh m_1H_1 - \left[1-H_d(2-m_1^2)\right](m_2^2-2)\frac{m_1}{m_2}\sinh m_1H_1\cosh m_2H_1}{\left[1-H_d(2-m_2^2)\right]\sinh m_2H_1\cosh m_1H_1 - \left[1-H_d(2-m_1^2)\right]\frac{m_1}{m_2}\sinh m_1H_1\cosh m_2H_1}\right]$$

(D-12)

APPENDIX E

BUCKLING OF A SANDWICH CYLINDER UNDER THERMALLY INDUCED HOOP STRESS

1. GOVERNING EQUATIONS

Appendix D treats the problem of determining the hoop stresses in a uniformly heated sandwich cylinder supported at either end by rigid unheated bulkheads. This Appendix develops a method for determining the cylinder temperature change, ΔT_{cr}, for which the cylinder will buckle in consequence of the induced hoop thermal stresses. Thus, it is assumed that the hoop thermal stresses will have already been determined by use of the technique of Appendix D.

For the present case, Donnell's equation, modified to apply to sandwich construction, takes the form (Reference 13).

$$D_s \nabla^8 w + 2t \left(1 - \frac{D_s}{D_q} \nabla^2\right) \left(\frac{E}{r^2} \frac{\partial^4 w}{\partial x^4} + \nabla^4 \sigma_y \frac{\partial^2 w}{\partial y^2}\right) = 0 \qquad \text{(E-1)}$$

The general solution for hoop stress, σ_y, as derived in Appendix D, is of the form

$$\sigma_y = A \cosh m_1 H_x + B \cosh m_2 H_x \qquad \text{(E-2)}$$

As described in Chapter VI, three separate cases must be considered:

(a) Fixed support condition. In this case the cylinder consists only of one bay fully fixed against rotation at each rigid bulkhead.

(b) Simple support condition - one bay. Again the cylinder consists only of one bay but the ends are no longer restrained against rotation at the bulkheads.

(c) Simple support condition - many bays. The cylinder is taken to be continuous over many bays as in a fuselage. The bulkheads provide no restraint against rotation but restrain completely all radial displacement.

In Chapter VI it was demonstrated that case (c) is derived from a combination of fixed support thermal stresses and a simply supported buckling mode. Thus no theoretical treatment of this case is necessary in this Appendix and only cases (a) and (b) are discussed here.

2. FIXED SUPPORT CONDITION

To analyze for fixed support conditions, the origin of coordinates is first shifted from the center of the cylinder to the left bulkhead (see sketch below). The hoop stress equation then takes the form

$$\sigma_y = E\,\alpha\,\Delta T\left[\,A\cosh m_1 (H_x - H_1) + B\cosh m_2 (H_x - H_1)\right] \qquad \text{(E-2a)}$$

Also, since the hyperbolic functions are not convenient for use in Equation (E-1), a transformation to an infinite cosine series is accomplished with Fourier analysis techniques, resulting in

$$\sigma_y = E\,\alpha\,\Delta T \sum_{p=0}^{\infty} \frac{C_p}{1+\delta_{0p}} \cos\frac{p\pi x}{2c} \qquad \text{(E-3)}$$

where δ_{0p} is the Kronecker delta $\left(\begin{array}{l}\delta_{ij} = 0,\ i \neq j \\ \delta_{ij} = 1,\ i = j\end{array}\right)$

and $$C_p = \left[\frac{2Am_1H_1 \sin m_1H_1}{\left(\frac{p\pi}{2}\right)^2 + (m_1H_1)^2} + \frac{2Bm_2H_1 \sinh m_2H_1}{\left(\frac{p\pi}{2}\right)^2 + (m_2H_1)^2}\right] \qquad \text{(E-4)}$$

for p even, and

$$C_p = 0 \qquad \text{(E-4a)}$$

for p odd.

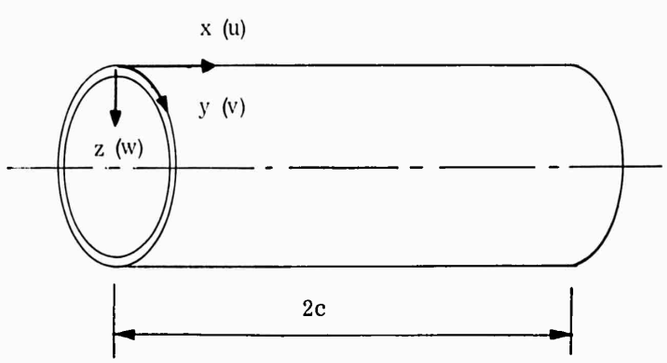

To achieve a solution for Equation (E-1) with use of Equation (E-3), Galerkin's method is employed. Thus, a deflection function which satisfies both the static and kinematic boundary conditions is selected. This function, which was employed by Anderson in Reference 28 is

$$w = \sin \frac{\pi y}{\lambda} \sum_{m=1}^{k} a_m \left[\cos (m-1)\frac{\pi x}{2c} - \cos(m+1) \frac{\pi x}{2c} \right] \qquad \text{(E-5)}$$

where $\lambda = \frac{\pi r}{n}$ is the half wavelength of the buckled shape in the circumferential direction and the coefficients a_m range from m=1 through m=k (the function for w is, of course, an infinite series with $k = \infty$ but is truncated at a finite value of k for numerical analysis). The unknown coefficients a_m are determined from the condition

$$\int_0^{\lambda} \int_0^{2c} w \cdot Q(w)\, dxdy = 0 \qquad \text{(E-6)}$$

where Q (w) is the differential equation (E-1) with σ_y from Equation (E-3).

After integration of Equation (E-6) and rearrangement of terms one obtains

$$\varepsilon_m \left[U_m (1 + \delta_{1m}) + U_{m+2} \right] - a_{m-2} U_m (1 - \delta_{1m})(1 - \delta_{2m}) - a_{m+2} U_m{}^{+2}$$

$$+ \prod \sum_{i=1}^{k} a_i \left[\left(\bar{C}_{m-i-2} - 2\bar{C}_{m-1} + \bar{C}_{m-i+2} - \bar{C}_{m+i-2} + 2\bar{C}_{m+1} - \bar{C}_{m+i+2} \right) \frac{4}{\pi^2} \right.$$

$$+ \frac{H_d}{H_1^2} \left\{ \left[(1+\beta^2)(m-i-2)^2 + 2(i+1)(m-i-2) + (i+1)^2 \right] \bar{C}_{m-i-2} \right.$$

$$-2 \left[(1+\beta^2)(m-i)^2 + 2i(m-i) + (i^2+1) \right] \bar{C}_{m-i} \qquad \text{(E-7)}$$

$$+ \left[(1+\beta^2)(m-i+2)^2 + 2(i-1)(m-i+2) + (i-1)^2 \right] \bar{C}_{m-i+2}$$

$$- \left[(1+\beta^2)(m+i-2)^2 - 2(i-1)(m+i-2) + (i-1)^2 \right] \bar{C}_{m+i-2}$$

$$+2 \left[(1+\beta^2)(m+i)^2 - 2i(m+1) + (i^2+1) \right] \bar{C}_{m+1}$$

$$\left. \left. - \left[(1+\beta^2)(m+i+2)^2 - 2(i+1)(m+i+2) + (i+1)^2 \right] \bar{C}_{m+i+2} \right] \right. = 0$$

$$\text{where } U_m = \frac{1}{\beta 2}\left[\left[(m-1)^2+\beta^2\right]^2 + \frac{32\,H_1{}^4}{\pi^4 H_d}\left[\frac{(m-1)^4}{\left[(m-1)^2+\beta^2\right]^2}\right] + \frac{8H_1{}^2}{\pi^2}\frac{(m-1)^4}{\left[(m-1)^2+\beta^2\right]}\right]$$

$$\overline{C}_k = \frac{C_k}{C_o} \quad , \quad \beta = \frac{2c}{\lambda} \qquad \text{and} \quad \Pi = \frac{c^2 t\, C_{ocr}}{D_s}$$

Equation (E-7) can now be written for m = 1, 2, 3, --- k, which yields k simultaneous equations. The condition of a vanishing determinant leads to the critical value of the buckling stress parameter Π . It is, however, more convenient as in Appendix A, to present the problem in matrix form and apply an iterative technique for the determination of Π for a number of values of the wavelength parameter β . When the simultaneous equations are written in matrix form, one obtains

$$\left[U\right]\left\{a\right\} + \Pi\left[\Sigma\right]\left\{a\right\} = 0$$

or

$$\frac{1}{\Pi}\left\{a\right\} = -\left[U\right]^{-1}\left[\Sigma\right]\left\{a\right\} \qquad \text{(E-8)}$$

It is found that the matrix $\left[U\right]^{-1}\left[\Sigma\right]$ has a checkerboard pattern, i.e., alternate terms are zero. This matrix can be rearranged to form two decoupled systems, corresponding to symmetric and antisymmetric failure modes, which can be treated separately. The symmetric mode leads, in all cases, to the lower critical stress. From the eigen value Π of the system the value of $Co_{cr} = C_o\, E\, \alpha\, \Delta\, T_{cr}$ can be computed leading to the critical temperature rise ΔT_{cr}.

Unfortunately, this approach demonstrated such poor convergence that it was not possible to determine the critical temperature even with m = 30. As noted in Chapter VI, however, a more critical mode of buckling than the present case can be defined (Case (c)) when the intent is to analyze a long cylinder supported over many rings.

3. SIMPLY SUPPORTED EDGES - ONE BAY

As in the case of built-in edges the expression for the hoop stress in the cylinder is transformed into the Fourier cosine series (Eq. E-3), where the coefficients C_p are given by Eq. E-4.

The analysis follows that of Hoff (Reference 14), suitably modified to include shear deformation terms. Hence, the displacement function is taken to have the form

$$w = \cos ny \sum a_m \cos \frac{m\pi x}{\lambda} \qquad \text{(E-9)}$$

Substitution of Equations (E-3) and (E-9) into (E-1) yields an expression involving double series. These series can be manipulated, as in Reference 14, to generate a set of linear simultaneous equations (see Equations 28 of Reference 14).

The general form of one such equation is the counterpart of Equation (E-7) of the fixed support case and the matrix form of these equations has the same appearance as Equation (E-8). The expression for U_m given by Hoff, however, must now include the shear deformation terms, i.e.

$$U_m = \frac{\left[\left(\frac{m\pi}{\lambda}\right)^2 + n^2\right]^4 + 4(1-\mu^2)\left(\frac{r}{h}\right)^2\left[1 + \frac{D_s}{r^2 D_q}\left\{\left(\frac{m\pi}{\lambda}\right)^2 + n^2\right\}\right]\left(\frac{m\pi}{\lambda}\right)^4}{2(1-\mu^2)\left(\frac{r}{h}\right)^2\left[1+\frac{D_s}{r^2 D_q}\left\{\left(\frac{m\pi}{\lambda}\right)^2 + n^2\right\}\right]\left[\left(\frac{m\pi}{\lambda}\right)^2 + n^2\right]^2 n^2} \quad \text{(E-10)}$$

In the present case the matrix associated with this term $\left(\left[U\right]\right)$ is a diagonal matrix and is therefore easily inverted. Using the matrix iterative techniques of Appendix A the eigenvalues of the system for a range of values of the wavelength parameter are computed and the minimum determined using a standard curve fitting procedure.

The eigenvalue thus determined, R in Hoff's notation, corresponds to the critical thermal strain $\alpha \triangle T_{cr}$.

APPENDIX F

SANDWICH CYLINDER STRESSES DUE TO INTERNAL AND EXTERNAL PRESSURE AND RADIAL TEMPERATURE GRADIENTS

The cylinder treated in this section is of the identical cross-section as those examined in Appendixes C, D, and E and is infinitely long. Now, however, a distinction must be made between the radii of the inner and outer skins. The inner radius is designated as r_i and the outer radius as r_o. The inner and outer skins are at constant temperatures T_i and T_o, respectively ($\Delta T = T_o - T_i$), and both internal and external pressures may be present. Also, the core is now assumed to have a modulus of elasticity in the radial direction (E_r) and zero stiffness in the circumferential and axial directions.

In this approach to the development of relationships for the stresses in the faces and core, each cylindrical component (the inner and outer faces and the core) is examined separately and finally combined using conditions of compatibility at the interfaces. Axial stresses are transmitted from one cylinder to the next only at the ends of the cylinders; such "end effect" stress systems are not considered in this development.

Sketched below is a representation of the forces acting on the skins and on the core. The unknown interface stress between the inner skin and the core is designated as q_i. At any radius r, the radial stress within the core must be

$$q = \frac{q_i r_i}{r} \tag{F-1}$$

and it follows that $q_o = q_i \frac{r_i}{r_o} = \frac{q_i}{R}$ (F-1a)

where $R = \frac{r_o}{r_i}$, (F-2)

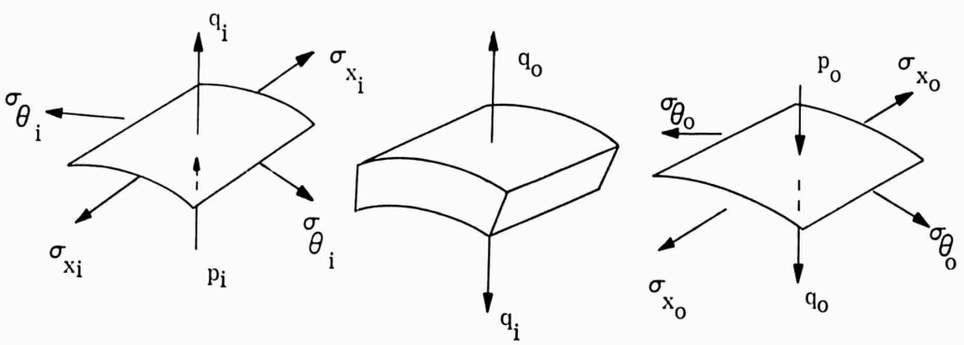

Inner Face Core Outer Face

while the radial strain due to this stress is

$$\epsilon_c = \frac{q_i r_i}{E_r r} \qquad \text{(F-3)}$$

By integration from r_i to r_o, one obtains the radial growth (i.e., the change in radial displacement between the inner and outer faces) due to this strain as follows:

$$\Delta w_{c_q} = \int_{r_i}^{r_o} \frac{q_i r_i}{E_r r} = \frac{q_i r_i}{E_r} \ln(R) \qquad \text{(F-4)}$$

The radial growth due to thermal strains is simply

$$\Delta w_{c_T} = \alpha \left(\frac{T_o + T_i}{2}\right) (r_o - r_i) \qquad \text{(F-4a)}$$

Considering now the total radial growth of the core (w_c) as being composed of both the growth due to thermal expansion and Δw_{c_q}, one obtains

$$\Delta w_c = \left[\frac{\alpha}{2}(T_o+T_i)(r_o-r_i) + \frac{q_i r_i}{E_r} \ln(R)\right] \qquad \text{(F-5)}$$

Radial displacement of the inner cylinder (w_i) is given by

$$w_i = r_i \left[\alpha T_i + \frac{(q_i + p_i) r_i}{Et} - \mu \frac{\sigma_{x_i}}{E}\right] \qquad \text{(F-7)}$$

where σ_{x_i} is the axial stress in the inner cylinder, while the strain in the axial direction is

$$\epsilon_{x_i} = \left[\alpha T_i + \frac{\sigma_{x_i}}{E} - \mu \frac{(q_i+p_i) r_i}{Et}\right] \qquad \text{(F-7)}$$

Similarly, for the outer cylinder, the radial displacemcnt and axial strain are

$$w_o = r_o \left[\alpha T_o - \mu \frac{\sigma_{x_o}}{E} - \frac{(q_o + p_o) r_o}{Et}\right] \qquad \text{(F-8)}$$

and

$$\epsilon_{x_o} = \left[\alpha T_o + \frac{\sigma_{x_o}}{E} + \mu \frac{(q_o+p_o) r_o}{Et}\right] \qquad \text{(F-9)}$$

where σ_{x_o} the the axial stress on the outer cylindcr.

From equilibrium, it is found that

$$\sigma_{x_o} = -\sigma_{x_i}\frac{r_i}{r_o} = -\frac{\sigma_{x_i}}{R} \tag{F-10}$$

and, from compatibility

$$\epsilon_{x_i} = \epsilon_{x_o} \tag{F-11}$$

$$w_i + \Delta w_c = w_o \tag{F-12}$$

Use of conditions (F-1) and (F-10) to (F-12) together with Equations (F-3) and (F-5) to (F-9) leads to the following two simultaneous equations in σ_{x_i} and q_i

$$\frac{(1+R)\,\sigma_{x_i}}{E} - \frac{2\mu r_i R\, q_i}{Et} = \alpha R \Delta T + \frac{\mu r_i R}{Et}(p_i + p_o R) \tag{F-13}$$

$$-\frac{2\mu\,\sigma_{x_i}}{E} + \frac{r_i(1+R+K)q_i}{Et} = \frac{\alpha}{2}(1+R)\Delta T - \frac{r_i}{Et}(p_i + p_o R^2) \tag{F-14}$$

Thus

$$\sigma_{x_i} = \frac{E\alpha\,\Delta T\, R\,((1+R)(1+\mu)+K) - \mu R(1-R-K)\frac{p_i r_i}{t} + \mu R^2(1-R+K)\frac{p_o r_i}{t}}{(1+R)(1+R+K) - 4\mu^2 R} \tag{F-15}$$

$$q_i = \frac{E\alpha\,\Delta T\,\frac{t}{2r_i}\,((1+R)^2 + 4\mu R) - p_i(1+R-2\mu^2 R) - p_o R^2(1+R-2\mu^2)}{(1+R)(1+R+K) - 4\mu^2 R} \tag{F-16}$$

where $K = \frac{Et}{E_r r_i}\ln R$

Using Equations (F-15) and (F-16), the equations for hoop and axial stress of Chapter VII are obtained by back substitution into the appropriate equations.

REFERENCES

1. Gallagher, R.H. and Huff, R.D.; "Thermal Stress Determination Techniques for Supersonic Transport Aircraft Structures, Part I–A Bibliography of Thermal Stress Analysis References, 1955-1962" ASD-TDR63-783, July 1963

2. Gallagher, R.H., Padlog, J. and Huff, R.D.; "Thermal Stress Determination Techniques for Supersonic Transport Aircraft Structures, Part III - Computer Programs for Beam, Plate and Cylindrical Shell Analysis" ASD–TDR63-783, July 1963.

3. Anon; "Sandwich Construction for Aircraft, Part II" ANC-23, 1955

4. Hoff, N.J.; "Thermal Buckling of Supersonic Wing Panels" Journal of Aeronautical Sciences, Vol. 23, 1956.

5. Klosner, J. and Forray, M.; "Buckling of Simply Supported Plates under Arbitrary Symmetrical Temperature Distributions" Journal of Aeronautical Sciences, Vol. 25, 1958.

6. van der Neut, A.; "Buckling Caused by Thermal Stresses" Chapter 11 "High Temperature Effects in Aircraft Structures" Agardograph 28, Pergamon Press, New York 1958.

7. Bijlaard, P.P.; "Thermal Stress and Deflections in Rectangular Sandwich Plates" Journal of Aerospace Sciences, Vol. 26, April 1959.

8. Ebcioglu, I.K.; "Thermo-Elastic Equations for a Sandwich Panel under Arbitrary Temperature Distribution, Transverse Load and Edge Compression" ASD-TR61-128, 1961.

9. Bijlaard, P.P., and Gallagher, R.H.; " Elastic Instability of a Cylindrical Shell under Arbitrary Circumferential Variation of Axial Stress" Journal of Aerospace Sciences, Vol. 27, November 1960.

10. Abir, D., and Nardo, S.V.; "Thermal Buckling of Circular Cylindrical Shells under Circumferential Temperature Gradients" Journal of Aerospace Sciences, Vol. 26, December 1959.

11. Leggett, D.M.A., and Hopkins, H.G., "Sandwich Panels and Cylinders under Compressive End Loads", A.R.C., R. and M.2282, 1942.

12. Teichmann, F.K., Wang, C-T., and Gerard, G.; "Buckling of Sandwich Cylinders under Axial Compression" Journal of Aeronautical Sciences, Vol. 18, June 1951.

13. Stein, M. and Mayers, J.; "Compressive Buckling of Simply Supported Curved Plates and Cylinders of Sandwich Construction", NACA TN2601, 1952.

14. Hoff, N.J.; "Buckling of Thin Cylindrical Shell under Hoop Stresses Varying in the Axial Direction" Journal of Applied Mechanics, Vol. 24, No. 3, September 1957.

15. Przemieniecki, J.S.;" Transient Temperature Distributions and Thermal Stresses in Fuselage Shells with Bulkheads or Frames", Journal of Royal Aeronautical Society, Vol. 60, No. 12, December 1956.

16. Johns, D.J.; "Thermal Stresses in Thin Cylindrical Shells, Stiffened by Plane Bulkheads for Arbitrary Temperature Distributions" College of Aeronautics, Cranfield, Note No. 83, July 1958.

17. Johns, D.J.; "Local Circumferential Buckling of Thin Circular Cylindrical Shells" NASA TN D-1510, 1962.

18. Anderson, M.S., "Thermal Buckling of Cylinders" NASA TN D-1510, 1962.

19. Yao, J.C., "Thermal-Stress Analysis of Sandwich-Type Cylindrical Shells by the Cross Method" Aerospace Engineering, Vol. 20, No. 8, August 1961.

20. Reissner, E.; "Finite Deflections of Sandwich Plates" Journal of Aeronautical Sciences, Vol. 15, July 1948.

21. Timoshenko, S., "Theory of Elastic Stability" McGraw Hill Book Co., New York, 1936, p. 350.

22. Gellatly, R.A.; "Buckling of Sandwich Panels with Particular Reference to Thermal Effects" Ph.D. Thesis, University of London, 1958.

23. Lewis, W.C.; "Deflection and Stresses in a Uniformly Loaded Simply Supported Rectangular Sandwich Panel" U.S. Forest Products Laboratory Report No. 1847-A, 1956.

24. Cunningham, J.H., and Jacobson, M.J.; "Design and Testing of Honeycomb Sandwich Cylinders under Axial Compression" NASA TN D-1510, 1962.

25. Norris, C.B., and Kuenzi, E.W.; "Buckling of Long Thin Plywood Cylinders in Axial Compression, Experimental Treatment" U.S. Forest Products Laboratory Report No. 1322-B, 1943.

26. March,H.W., and Kuenzi E.W.; "Buckling of Cylinders of Sandwich Construction in Axial Compression" U.S. Forest Products Laboratory Report No. 1830, 1957.

27. Eakin,E.C.; "Honeycomb Cylinder Tests" Douglas Aircraft Company Report No. SM-37719, January 1962.

28. Anderson,M,S.;" Combinations of Temperature and Axial Compression Required for Buckling of a Ring-Stiffened Cylinder" NASA TN D-1224, 1962.

Aeronautical Systems Division, Flight Dynamics Lab., Wright-Patterson AFB, Ohio.
Rpt. Nr. ASD-TDR-63-783, Part II,
THERMAL STRESS DETERMINATION TECHNIQUES FOR SUPERSONIC TRANSPORT AIRCRAFT STRUCTURES, PART II - DESIGN DATA FORSANDWICH PLATES AND CYLINDERS UNDER APPLIED LOADS AND THERMAL GRADIENTS.
Technical Documentary Rpt., Jan. 1964
117 pp., incl. illus., tables.

Unclassified Report

(over)

UNCLASSIFIED

1. Supersonic Planes
2. Transport Planes
3. Structures
4. Sandwich Panels
5. Stresses
6. Thermal Stresses

I AFSC Project 9056
II Contract AF33(657)-8936
III Textron's Bell Aerosystems Company, Buffalo, N.Y.
IV Gellatly, R.A. and Gallagher, R.H.

V ASD-TDR-63-783, Part II
VI Avail fr. DDC
VII Not avail fr. OTS

Structural design data are presented for various applied load and thermal gradient conditions for flat rectangular sandwich panels and sandwich cylinders. The flat panel solutions pertain to instability under nonuniform stress, and also to the stresses and displacements resulting from normal pressures and temperature gradients across the panel thickness in the presence of uniform midplane compression.

Sandwich cylinder design data are given for buckling under nonuniform circumferential and axial stress, respectively, and for stresses due to radial or axial temperature gradients. The range of stiffness parameters extend, at one limit, to the isotropic forms of construction.

Aeronautical Systems Division, Flight Dynamics Lab., Wright-Patterson AFB, Ohio.
Rpt. Nr. ASD-TDR-63-783, Part II,
THERMAL STRESS DETERMINATION TECHNIQUES FOR SUPERSONIC TRANSPORT AIRCRAFT STRUCTURES, PART II - DESIGN DATA FORSANDWICH PLATES AND CYLINDERS UNDER APPLIED LOADS AND THERMAL GRADIENTS.
Technical Documentary Rpt., Jan. 1964
117 pp., incl. illus., tables.

Unclassified Report

(over)

UNCLASSIFIED

1. Supersonic Planes
2. Transport Planes
3. Structures
4. Sandwich Panels
5. Stresses
6. Thermal Stresses

I AFSC Project 9056
II Contract AF33(657)-8936
III Textron's Bell Aerosystems Company, Buffalo, N.Y.
IV Gellatly, R.A. and Gallagher, R.H.

V ASD-TDR-63-783, Part II
VI Avail fr. DDC
VII Not avail fr. OTS

Structural design data are presented for various applied load and thermal gradient conditions for flat rectangular sandwich panels and sandwich cylinders. The flat panel solutions pertain to instability under nonuniform stress, and also to the stresses and displacements resulting from normal pressures and temperature gradients across the panel thickness in the presence of uniform midplane compression.

Sandwich cylinder design data are given for buckling under nonuniform circumferential and axial stress, respectively, and for stresses due to radial or axial temperature gradients. The range of stiffness parameters extend, at one limit, to the isotropic forms of construction.

Aeronautical Systems Division, Flight Dynamics Lab., Wright-Patterson AFB, Ohio.
Rpt. Nr. ASD-TDR-63-783, Part II,
THERMAL STRESS DETERMINATION TECHNIQUES FOR SUPERSONIC TRANSPORT AIRCRAFT STRUCTURES, PART II - DESIGN DATA FORSANDWICH PLATES AND CYLINDERS UNDER APPLIED LOADS AND THERMAL GRADIENTS.
Technical Documentary Rpt., Jan. 1964
117 pp., incl. illus., tables.

Unclassified Report

(over)

UNCLASSIFIED

1. Supersonic Planes
2. Transport Planes
3. Structures
4. Sandwich Panels
5. Stresses
6. Thermal Stresses

I AFSC Project 9056
II Contract AF33(657)-8936
III Textron's Bell Aerosystems Company, Buffalo, N.Y.
IV Gellatly, R.A. and Gallagher, R.H.

V ASD-TDR-63-783, Part II
VI Avail fr. DDC
VII Not avail fr. OTS

Structural design data are presented for various applied load and thermal gradient conditions for flat rectangular sandwich panels and sandwich cylinders. The flat panel solutions pertain to instability under nonuniform stress, and also to the stresses and displacements resulting from normal pressures and temperature gradients across the panel thickness in the presence of uniform midplane compression.

Sandwich cylinder design data are given for buckling under nonuniform circumferential and axial stress, respectively, and for stresses due to radial or axial temperature gradients. The range of stiffness parameters extend, at one limit, to the isotropic forms of construction.

Aeronautical Systems Division, Flight Dynamics Lab., Wright-Patterson AFB, Ohio.
Rpt. Nr. ASD-TDR-63-783, Part II,
THERMAL STRESS DETERMINATION TECHNIQUES FOR SUPERSONIC TRANSPORT AIRCRAFT STRUCTURES, PART II - DESIGN DATA FORSANDWICH PLATES AND CYLINDERS UNDER APPLIED LOADS AND THERMAL GRADIENTS.
Technical Documentary Rpt., Jan. 1964
117 pp., incl. illus., tables.

Unclassified Report

(over)

UNCLASSIFIED

1. Supersonic Planes
2. Transport Planes
3. Structures
4. Sandwich Panels
5. Stresses
6. Thermal Stresses

I AFSC Project 9056
II Contract AF33(657)-8936
III Textron's Bell Aerosystems Company, Buffalo, N.Y.
IV Gellatly, R.A. and Gallagher, R.H.

V ASD-TDR-63-783, Part II
VI Avail fr. DDC
VII Not avail fr. OTS

Structural design data are presented for various applied load and thermal gradient conditions for flat rectangular sandwich panels and sandwich cylinders. The flat panel solutions pertain to instability under nonuniform stress, and also to the stresses and displacements resulting from normal pressures and temperature gradients across the panel thickness in the presence of uniform midplane compression.

Sandwich cylinder design data are given for buckling under nonuniform circumferential and axial stress, respectively, and for stresses due to radial or axial temperature gradients. The range of stiffness parameters extend, at one limit, to the isotropic forms of construction.

Aeronautical Systems Division, Flight Dynamics Lab., Wright-Patterson AFB, Ohio.
Rpt. Nr. ASD-TDR-63-783, Part II,
THERMAL STRESS DETERMINATION TECHNIQUES FOR SUPERSONIC TRANSPORT AIRCRAFT STRUCTURES, PART II - DESIGN DATA FORSANDWICH PLATES AND CYLINDERS UNDER APPLIED LOADS AND THERMAL GRADIENTS.
Technical Documentary Rpt., Jan. 1964
117 pp., incl. illus., tables.

Unclassified Rcport

(over)

UNCLASSIFIED

1. Supersonic Planes
2. Transport Planes
3. Structures
4. Sandwich Panels
5. Stresses
6. Thermal Stresses

I AFSC Prcject 9056
II Contract AF33(657)-8936
III Textron's Bell Aerosystems Company, Buffalo, N.Y.
IV Gellatly, R.A. and Gallagher, R.H.

Structural design data are presentcd for various applied load and thermal gradient conditions for flat rectangular sandwich panels and sandwich cylinders. The flat panel solutions pertain to instability under nonuniform stress, and also to thc stresses and displacements resulting from normal pressures and temperature gradients across the panel thickness in the presencc of uniform midplane compression.

Sandwich cylinder design data are given for buckling under nonuniform circumferential and axial stress, rcspectively, and for stresses due to radial or axial temperature gradients. The range of stiffness parameters extend, at one limit, to the isotropic forms of construction.

V ASD-TDR-63-783, Part II
VI Avail fr. DDC
VII Not avail fr. OTS

Aeronautical Systems Division, Flight Dynamics Lab., Wright-Patterson AFB, Ohio.
Rpt. Nr. ASD-TDR-63-783, Part II,
THERMAL STRESS DETERMINATION TECHNIQUES FOR SUPERSONIC TRANSPORT AIRCRAFT STRUCTURES, PART II - DESIGN DATA FORSANDWICH PLATES AND CYLINDERS UNDER APPLIED LOADS AND THERMAL GRADIENTS.
Technical Documentary Rpt., Jan. 1964
117 pp., incl. illus., tables.

Unclassified Report

(over)

UNCLASSIFIED

1. Supersonic Planes
2. Transport Planes
3. Structures
4. Sandwich Panels
5. Stresses
6. Thermal Stresses

I AFSC Project 9056
II Contract AF33(657)-8936
III Textron's Bell Aerosystems Company, Buffalo, N.Y.
IV Gellatly, R.A. and Gallagher, R.H.

Structural design data are presented for various applied load and thermal gradient conditions for flat rectangular sandwich panels and sandwich cylinders. The flat panel solutions pertain to instability under nonuniform stress, and also to the stresses and displacements resulting from normal pressures and temperature gradients across the panel thickness in the presence of uniform midplane compression.

Sandwich cylinder design data are given for buckling under nonuniform circumferential and axial stress, respectively, and for stresses due to radial or axial temperature gradients. The range of stiffness parameters extend, at one limit, to the isotropic forms of construction.

V ASD-TDR-63-783, Part II
VI Avail fr. DDC
VII Not avail fr. OTS

Aeronautical Systems Division, Flight Dynamics Lab., Wright-Patterson AFB, Ohio.
Rpt. Nr. ASD-TDR-63-783, Part II,
THERMAL STRESS DETERMINATION TECHNIQUES FOR SUPERSONIC TRANSPORT AIRCRAFT STRUCTURES, PART II - DESIGN DATA FORSANDWICH PLATES AND CYLINDERS UNDER APPLIED LOADS AND THERMAL GRADIENTS.
Technical Documentary Rpt., Jan. 1964
117 pp., incl. illus., tables.

Unclassified Report

(over)

UNCLASSIFIED

1. Supersonic Planes
2. Transport Planes
3. Structures
4. Sandwich Panels
5. Stresses
6. Thermal Stresses

I AFSC Project 9056
II Contract AF33(657)-8936
III Textron's Bell Aerosystems Company, Buffalo, N.Y.
IV Gellatly, R.A. and Gallagher, R.H.
V ASD-TDR-63-783, Part II
VI Avail fr. DDC
VII Not avail fr. OTS

Structural design data are presented for various applied load and thermal gradient conditions for flat rectangular sandwich panels and sandwich cylinders. The flat panel solutions pertain to instability under nonuniform stress, and also to the stresses and displacements resulting from normal pressures and temperature gradients across the panel thickness in the presence of uniform midplane compression.

Sandwich cylinder design data are given for buckling under nonuniform circumferential and axial stress, respectively, and for stresses due to radial or axial temperature gradients. The range of stiffness parameters extend, at one limit, to the isotropic forms of construction.

Aeronautical Systems Division, Flight Dynamics Lab., Wright-Patterson AFB, Ohio.
Rpt. Nr. ASD-TDR-63-783, Part II,
THERMAL STRESS DETERMINATION TECHNIQUES FOR SUPERSONIC TRANSPORT AIRCRAFT STRUCTURES, PART II - DESIGN DATA FORSANDWICH PLATES AND CYLINDERS UNDER APPLIED LOADS AND THERMAL GRADIENTS.
Technical Documentary Rpt., Jan. 1964
117 pp., incl. illus., tables.

Unclassified Report

(over)

UNCLASSIFIED

1. Supersonic Planes
2. Transport Planes
3. Structures
4. Sandwich Panels
5. Stresses
6. Thermal Stresses

I AFSC Project 9056
II Contract AF33(657)-8936
III Textron's Bell Aerosystems Company, Buffalo, N.Y.
IV Gellatly, R.A. and Gallagher, R.H.
V ASD-TDR-63-783, Part II
VI Avail fr. DDC
VII Not avail fr. OTS

Structural design data are presented for various applied load and thermal gradient conditions for flat rectangular sandwich panels and sandwich cylinders. The flat panel solutions pertain to instability under nonuniform stress, and also to the stresses and displacements resulting from normal pressures and temperature gradients across the panel thickness in the presence of uniform midplane compression.

Sandwich cylinder design data are given for buckling under nonuniform circumferential and axial stress, respectively, and for stresses due to radial or axial temperature gradients. The range of stiffness parameters extend, at one limit, to the isotropic forms of construction.